frontiers | Research Topics

Recent advances in thermal and nonthermal ablative technologies of the thyroid

Edited by
Pia Pace-Asciak and Ralph P. Tufano

Published in
Frontiers in Endocrinology

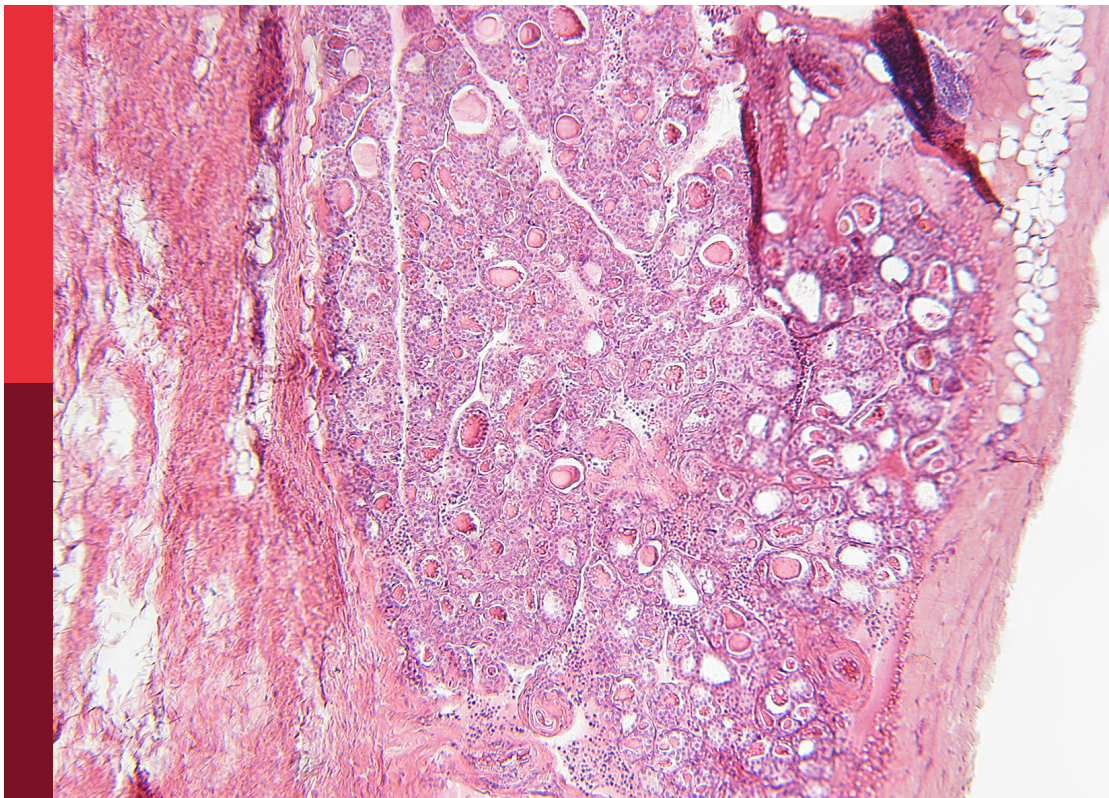

ISSN 1664-8714
ISBN 978-2-8325-6324-3
DOI 10.3389/978-2-8325-6324-3

About Frontiers

Frontiers is more than just an open access publisher of scholarly articles: it is a pioneering approach to the world of academia, radically improving the way scholarly research is managed. The grand vision of Frontiers is a world where all people have an equal opportunity to seek, share and generate knowledge. Frontiers provides immediate and permanent online open access to all its publications, but this alone is not enough to realize our grand goals.

Frontiers journal series

The Frontiers journal series is a multi-tier and interdisciplinary set of open-access, online journals, promising a paradigm shift from the current review, selection and dissemination processes in academic publishing. All Frontiers journals are driven by researchers for researchers; therefore, they constitute a service to the scholarly community. At the same time, the *Frontiers journal series* operates on a revolutionary invention, the tiered publishing system, initially addressing specific communities of scholars, and gradually climbing up to broader public understanding, thus serving the interests of the lay society, too.

Dedication to quality

Each Frontiers article is a landmark of the highest quality, thanks to genuinely collaborative interactions between authors and review editors, who include some of the world's best academicians. Research must be certified by peers before entering a stream of knowledge that may eventually reach the public - and shape society; therefore, Frontiers only applies the most rigorous and unbiased reviews. Frontiers revolutionizes research publishing by freely delivering the most outstanding research, evaluated with no bias from both the academic and social point of view. By applying the most advanced information technologies, Frontiers is catapulting scholarly publishing into a new generation.

What are Frontiers Research Topics?

Frontiers Research Topics are very popular trademarks of the *Frontiers journals series*: they are collections of at least ten articles, all centered on a particular subject. With their unique mix of varied contributions from Original Research to Review Articles, Frontiers Research Topics unify the most influential researchers, the latest key findings and historical advances in a hot research area.

Find out more on how to host your own Frontiers Research Topic or contribute to one as an author by contacting the Frontiers editorial office: frontiersin.org/about/contact

Recent advances in thermal and nonthermal ablative technologies of the thyroid

Topic editors

Pia Pace-Asciak — University of Toronto, Canada

Ralph P. Tufano — The Johns Hopkins Hospital, Johns Hopkins Medicine, United States

Citation

Pace-Asciak, P., Tufano, R. P., eds. (2025). *Recent advances in thermal and nonthermal ablative technologies of the thyroid*. Lausanne: Frontiers Media SA. doi: 10.3389/978-2-8325-6324-3

Table of contents

frontiers | Frontiers in Endocrinology

TYPE Editorial
PUBLISHED 24 April 2025
DOI 10.3389/fendo.2025.1601452

OPEN ACCESS

EDITED AND REVIEWED BY
Terry Francis Davies,
Icahn School of Medicine at Mount Sinai, United States

*CORRESPONDENCE
Pia Pace-Asciak
Pia.Pace-Asciak@unityhealth.to

RECEIVED 27 March 2025
ACCEPTED 02 April 2025
PUBLISHED 24 April 2025

CITATION
Pace-Asciak P and Tufano RP (2025) Editorial: Recent advances in thermal and nonthermal ablative technologies of the thyroid.
Front. Endocrinol. 16:1601452.
doi: 10.3389/fendo.2025.1601452

Editorial: Recent advances in thermal and nonthermal ablative technologies of the thyroid

Pia Pace-Asciak[1]* and Ralph P. Tufano[2]

[1]Department of Otolaryngology – Head and Neck Surgery, University of Toronto, Toronto, ON, Canada, [2]Head and Neck Endocrine Surgery, Sarasota Memorial Care System, Florida State University School of Medicine, Sarasota, FL, United States

KEYWORDS

thyroid disease, radiofrequency ablation, laser ablation, benign and malignant thyroid nodules, ablative therapy

Editorial on the Research Topic

Recent advances in thermal and nonthermal ablative technologies of the thyroid

The field of thyroidology is rapidly expanding to include alternatives beyond surgery such as minimally invasive thermal and nonthermal ablative techniques for benign and carefully selected malignant thyroid nodules. The patient-centered, minimally invasive approach to thyroid nodules has been used globally for years and is now permeating North America. The main appeal for these newer approaches is that compared to surgery it avoids the need for a general anesthetic, an incision, and is associated with a quick recovery and low risk for hypothyroidism. We compiled a series of articles that reflect this exciting time in thyroid research with articles that look at different therapeutic and diagnostic approaches for treating benign and malignant thyroid nodules. Within this diverse set of articles, we share quality research that looks at ways to individualize treatment ranging from isolating biomarkers at the microscopic genetic level for autoimmune thyroiditis spanning to novel diagnostic and clinical approaches for treating thyroid nodules with ablative technologies.

With the introduction of any new procedure, there is always a learning curve to achieve proficiency. This is a timely topic given the number of new centres bringing thermal ablation to their institution and wanting safe alternatives for their patients. According to the literature, physicians with prior experience doing their own thyroid ultrasounds and ultrasound guided fine needle biopsy (FNA) may have to carry out at least 20-30 radiofrequency ablation (RFA) procedures before reaching a safe and competent level (1). Chytiris et al., explore this concept further by providing insight into the learning curve for safely and effectively ablating non-functioning thyroid nodules with the nodule volume considered. We felt this paper was important since the authors provide guidance to novice operators on the various factors (such as technical ability and nodule characteristics) involved in successful and safe ablation.

Ultrasound is the gold standard for risk stratifying whether biopsy is warranted. Traditional grey scale ultrasound can be ineffective for managing isoechoic thyroid nodules and ruling out sonographic features of cancer (2). Most of these nodules are benign but can lead to unnecessary biopsies in the process of ruling out malignancy. Goundan et al. discuss the use of quantitative ultrasound (QUS) as a novel imaging method to assess the tissue

microarchitecture of the nodule as a means of further risk stratifying isoechoic and hypoechoic thyroid nodules. Improving accuracy of imaging by subtyping the nodule characteristics may lead to less FNA biopsies, and improved quality of care.

We have included articles that describe methods for ensuring safety and efficacy when using Radiofrequency ablation (RFA). By pushing the boundaries and indications of RFA, Teliti et al. ensure patient safety by monitoring the recurrent laryngeal nerve with flexible laryngoscopy in the awake patient while using RFA in bilateral thyroid nodules. As this technology continues to evolve, innovative techniques emerge to ensure efficacy and safety but also accuracy. Sarkis et al. use a novel guide when performing RFA of thyroid nodules to provide a robust in line visualisation of the 7 mm or 10 mm radiofrequency active probe tip to ensure safety while near the danger triangle and complete ablation of the conceptual subunits during RFA to avoid later regrowth. Furthermore, Chuanke et al. demonstrates long-term volume reduction in up to 6 years post treatment, with stabilization 2 years post treatment. Comparing preoperative contrast-enhanced ultrasonography (CEUS) in the target area with postoperative CEUS to ensure complete ablation particularly along the margins of the nodule is a useful technique ensuing long-term success. In addition, the use of percutaneous laser ablation has been shown to effectively reduce nodule volume and alleviate associated compressive symptoms in benign nodules. Malik et al. demonstrate sustained reduction long-term (up to 18 months) post laser ablation with a thin percutaneous optic fiber creating a predictable zone of coagulation with a type of image guidance (spatial overlay) for treatment planning to ensure all zones are equally targeted.

While early studies indicate that thermal ablation does not appear to compromise the overall survival rate or increase the risk of recurrence, more extensive long-term data are required to better understand its role in the management of thyroid cancer. The use of thermal ablation, such as RFA, in the treatment of low-risk papillary thyroid carcinoma (PTC) is an area of growing interest. PTC, particularly in its low-risk form, has a relatively good prognosis, and many patients may not require aggressive surgical intervention or treatment at all. For these individuals, thermal ablation may provide a less invasive option, with the potential to avoid the risks associated with thyroidectomy. Gong et al. compare the efficacy, safety and impact on the quality of life between thermal ablation (RFA and laser) and surgical interventions in patients with papillary microcarcinoma. A superior quality of life and better functional outcomes were noted in the thermal ablation group compared to the surgery group underscoring the need to incorporate such treatments for low-risk disease.

As the use of RFA expands, its application in low-risk papillary thyroid carcinoma offers a potentially transformative approach to treatment, though more long-term data are needed to fully evaluate its role in oncological management. On the other end of the spectrum, newer studies continue to push the boundaries of traditional treatment methods and use creative multimodal solutions for more aggressive thyroid disease. Wan et al. explore the clinical benefits of using ultrasound guided ^{125}Iodine seed implantation for iodine-refractory differentiated thyroid cancer (RAIR-DTC). These authors employ a localized treatment to tumor cells which causes minimal damage to surrounding structures by emitting energy over a long period of time compared to doses of external beam radiation which causes lethal damage to surrounding tissues. Akin to the concept of minimally invasive thermal ablation, this paper employs other methods for targeted local tumor ablation with minimal side effects.

Complications can and do happen despite the excellent safety profile of minimally invasive treatments. Major complications are rare with minimally invasive techniques but do exist. Ferraro et al. review the literature and share a case report of thyroid nodule rupture post RFA and propose a treatment algorithm for managing major complications. Chuanke et al. also share a complication of Horner's syndrome post cervical chain injury for readers so awareness and consent can be appropriately obtained.

At a more microscopic level, the genetics of thyroid disease can dictate the trajectory of disease outcome. With autoimmune thyroiditis, understanding the complex genetic expression of T cell exhaustion (Tex) and its role in Graves' disease (GD) can be helpful to tailor therapeutics. Jiang et al. examine gene profiling in GD to investigate how Tex related gene CBL is expressed in autoimmune thyroid disease and to subtype its expression. By shedding light on the genetic expression of the immune response within the thyroid, it introduces a novel research avenue for developing molecularly targeted drugs for each subtype. Once again, another example of how the field of thyroidology is moving away from a "one size fits all" approach to a more tailored and individualized one.

We hope you enjoy the diverse topics within our Research Topic on ablative technology and become inspired to develop innovative approaches within your own centres for further improving the management of both benign and malignant thyroid disease.

Author contributions

PP: Validation, Conceptualization, Supervision, Writing – review & editing, Data curation, Writing – original draft. RT: Writing – original draft, Writing – review & editing, Supervision.

Conflict of interest

The authors declare that the research was conducted in the absence of any commercial or financial relationships that could be construed as a potential conflict of interest.

Generative AI statement

The author(s) declare that no Generative AI was used in the creation of this manuscript.

Publisher's note

References

1. Bom WJ, Joosten FBM, van Borren MMGJ, Bom EP, van Eekeren RRJP, de Boer H. Radiofrequency ablation for symptomatic, non-functioning, thyroid nodules: a single- center learning curve. *Endocr Connect*. (2022) 11:e210304. doi: 10.1530/EC-21–0304

2. Molina-Vega M, Rodríguez-Pérez CA, Álvarez-Mancha AI, Baena-Nieto G, Riestra M, Alcázar V, et al. Clinical and ultrasound thyroid nodule characteristics and their association with cytological and histopathological outcomes: A retrospective multicenter study in high-resolution thyroid nodule clinics. *J Clin Med.* (2019) 8:2172. doi: 10.3390/jcm8122172

frontiers | Frontiers in Endocrinology

TYPE Original Research
PUBLISHED 02 February 2024
DOI 10.3389/fendo.2024.1326188

OPEN ACCESS

EDITED BY
Pia Pace-Asciak,
University of Toronto, Canada

REVIEWED BY
Zbigniew Adamczewski,
Medical University of Lodz, Poland
Gerdi Tuli,
Regina Margherita Hospital, Italy
Yuxuan Qiu,
Sichuan University, China
Xiao-Yan Zhang,
Chinese Academy of Medical Sciences and Peking Union Medical College Hospital, China

*CORRESPONDENCE
Poorani N. Goundan
poorani.goundan@bmc.org

RECEIVED 23 October 2023
ACCEPTED 15 January 2024
PUBLISHED 02 February 2024

CITATION
Goundan PN, Lye T, Markel A, Mamou J and Lee SL (2024) Improved cancer risk stratification of isoechoic thyroid nodules to reduce unnecessary biopsies using quantitative ultrasound.
Front. Endocrinol. 15:1326188.
doi: 10.3389/fendo.2024.1326188

Improved cancer risk stratification of isoechoic thyroid nodules to reduce unnecessary biopsies using quantitative ultrasound

Poorani N. Goundan[1]*, Theresa Lye[2,3], Andrew Markel[2,4], Jonathan Mamou[2] and Stephanie L. Lee[1]

[1]Section of Endocrinology, Diabetes, Nutrition and Metabolism, Boston Medical Center, Chobanian Avedisian School of Medicine, Boston, MA, United States, [2]Department of Radiology, Weill Cornell Medicine, New York, NY, United States, [3]Topcon Advanced Biomedical Imaging Laboratory, Topcon Healthcare, Oakland, NJ, United States, [4]Department of Biomedical Engineering, Tulane University, New Orleans, LA, United States

Objective: Gray-scale ultrasound (US) is the standard-of-care for evaluating thyroid nodules (TNs). However, the performance is better for the identification of hypoechoic malignant TNs (such as classic papillary thyroid cancer) than isoechoic malignant TNs. Quantitative ultrasound (QUS) utilizes information from raw ultrasonic radiofrequency (RF) echo signal to assess properties of tissue microarchitecture. The purpose of this study is to determine if QUS can improve the cancer risk stratification of isoechoic TNs.

Methods: Patients scheduled for TN fine needle biopsy (FNB) were recruited from the Thyroid Health Clinic at Boston Medical Center. B-mode US and RF data (to generate QUS parameters) were collected in 274 TNs (163 isoechoic, 111 hypoechoic). A linear combination of QUS parameters (CQP) was trained and tested for isoechoic [CQP(i)] and hypoechoic [CQP(h)] TNs separately and compared with the performance of conventional B-mode US risk stratification systems.

Results: CQP(i) produced an ROC AUC value of 0.937+/- 0.043 compared to a value of 0.717 +/- 0.145 ($p > 0.05$) for the American College of Radiology Thyroid Imaging, Reporting and Data System (ACR TI-RADS) and 0.589 +/- 0.173 ($p > 0.05$) for the American Thyroid Association (ATA) risk stratification system. In this study, CQP(i) avoids unnecessary FNBs in 73% of TNs compared to 55.8% and 11.8% when using ACR TI-RADS and ATA classification system.

Conclusion: This data supports that a unique QUS-based classifier may be superior to conventional US stratification systems to evaluate isoechoic TNs for cancer and should be explored further in larger studies.

KEYWORDS

thyroid nodule, thyroid cancer, fine needle aspiration, thyroid ultrasonography, thyroid cytology

Introduction

A long-standing concern in the management of thyroid nodules (TNs) is the ineffectiveness of risk stratification of isoechoic TNs as cancer or benign using gray-scale ultrasound (US). The American Thyroid Association (ATA) TN classification system and the American College of Radiology Thyroid Imaging, Reporting and Data System (ACR TI-RADS) use high-risk US features including hypoechogenicity, irregular margins and microcalcification to assign a risk level for malignancy (1, 2). The high-risk features identified in these systems are, however, more specific for the classic papillary thyroid cancer subtype. Isoechoic TNs are very common and are more likely to undergo fine needle biopsy (FNB) due to their larger size (3). While a majority of isoechoic TNs are benign, some malignant TNs (follicular thyroid cancer, follicular variant of papillary thyroid cancer and 20% of classic papillary thyroid cancer) demonstrate an isoechoic appearance on US (4, 5). The current ACR TI-RADS TN classification system would not biopsy and completely miss these isoechoic cancers if partially cystic in appearance. The ATA classification system classifies isoechoic TNs as low suspicion and recommends FNB for a size greater than 1.5 cm regardless of other high-risk features such as hyperechoic foci or invasive margins. Follicular cancer and those that behave similarly have a higher risk for distant metastatic disease compared to papillary thyroid cancer making it important that these TNs undergo FNB appropriately (6). At the same time, considerable health care cost and patient and provider anxiety associated with invasive procedures (i.e., FNB, surgery) for benign disease highlight the need to avoid unnecessary FNBs in benign TNs. Therefore, an imaging technique that uniquely allows analysis of isoechoic TNs to reduce unnecessary invasive FNBs in benign TNs without missing cancer will improve the quality of medical care provided to patients with TNs.

Quantitative US (QUS) is an imaging method that utilizes data from raw ultrasonic radiofrequency (RF) echo signals to assess properties of tissue microarchitecture (7–11). Most of the information contained in RF data is discarded in B-mode gray-scale US imaging that is typically used in clinical care. QUS generates numerical parameters that are a function of the underlying microstructure of the interrogated tissue (e.g., effective scatterer size and effective acoustic concentration) (8, 9). Our group has previously demonstrated the use of this clinically novel US technique in the risk stratification of TNs (12). The area under the receiver operating characteristics (ROC) curve of a linear QUS-based classifier (combination of QUS parameters or CQP) was 0.857 +/- 0.033, and statistically the same as that of ACR TI-RADS and ATA risk classification system for discriminating between malignant and benign TNs ($p = 0.327$ and $p = 0.041$, respectively) but without the limiting factor of clinician inexperience in thyroid sonography. This CQP classifier also demonstrated a 44 to 66% reduction in unnecessary FNBs which outperformed the reduction using the ACR TI-RADS and ATA risk classification systems with a negative predictive value of 97 to 100%. We now report the outcomes of a preliminary study in which different QUS-based classifiers were created for isoechoic and hypoechoic TNs to determine if cancer-risk stratification improves.

Materials and methods

The study was performed following institutional review board approval. Details regarding subject recruitment, data collection, RF data processing have been outlined in a prior publication (12). Briefly, patients with one or more TNs who were either undergoing an FNB or had a prior FNB were recruited from the Thyroid Health Clinic at Boston Medical Center. A GE LOGIQ-E9 US scanner (GE Healthcare, Chicago, IL) was used for acquiring RF data utilized for computing QUS parameters using the reference phantom method (13). RF data capture is available natively on the LOGIQ-E9 and therefore no modification of the instrument was necessary. A software key provided by the manufacturer had to be input once to activate RF data capture. TNs with significant cystic area or macrocalcification anterior to the region of interests were not included in the analysis due to interference with US wave propagation. Non-invasive follicular thyroid neoplasms with papillary like features (NIFTPs) were not included due to small numbers in the data set. Investigators who are experienced ultrasonographers reviewed gray-scale US images from the picture and archiving, and communications system (PACS) and determined the echogenicity of TNs. TNs that were designated as isoechoic or hyperechoic were categorized as isoechoic for this study. TNs that were designated as mildly hypoechoic or very hypoechoic were categorized as hypoechoic. A combination of cytology, molecular testing using ThyroSeq genomic classifier (v2 or v3) (CBLPath, Inc., Rye Brook, NY) and surgical pathology was used to classify TNs as benign or cancer. A TN was categorized as benign if it had benign cytology (Bethesda II), or indeterminate cytology (Bethesda III or IV) without any high-risk molecular test result or if surgical pathology did not show any evidence of malignancy. A TN was classified as cancer if found to have Bethesda VI cytology or if surgical pathology demonstrated malignancy. In one subject, a TN with high-risk US features was categorized as malignant based on the presence of a suspicious cervical node that was positive for metastatic thyroid cancer on FNB. Similar methods described in prior publications and in our prior study were used for RF data processing and QUS parameter estimation (7, 12, 14). A combination of QUS parameters were tested using a Fisher linear discriminant approach and classification performance was assessed using ROC curves. Statistical analysis for the study was performed using the MATLAB statistical toolbox (The MathWorks, Inc., Natick, MA).

An optimal linear combination of QUS parameters (CQP) was derived individually for isoechoic TNs [CQP(i)] and hypoechoic TNs [CQP(h)]. The performance of these classifiers was compared to a classifier that was trained using TNs irrespective of echogenicity [CQP(c)] and also to currently used gray-scale TN classification system, ACR TI-RADS and ATA classification system.

10.3389/fendo.2024.1326188

Results

A total of 274 TNs were included in the final analysis. Of these, 163 were categorized as isoechoic (158 benign and 5 cancer) and 111 as hypoechoic (86 benign and 25 cancer) [Table 1]. The prevalence of malignancy in TNs categorized as isoechoic was 3.1% and in those categorized as hypoechoic was 22.5%.

(A) Performance of CQP(i) compared to gray-scale US:

The optimal linear combination of QUS parameters (Nakagami shape parameter, intercept, effective scatterer size, and acoustic concentration) for isoechoic TNs – CQP(i) was determined [21.1875 x Avg_NakShapeParam + 2.6668 x Avg_Intercept - 0.89063 x Avg_EffectiveScattererSize - 2.41 x Avg_AcousticConcentration + 25.9495 x NStd_NakShapeParam]. CQP(i) performed with an ROC AUC of 0.937+/- 0.043 [95% CI 0.853 – 1.000] compared to the performance of ACR TI-RADS, 0.717 +/- 0.145 [95% CI 0.436-1.000, p >0.05] and ATA risk stratification system, 0.589 +/- 0.173 [95% CI 0.250 – 0.929, p >0.05] [Table 2]. Using the CQP(i) threshold of -61.341 for FNB (i.e., a TN chosen for FNB if the CQP(i) value for the TN is equal or less than the threshold), 119 of 163 (73%) TNs were excluded from FNB with a missed malignancy rate of zero among isoechoic TNs (i.e., all malignant TNs would be selected for FNB). With ACR TI-RADS, FNB would not have been recommended in 91 (55.8%) TNs and one malignant TN would have been missed. With the ATA risk stratification system, FNB could be avoided in 19 (11.7%) TNs, with no missed malignant TN. The reduction in FNB for the ATA system is low in the study as the patient population from which subject recruitment occurred had TNs for which FNB was recommended clinically based primarily on the ATA risk stratification system.

When comparing the TNs for which FNB was not recommended, between the CQP(i) and ACR TI-RADS, there was an overlap of 67 TNs in this category. However, 52 TNs for which FNB was not recommended per CQP(i) met criteria for FNB per ACR TI-RADS. Conversely, 23 TNs for which FNB was not recommended per ACR TI-RADS met criteria per the CQP (i) threshold.

The malignant TN missed by the ACR TI-RADS classification system was a 5 cm solid cystic nodule with isoechoic echotexture, with a smooth margin and without any echogenic foci. The surgical pathology of this TN demonstrated a follicular variant papillary thyroid cancer without lymphovascular invasion, extrathyroidal extension or metastatic nodes. Given the size of this TN, it is likely that many clinicians would have chosen to perform an FNB for the TN even if they used ACR TI-RADS system in their clinical practice. When the performance of each TN classification method was revised after removing this nodule, the CQP(i) produced an ROC AUC performance of 0.929 +/- 0.053 [95% CI 0.825-1.000] compared to the performance of ACR TI-RADS of 0.854 +/- 0.095 [95% CI 0.668-1.000] and the performance of ATA risk stratification system of 0.729 +/- 0.149 [95% CI 0.406-1.000].

(B) Performance of CQP(h) compared to gray-scale US:

The optimal linear combination of QUS parameters (acoustic concentration, intercept, midband fit, Nakagami shape parameter, spectral slope) for hypoechoic TNs – CQP(h) was determined [0.062268 x Avg_AcousticConcentration - 0.62066 x Std_Intercept - 0.41233 x Std_MidbandFit - 10.5011 x NStd_NakShapeParam + 0.092736 x NStd_SpectralSlope]. CQP (h) performed with an ROC AUC of 0.822 +/0.051 [95% CI 7.22-0.921], compared to 0.810 +/- 0.049 [95% CI 0.714 – 0.907, p >0.05] for ACR TI-RADS and 0.822 +/- 0.049 [95% CI 0.729 – 0.918, p >0.05] for ATA risk stratification system [Table 2]. When CQP(h) threshold of -3.079 to perform an FNB in hypoechoic TNs was chosen, 24 of 86 (21.6%) TNs could be excluded from FNB without missing any malignant TNs. ACR TI-RADS would avoid a FNB in 20 (18%) TNs, and miss one malignant TN (a 1.4 cm hypoechoic TN that was found on surgical pathology to be a follicular variant papillary thyroid cancer without lymphovascular invasion, extrathyroidal extension or metastatic lymph nodes). With the ATA risk stratification system, FNB was avoided in 2 TNs with no missed malignant TNs.

When comparing the TNs for which FNB was not recommended, between the CQP(h) and ACR TI-RADS there was an overlap of 8 TNs in this category. There were 16 TN for which FNB was not recommended per CQP(h) that met criteria for FNB per ACR TI-RADS and there were 11 TNs for which FNB was not recommended per ACR TI-RADS that met criteria per the CQP (h) threshold.

(C) Performance of CQP(i) and CQP(h) compared to a common classifier - CQP(c):

The performance of an optimal linear classifier trained on TNs irrespective of echogenicity, CQP(c) [7.086 x Avg_NakShapeParam – 0.8791x Avg_SpectralSlope + 0.1900 x Avg_AcousticConcentration – 0.6343 x Std_Intercept + 0.1049 x Std_SpectralSlope] was compared to the echogenicity specific classifiers CQP(i) and CQP(h) [Table 3]. Using a biopsy threshold of 6.638, the number of TNs excluded from FNB without missing any cancer was 91 (33.2%) when CQP(c) was applied to all TN. Specifically, for isoechoic TNs, 74 (45.4%) FNBs could be avoided which is fewer compared to when CQP(i) was used.

TABLE 1 TN characteristics and categorization.

	Isoechoic TN	Hypoechoic TN
No. of nodules	163	111
Average maximal diameter (cm)	2.8 [range 1 - 7]	2.2 [range 0.9 – 7.5]
Final Classification		
Benign, n	158 (96.9%)	86 (77.5%)
Cancer, n	5 (3.1%)	25 (22.5%)
- cPTC	3 (60%)	15 (60%)
- fvPTC	2 (40%)	3 (12%)
- FTC	0	2 (8%)
- Anaplastic thyroid cancer	0	1 (4%)
- Bethesda VI cytology	0	3 (12%)
- Cytology of cervical nodule positive for thyroid malignancy	0	1 (4%)

TN, thyroid nodule; cPTC, classic papillary thyroid cancer; fvPTC, follicular variant papillary thyroid cancer; FTC, follicular thyroid cancer.

TABLE 2 Comparison of results of individual QUS-based classifiers for isoechoic and hypoechoic TNs compared to ACR TI-RADS and ATA risk stratification system.

	Isoechoic TN (163)			Hypoechoic TN (111)		
	AUC	FNB reduction	Missed cancers, n	AUC	FNB reduction	Missed cancers, n
QUS-based classifier	0.937*	73% (119/163)	0	0.822**	21.6% (24/111)	0
ACR TI-RADS	0.717	55.8% (91/163)	1	0.810	18% (20/111)	1
ATA system	0.589	11.7% (19/163)	0	0.820	1.8% (2/111)	0

TN, thyroid nodule; *based on CQP(i); **based on CQP(h).

When CQP(c) was applied for hypoechoic TNs, 17 (15.3%) FNBs could be avoided.

Discussion

TNs are made up of a heterogeneous group of histology that includes benign hyperplasia and adenomas, differentiated (papillary and follicular), poorly differentiated, anaplastic and medullary thyroid cancer, thyroid lymphoma and metastatic disease to the thyroid gland (15). All of these subtypes vary in their histological appearance. For example, classic papillary thyroid cancer is characterized by papillary arrangements with a vascular core and psammoma calcification while in follicular thyroid cancer sheets of follicular cells with reduced amounts of colloid are seen with hallmark vascular or capsular invasion. Certain gray-scale US features, such as echogenicity, reflect these differences in the TN architecture. However, while these are more effective in identifying classic papillary thyroid cancers that are hypoechoic and have punctate echogenic foci, it is less the case for the other subtypes.

It is also important to note that we are shifting from an emphasis on TN US to diagnose cancer to a recognition that the management of TNs should also prioritize avoiding unnecessary invasive procedures. Up to 90 to 95% of TNs are benign (16, 17). The incurred cost from FNB, molecular testing and surgery for benign TN is exorbitant (18, 19). In addition, it adds to patient and provider anxiety and increases the risk for post-surgical complications including nerve injury and hypocalcemia. These complications can be reduced, however not eliminated, through various measures such as undergoing surgery by a high-volume thyroid surgeon and use of neuromonitoring devices during surgery.

Creating a separate QUS-based linear classifier for isoechoic and hypoechoic TNs demonstrated improved TN risk stratification, specifically for isoechoic TNs, compared to applying a single classifier for all TNs. The ROC AUC performance of CQP(i) was greater than that of ACR TI-RADS and ATA classification system, but not statistically significantly in the setting of inadequate TN numbers. However, CQP(i) reduces unnecessary FNBs by 73% in isoechoic TNs compared to 55.8% by ACR TI-RADS. Figure 1 demonstrates two TNs that were both classified as isoechoic. One TN was isoechoic, solid and taller-than-wide and biopsied based on the TI-RADS classification system because the size was >1.5 cm, but was benign by cytology. The second TN was isoechoic and partially cystic and would not have been biopsied based on the TI-RADS classification system. It was found to be a follicular variant of papillary thyroid cancer. These two nodules have very different QUS-based CQP(i) values that would not have recommended a biopsy of the benign isoechoic, solid nodule but would have biopsied the partially cystic isoechoic papillary thyroid cancer. In addition, CQP(i) and CQP(h) together can reduce unnecessary FNB by 52.2% in all TNs without missing a malignant TN. This is improved compared to the reduction in unnecessary FNBs when a single QUS-based classifier is applied to all TNs (45.4%). The relevance of these findings is further highlighted by the fact that 60% of the TNs in the study were isoechoic and 97% of the isoechoic TNs were benign. Of note, while a majority of classic papillary thyroid cancers were hypoechoic, 17% in the study were classified as isoechoic. Follicular thyroid cancers, which are often isoechoic, in the current study were categorized as hypoechoic.

The data demonstrated differences in how the QUS-based classifier and gray-scale US categorized TNs. 43.7% of TNs that did not meet criteria for FNB by the CQP(i) classifier, were recommended for FNB by ACR TI-RADS. 25.3% TNs that did

TABLE 3 Comparison of performance of CQP(c), CQP(i) and CQP(h) in isoechoic and hypoechoic TNs.

FNB criteria	CQP(c)	CQP(c)		CQP(i)	CQP(h)
TN category	All TNs	Isoechoic TNs	Hypoechoic TNs	Isoechoic TNs	Hypoechoic TNs
N	274	163	111	163	111
True Negative, n	91 (33.2%)	74 (45.4%)	17 (15.3%)	119 (73%)	24 (21.6%)
False Positive, n	153 (55.8%)	84 (51.5%)	69 (62.2%)	39 (23.9%)	62 (55.9%)
True positive, n	30 (10.9%)	5 (3.1%)	25 (22.5%)	5 (3.1%)	25 (22.5%)

TN, thyroid nodule.

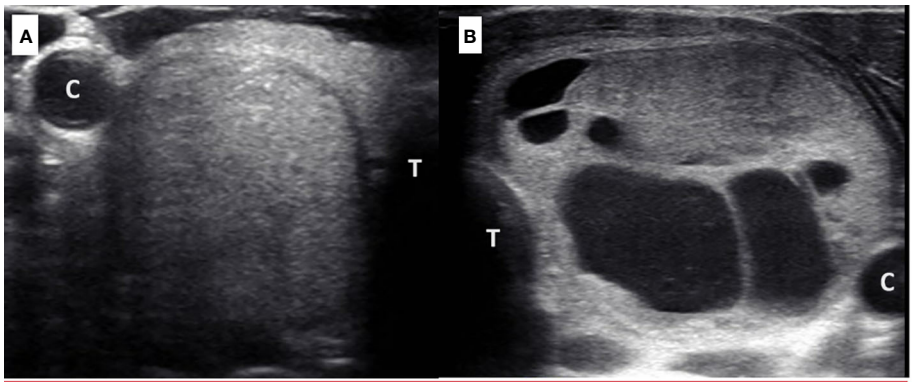

FIGURE 1
TNs **(A, B)** described with gray-scale US as isoechoic. Nodule **(A)** (right mid 2.6 cm isoechoic TN with well-defined margins, taller-than-wide configuration and no microcalcification; biopsy recommended for TI-RADS 4 if size greater than 1.5 cm) was benign by cytology. TN A had a CQP(i) value of -55.878 (biopsy is not recommended). Nodule **(B)** (left 5.1 cm isoechoic, mixed solid cystic TN with well-defined margins and no microcalcification; biopsy not recommended for TI-RADS 2) was malignant (follicular variant of papillary thyroid cancer) by pathology. TN B had a CQP(i) value of -64.560 measured in the solid region of the nodule (biopsy is recommended). [C, carotid artery; T, trachea].

not meet criteria for FNB by ACR TI-RADS were recommended for FNB by the QUS-based classifier. This suggests that the two risk stratification systems are likely assessing different attributes of the TNs and may have a synergistic effect when combined to reduce unnecessary FNBs in TNs. For instance, if one considers combining the CQP(i) and ACR-TI-RADS in the simplest way: a TN is recommended to undergo FNB only if both recommend it, then 142/163 (87%) TNs would have not been recommended for FNB (this includes one malignant TN for which ACR TI-RADS recommend deferring FNB). This demonstrates the tremendous clinical value of combining the microstructural information provided by QUS parameters with the gray-scale US features assessed by an expert ultrasonographer.

Interestingly, the performance of CQP(h), ACR TI-RADS and ATA risk stratification system for hypoechoic TNs was similar. Published literature has demonstrated the ROC AUC performance of gray-scale US in various practice settings ranges from 0.76 to 0.88 (20–23). QUS is not prone to the operator and machine variability seen with gray-scale US, and it can potentially be a useful tool to improve the performance of a less experienced ultrasonographer assessing TNs.

Similar to our prior study, we did not include TNs with a final surgical pathology of NIFTPs due to the low numbers in this preliminary data set. Our institution historically has a low prevalence of NIFTP, which represents 2.3% of all papillary neoplasia (24). In addition, the prevalence of malignancy in isoechoic TNs is low which limits the interpretation of results in our current study. These two concerns can be better addressed in future studies with larger number of subjects. TNs with significant macrocalcification or cystic areas anterior to region of interest in the TN were also excluded because these structures prevent or change the propagation of US RF signal preventing QUS analysis. The authors recognize while TNs were separated into iso- and hypoechoic, these groups are still heterogeneous in their pathology. While echogenicity was chosen in this study to categorize TNs, in future studies the use of other gray-scale US features in combination with QUS should be explored. Secondly, hypoechoic echogenicity can be further categorized as mildly hypoechoic and very or markedly hypoechoic, the latter associated with a higher risk for malignancy (25–27). This needs to be taken into consideration when planning future studies. In this preliminary analysis, the categorization of TNs based on the echogenicity was done manually by the investigators. There can be inter-observer and machine variability. In the future, exploring an objective method for determining echogenicity using either QUS or other techniques should be considered.

For many years we have adhered to a tradition of treating all TNs the same while imaging. Our study is an attempt to apply an algorithmic approach to TN imaging. Our preliminary results are promising and builds compelling case to explore TN imaging keeping heterogeneity in TN histology in mind.

Data availability statement

The raw data supporting the conclusions of this article will be made available by the authors, without undue reservation.

Ethics statement

The studies involving humans were approved by Boston Medical Center and Boston University Medical Campus. The studies were conducted in accordance with the local legislation and institutional requirements. The participants provided their written informed consent to participate in this study.

Author contributions

PG: Formal analysis, Methodology, Writing – original draft, Writing – review & editing. TL: Formal analysis, Methodology, Writing – review & editing. AM: Formal analysis, Writing – review & editing. JM: Formal analysis, Methodology, Writing – review & editing. SL: Formal analysis, Methodology, Writing – review & editing, Writing – original draft.

Funding

The author(s) declare financial support was received for the research, authorship, and/or publication of this article. The work was supported by the National Institutes of Health grant R21 CA212744 awarded to the Boston Medical Center, SL, Principal Investigator.

Conflict of interest

The authors declare that the research was conducted in the absence of any commercial or financial relationships that could be construed as a potential conflict of interest.

Publisher's note

References

1. Haugen BR, Alexander EK, Bible KC, Doherty GM, Mandel SJ, Nikiforov YE, et al. 2015 American thyroid association management guidelines for adult patients with thyroid nodules and differentiated thyroid cancer: the American thyroid association guidelines task force on thyroid nodules and differentiated thyroid cancer. *Thyroid* (2016) 26(1):1–133. doi: 10.1089/thy.2015.0020

2. Tessler FN, Middleton WD, Grant EG, Hoang JK, Berland LL, Teefey SA, et al. ACR thyroid imaging, reporting and data system (TI-RADS): white paper of the ACR TI-RADS committee. *J Am Coll Radiol* (2017) 14(5):587–95. doi: 10.1016/j.jacr.2017.01.046

3. Molina-Vega M, Rodríguez-Pérez CA, Álvarez-Mancha AI, Baena-Nieto G, Riestra M, Alcázar V, et al. Clinical and ultrasound thyroid nodule characteristics and their association with cytological and histopathological outcomes: A retrospective multicenter study in high-resolution thyroid nodule clinics. *J Clin Med* (2019) 8 (12):2172. doi: 10.3390/jcm8122172

4. Jeh SK, Jung SL, Kim BS, Lee YS. Evaluating the degree of conformity of papillary carcinoma and follicular carcinoma to the reported ultrasonographic findings of Malignant thyroid tumor. *Korean J Radiol* (2007) 8(3):192–7. doi: 10.3348/kjr.2007.8.3.192

5. Kim DS, Kim JH, Na DG, Park SH, Kim E, Chang KH, et al. Sonographic features of follicular variant papillary thyroid carcinomas in comparison with conventional papillary thyroid carcinomas. *J Ultrasound Med* (2009) 28(12):1685–92. doi: 10.7863/jum.2009.28.12.1685

6. Pereira M, Williams VL, Hallanger Johnson J, Valderrabano P. Thyroid cancer incidence trends in the United States: association with changes in professional guideline recommendations. *Thyroid* (2020) 30(8):1132–40. doi: 10.1089/thy.2019.0415

7. Feleppa EJ, Mamou J, Porter CR, Machi J. Quantitative ultrasound in cancer imaging. *Semin Oncol* (2011) 38(1):136–50. doi: 10.1053/j.seminoncol.2010.11.006

8. Oelze ML, Mamou J. Review of quantitative ultrasound: envelope statistics and backscatter coefficient imaging and contributions to diagnostic ultrasound. *IEEE Trans Ultrason Ferroelectr Freq Control* (2016) 63(2):336–51. doi: 10.1109/TUFFC.2015.2513958

9. Oelze ML, Zachary JF, O'Brien WD Jr. Characterization of tissue microstructure using ultrasonic backscatter: theory and technique for optimization using a Gaussian form factor. *J Acoust Soc Am* (2002) 112(3 Pt 1):1202–11. doi: 10.1121/1.1501278

10. Lizzi FL, Greenebaum M, Feleppa EJ, Elbaum M, Coleman DJ. Theoretical framework for spectrum analysis in ultrasonic tissue characterization. *J Acoust Soc Am* (1983) 73(4):1366–73. doi: 10.1121/1.389241

11. Feleppa EJ, Lizzi FL, Coleman DJ, Yaremko MM. Diagnostic spectrum analysis in ophthalmology: a physical perspective. *Ultrasound Med Biol* (1986) 12(8):623–31. doi: 10.1016/0301-5629(86)90183-3

12. Goundan PN, Mamou J, Rohrbach D, Smith J, Patel H, Wallace KD, et al. A preliminary study of quantitative ultrasound for cancer-risk assessment of thyroid nodules. *Front Endocrinol (Lausanne)* (2021) 12:627698. doi: 10.3389/fendo.2021.627698

13. Yao LX, Zagzebski JA, Madsen EL. Backscatter coefficient measurements using a reference phantom to extract depth-dependent instrumentation factors. *Ultrason Imaging* (1990) 12(1):58–70. doi: 10.1177/016173469001200105

14. Mamou J, Coron A, Oelze ML, Saegusa-Beecroft E, Hata M, Lee P, et al. Three-dimensional high-frequency backscatter and envelope quantification of cancerous human lymph nodes. *Ultrasound Med Biol* (2011) 37(3):345–57. doi: 10.1016/j.ultrasmedbio.2010.11.020

15. WHO. *Classification of Tumours of Endocrine Organs. 4th ed Vol. 10.* Lyon, France: WHO/IARC Press (2017).

16. Brander A, Viikinkoski P, Nickels J, Kivisaari L. Thyroid gland: US screening in a random adult population. *Radiol* (1991) 181(3):683–7. doi: 10.1148/radiology.181.3.1947082

17. Werk EE Jr, Vernon BM, Gonzalez JJ, Ungaro PC, McCoy RC. Cancer in thyroid nodules. A community hospital survey. *Arch Intern Med* (1984) 144(3):474–6. doi: 10.1001/archinte.1984.00350150058018

18. Wu JX, Lam R, Levin M, Rao J, Sullivan PS, Yeh MW. Effect of Malignancy rates on cost-effectiveness of routine gene expression classifier testing for indeterminate thyroid nodules. *Surgery* (2016) 159(1):118–26. doi: 10.1016/j.surg.2015.05.035

19. Nishino M, Nikiforova M. Update on molecular testing for cytologically indeterminate thyroid nodules. *Arch Pathol Lab Med* (2018) 142(4):446–57. doi: 10.5858/arpa.2017-0174-RA

20. Ahmadi S, Oyekunle T, Jiang X, Scheri R, Perkins J, Stang M, et al. A direct comparison of the ATA and RI-RADS ultrasound scoring systems. *Endocr Pract* (2019) 25(5):413–22. doi: 10.4158/EP-2018-0369

21. Jin ZQ, Yu HZ, Mo CJ, Su RQ. Clinical study of the prediction of Malignancy in thyroid nodules: modified score versus 2017 American college of radiology's thyroid imaging reporting and data system ultrasound lexicon. *Ultrasound Med Biol* (2019) 45 (7):1627–37. doi: 10.1016/j.ultrasmedbio.2019.03.014

22. Lim-Dunham JE, Toslak IE, Reiter MP, Martin B. Assessment of the American college of radiology thyroid imaging reporting and data system for thyroid nodule Malignancy risk stratification in a pediatric population. *AJR Am J Roentgenol* (2019) 212(1):188–94. doi: 10.2214/AJR.18.20099

23. Shen Y, Liu M, He J, Wu S, Chen M, Wan Y, et al. Comparison of different risk-stratification systems for the diagnosis of benign and Malignant thyroid nodules. *Front Oncol* (2019) 9:378. doi: 10.3389/fonc.2019.00378

24. Chung R, Guan H, Ponchiardi C, Cerda S, Marwaha N, Yilmaz OH, et al. Noninvasive follicular thyroid neoplasm with papillary-like nuclear features: epidemiology and long-term outcomes in a strictly defined cohort. *Thyroid* (2021) 31(1):68–75. doi: 10.1089/thy.2019.0616

25. Lee JY, Lee CY, Hwang I, You SH, Park SW, Lee B, et al. Malignancy risk stratification of thyroid nodules according to echotexture and degree of hypoechogenicity: a retrospective multicenter validation study. *Sci Rep* (2022) 12 (1):16587. doi: 10.1038/s41598-022-21204-5

26. Kim EK, Park CS, Chung WY, Oh KK, Kim DI, Lee JT, et al. New sonographic criteria for recommending fine-needle aspiration biopsy of nonpalpable solid nodules of the thyroid. *AJR Am J Roentgenol* (2002) 178(3):687–91. doi: 10.2214/ajr.178.3.1780687

27. Moon WJ, Jung SL, Lee JH, Na DG, Baek JH, Lee YH, et al. Thyroid Study Group, Korean Society of Neuro- and Head and Neck Radiology. Benign and Malignant thyroid nodules: US differentiation–multicenter retrospective study. *Radiol* (2008) 247(3):762–70. doi: 10.1148/radiol.2473070944

frontiers | Frontiers in Endocrinology

TYPE Review
PUBLISHED 02 April 2024
DOI 10.3389/fendo.2024.1355383

OPEN ACCESS

EDITED BY
Pia Pace-Asciak,
University of Toronto, Canada

REVIEWED BY
Hongwei Cheng,
University of Macau, China
Tzu-Yen Huang,
Kaohsiung Medical University, Taiwan

*CORRESPONDENCE
Chelsey K. Baldwin
cbaldwin@mfa.gwu.edu

RECEIVED 13 December 2023
ACCEPTED 18 March 2024
PUBLISHED 02 April 2024

CITATION
Ferraro T, Sajid S, Hodak SP and Baldwin CK (2024) Thyroid nodule rupture after radiofrequency ablation: case report and literature review.
Front. Endocrinol. 15:1355383.
doi: 10.3389/fendo.2024.1355383

Thyroid nodule rupture after radiofrequency ablation: case report and literature review

Tatiana Ferraro[1,2], Sameeha Sajid[2], Steven P. Hodak[3] and Chelsey K. Baldwin[3]*

[1]Division of Otolaryngology-Head and Neck Surgery, The George Washington University School of Medicine and Health Sciences, Washington, DC, United States, [2]Department of Endocrinology, The George Washington University School of Medicine & Health Sciences, Washington, DC, United States, [3]Department of Medicine, Diabetes and Endocrinology Section, New York University School of Medicine, New York, NY, United States

Purpose: Radiofrequency ablation (RFA) is an effective and safe modality for the treatment of thyroid nodules. Nodule rupture is a major complication of RFA. There is little known on the natural history of nodule rupture due to a lack of clinical experience and no consensus on its management. A comprehensive review of nodule rupture presentation, diagnosis, and management is needed.

Methods: We report a case of nodule rupture and conduct a literature review. A total of 33 patients experiencing nodule rupture after RFA were included, and their clinical presentation, management, and outcomes were collected and analyzed.

Results: Nodule rupture presents with acute swelling (90.3%) and pain (77.4%) within 7 months of RFA procedure, most commonly due to disruption of the anterior thyroid capsule (87%), and can be diagnosed with ultrasonography. Most ruptures can be managed conservatively, exemplified by our reported case. There are no reported cases of long-term sequalae.

Conclusion: Nodule rupture is the second most common major complication of RFA. Based on the available evidence, we propose a treatment algorithm for nodule rupture and recommendations for future data collection to address gaps in our understanding of rupture etiology and effective management.

KEYWORDS

radiofrequency ablation, thyroid nodule rupture, minimally invasive techniques, thermal ablation, thyroid nodule

1 Introduction

Radiofrequency ablation (RFA) is a minimally invasive technique that is an effective and safe treatment modality for benign symptomatic thyroid nodules. Average nodule volume reduction of 67.7%–84.8% at 12 months following RFA has been reported (1–4) leading to symptomatic and cosmetic improvement as measured by patient health-related quality of life scores (3). However, RFA is associated with a number of possible adverse events. These include minor complications such as local pressure, pain, vasovagal reaction, cough, hematoma, vomiting, and skin burns, and major complications such as both transient and permanent voice changes, hypo/hyperthyroidism, nerve plexus injury, and nodule rupture (5).

Following voice injury, nodule rupture is the second most common major complication associated with RFA occurring in 0.2%–2.5% of cases (1, 3). Nodule rupture usually requires a significant escalation of follow-up intensity and sequelae, may range from local discomfort to formation of an abscess with mass effect on the trachea requiring urgent surgical management (3, 6). Nodule rupture is defined by the disruption of the thyroid capsule with extravasation of nodule contents into the extra thyroidal space (5). The pathophysiology of nodule rupture is unknown. Reported management strategies include conservative measures of pain control and antibiotic therapy, and invasive measures including surgical evacuation and thyroid lobectomy (1, 2, 6). Currently, there is a paucity of data on nodule rupture including consensus on etiology and management despite the increasing number of clinicians performing RFA procedure for thyroid structural disease. In this study, we report our experience with a case of nodule rupture and review the available literature for risk factors, etiology, methods of diagnosis, and management. Finally, we propose a standard of data collection to improve our understanding of this serious complication of RFA.

2 Case report

Informed consent was provided for all clinical information and images associated with this publication.

A 47-year-old man with a history of congenital heart disease presented seeking alternatives to surgical management for a cosmetically bothersome left lobe thyroid nodule associated with compressive symptoms while wearing a buttoned collar. Ultrasound of the thyroid revealed a solid, mildly hypoechoic nodule nearly replacing the left lobe measuring 42 × 23 × 29 mm (14.7 mL) (Figure 1). Fine needle aspiration demonstrated benign cytology. The patient was biochemically euthyroid with a baseline TSH of 1.37 mIU/L (0.4–4.1 mIU/L). The patient opted to undergo radiofrequency ablation. On the day of the procedure, the patient was given 1 mg of Xanax for anxiolytic effect, and 1% lidocaine without epinephrine was infiltrated in the skin at the planned needle entry site and around the anterior thyroid capsule to provide local analgesia. A 7-cm-length, 18-ga, 1-cm active tip, internally cooled radiofrequency (RF) electrode (Well-Point RF Electrode, Taewoong Medical, Seoul Korea) was used via the trans-isthmic approach with moving shot technique. Power was initiated at 35 W, and a maximum power of 60 W was used. The patient tolerated the procedure well with only transient pauses for discomfort. Upon completion, ultrasound imaging confirmed typical hypo- and hyperechoic changes consistent with treatment effect throughout the entire volume of the nodule; there was no evidence of immediate complication, and the patient was discharged 60 min after the completion of the case.

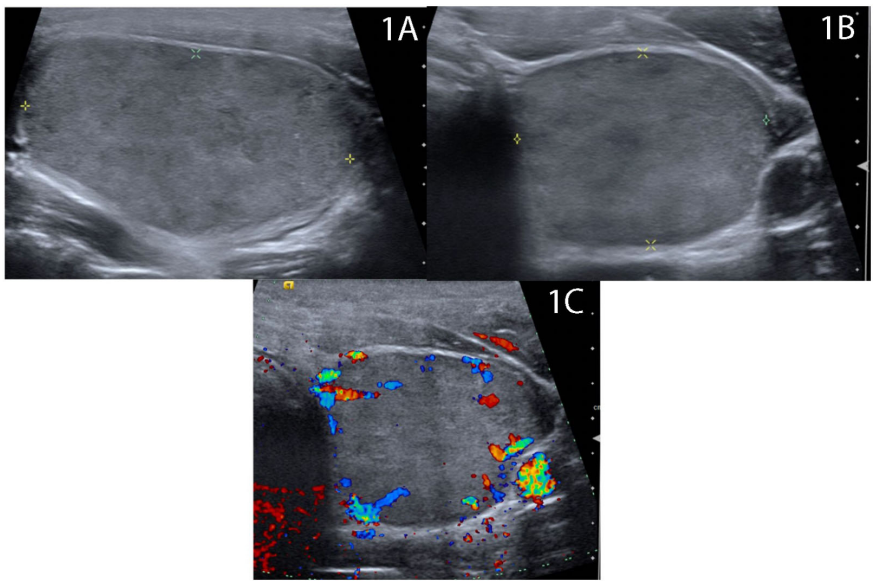

FIGURE 1
Baseline ultrasound demonstrates 4.2 cm solid homogenous, mildly hypoechoic nodule thyroid nodule replacing the majority of the left thyroid lobe in **(A)** longitude and **(B)** transverse views with **(C)** scant peripheral vascularity.

One week post-RFA, the patient reported transient anterior neck discomfort associated with mild erythema for 24 h, which resolved without intervention (Figure 2A). Ultrasound performed within 1 day of complaint demonstrated the continued presence of expected post-treatment changes including a non-distinct anterior border in close proximity to the treatment zone, however, with no evidence of extrathyroidal fluid extravasation (Figure 3A) or evidence of active bleeding (Figure 3B).

At 4 weeks post-RFA, the patient reported mild, recurrent 3/10 anterior neck pain associated with redness and swelling (Figure 2B). The maximum temperature measured at home was 100.0°F. The patient also reported dental work 2 days prior to recurrent pain. The patient presented to a local facility for evaluation, and contrast-enhanced neck CT showed a 3.3 cm × 2.1 cm × 3.5 cm (AP × TR × CC) low-density perithyroidal fluid collection contiguous with the treated thyroid nodule with peripheral enhancement deep to the sternocleidomastoid muscle associated with edema and reticulation of the overlying subcutaneous tissue and skin (Figure 4) consistent with thyroid nodule rupture. Findings were confirmed on subsequent ultrasonography (Figure 5). Because of the recent dental procedure and concern for potential infection, Augmentin 500–200 mg daily for 10 days was initiated and surveillance was continued.

The patient reported resolution of pain after 3 days with persistent prominence of the left neck. Over the course of the next 3 months, the patient reported slow resolution of neck fullness. Progress was monitored with ultrasound imaging over the course of 1 year following RFA (Figure 5) demonstrating progressive resolution of rupture findings. Ultimately, there was a 93% nodule volume reduction from baseline without development of recurrent pain or thyroid hormone dysfunction [TSH of 1.51 mIU/L (0.4–4.1)] at 1 year post-RFA.

3 Literature review

We identified seven studies in the literature that reported a total of 33 cases of nodule rupture after radiofrequency ablation (RFA). Studies predominantly included benign thyroid nodules (BTN) but also included malignant nodules. All cases of nodule rupture occurred in BTN (Table 1). Study inclusion criteria included English Language and report of thyroid nodule rupture. Best judgment was used to eliminant redundant cases used in serial publications.

4 Discussion

4.1 Presentation and diagnosis

Nodule rupture is the second most common major complication of radiofrequency ablation occurring at a frequency of 0.21%–2.5% (1, 3). Nodule rupture is not unique to RFA and has been reported following microwave and laser ablation as well (7, 8).

Nodule rupture after RFA typically presents with acute swelling (90.3%), pain (77.4%), and erythema (16.1%) of the anterior neck (Table 1). Relatively few patients have fever (6.5%), and only one patient reported cough associated with a medial rupture content compressing the trachea (2). Onset of symptoms ranges from 16 to 195 days post-procedure with an average of 48.8 days (Table 1), suggesting that rupture typically presents within the first 2 months following RFA, however should be considered up to 7 months post-procedure (1, 5).

The diagnosis of nodule rupture is confirmed by imaging demonstrating the disruption of the thyroid capsule with nodule contents extravasating into the extrathyroidal space. Extrathyroidal contents most commonly spread within the soft tissue with inflammatory response consistent with phlegmon and less commonly form organized abscess (1). Thyroid ultrasonography is sensitive for the diagnosis of rupture; however, patients presenting to emergency services are more likely to be diagnosed by CT (1). Familiarity with ultrasonographic findings consistent with nodule rupture would obviate the need for unnecessary diagnostic procedures such as CT or aspiration and expedite correct diagnosis (2).

Nodule ruptures can be classified by the location of thyroid capsule disruption: anterior, posterolateral, and medial (Figure 6) (2). Anterior ruptures are characterized by disruption of the anterior thyroid border and extension of nodular contents into the anterior extrathyroidal area, which may invade the strap muscles. Anterior nodule ruptures are the most common classification subtype (2, 6); experts propose that the relative

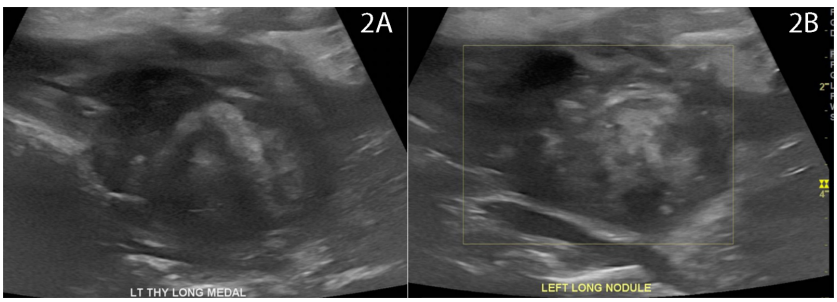

FIGURE 2
Photograph of patient neck at **(A)** 7 days post-RFA at time of initial complaint of transient redness and discomfort with spontaneous recovery and **(B)** at time of recurrent symptoms of pain, swelling, and redness at 1 month post-RFA prompting CT neck demonstrating findings of nodule rupture.

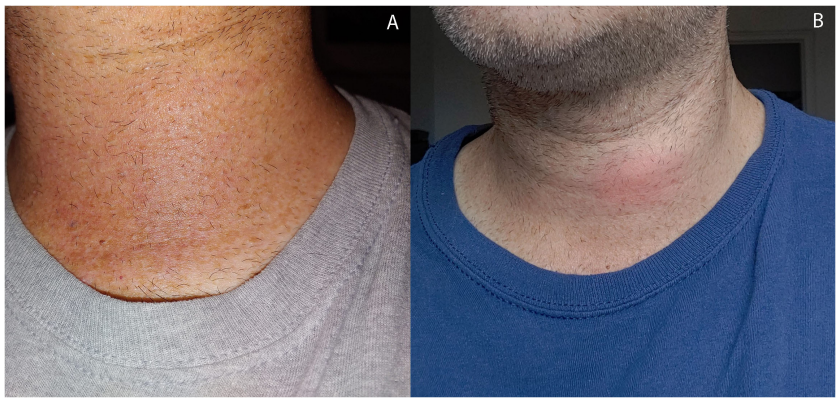

FIGURE 3
Ultrasound 7 days post-RFA with patient reported symptoms of transient erythema and fullness. Ultrasound without extrathyroidal mass but classic artifacts typical of immediate post-RFA including areas of **(A)** hyperechoic and hypoechoic changes with a non-distinct anterior border **(B)** without evidence of active bleeding.

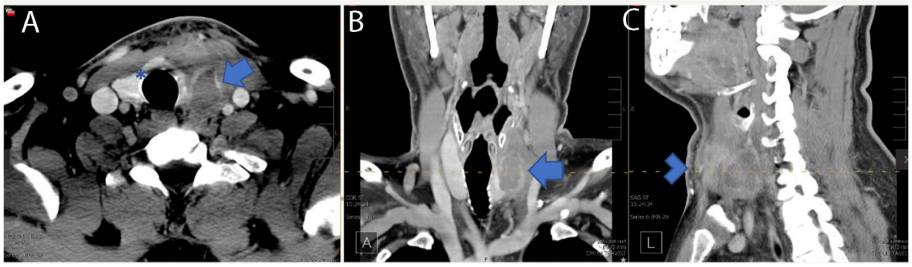

FIGURE 4
Four weeks post-RFA contrasted neck CT demonstrating a 3.3 cm × 2.1 cm × 3.5 cm (AP × TR × CC) low-density perithyroidal fluid collection with peripheral enhancement (arrow) deep to the sternocleidomastoid muscle with disruption of the anterior capsule (Asterix) associated with edema and reticulation of the overlying subcutaneous tissue and skin (arrowhead) consistent with nodule rupture. Features of the nodule rupture are shown in **(A)** transverse, **(B)** coronal, and **(C)** sagittal planes.

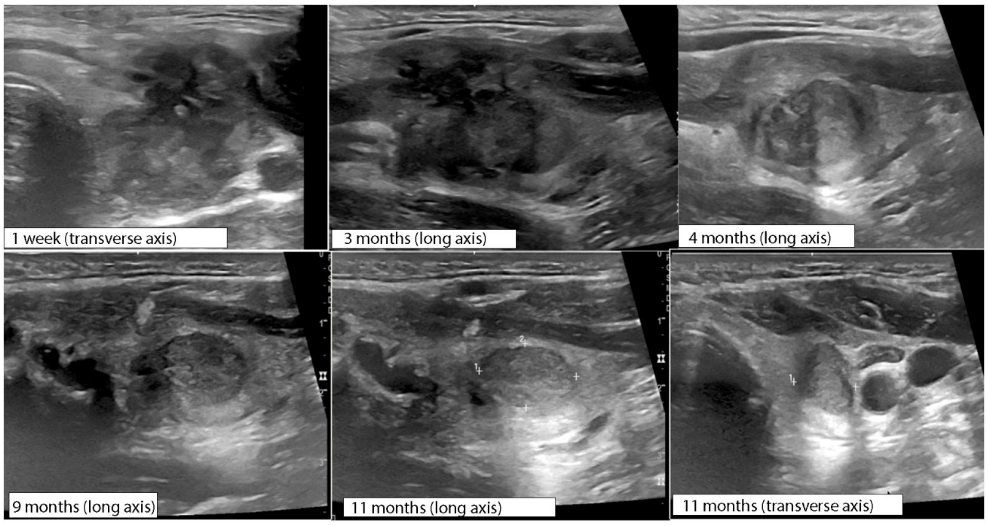

FIGURE 5
Serial ultrasound changes for 1 year following initial RFA procedure measured at time post-rupture, monitoring nodule rupture resolution.

TABLE 1 Characteristics, procedure, management of nodule rupture in eight case reports/series.

Study	Age Mean + range (years)	Gender (% male)	Mean nodule volume (mL)	Rate of rupture/ nodules treated	Mean time to onset of symptoms (days)	RUP (min)	Mean total energy used (kcal)	Mean max power of all RFA sessions (W)	Symptoms	Method of diagnosis	Location of nodule rupture	Peri-rupture complications	Outcome
Baek 2012 & Kim 2017 (N=3)	–	–	37.5 (range, 17.4–71.5)	3/875 = 0.34%	34 days (range, 22–50)	–	–	–	Swelling 100% Pain 100%	US 66% US&CT33%	Anterior 100%	Internal Bleeding 66% Abscess 33%	CR 100%
Shin 2011 (N=6)	43 (28–60) years	33% male	22.5 (range, 2.12–57.47)	6/2616 = 0.2%	38.5 days (range, 9–60)	23.7	–	83.2 W (range, 50–130)	Swelling 100% Pain 100%	US Only 33% CT only 17% US&CT 50%	Anterior 100%	–	CR 100%
Che 2015 (N=1)	–	100% male	–	1/200 = 0.5%	7 days	–	–	–	–	–	–	–	CR 2 weeks
Valcalvi 2015 (N=1)	–	–	–	1/40 = 2.5%	26 days	–	–	–	–	–	–	Fasciitis	CR
Chung 2019 (N=12)	40.6 (16–75) years	25% male	17.18 mL (range, 0.19–75.13)	–	50.5 days (range, 11–156)	12.2	–	57.5 W (range, 30–110)	Sudden Swelling 83.3% Pain 83.3% Cough 8.3% Fever 8.3%	US only 83.3% CT only 8.3% US & CT 8.3%	Anterior 75% Posterolateral 16.7% Medial 8.3%	–	CR ~100% (11/11)*
Chen 2021 (N=9)	38.9 (range, 27–48) yrs	22.2% male	73.9 mL (range 7.7–198)	9/818 = 1.1%	51.4 days (range, 19–195)	29.3 (Std dv 13.5)	16.6 kcal (range, 1.5–33.3)	58.8 W (range, 30–70)	Swelling 88.9% Pain 33.3% Erythema 44.4% Fever 11.1%	CT only 33.3% US only 66.7%	Anterior 88.9% Medial 11.1%	–	CR 100%
Our case study (N=1)	47	100% male	14.67 mL	–	21 days	–	–	60 W	Swelling 100% Pain 100% Erythema 100%	CT & US	Anterior 100%	–	CR
All Studies (N=33)	41.5 (16–75)	36.4% male (12/33)	36.57 mL (0.19–198)	0.44% (20/4,549)	48.8 days (7–195)	20.5 min	16.6 kcal	64.9 W	Swelling 90.3% (28/31) Pain 77.4% (24/31) Erythema 16.1% (5/31) Fever 6.5% (2/31) Cough (1/31) =3.2%	US Only 64.5% (20/31) CT Only 16.1% (5/31) US & CT 19.4% (6/31)	Ant 27/31 = 87.1% posterolateral= 2/31 = 6.5% medial= 2/31 = 6.5%	Superimposed infection (abscess or fasciitis) =6.0% (2/33)	CR 100% (32/32)

Abx, antibiotics; HA, hospital admission; I&D, incision and drainage; SD, surgical debridement; NR, not reported; CR, complete recovery; –, data not reported; RUP, ablation time in minutes; of the RFA session immediately prior to rupture; Mean Max Power= the average obtained for maximum power achieved across all RFA sessions; *Chung 2019 study one patient without report of management technique so eliminated from this chart bring n = 11.

10.3389/fendo.2024.1355383

10.3389/fendo.2024.1355383

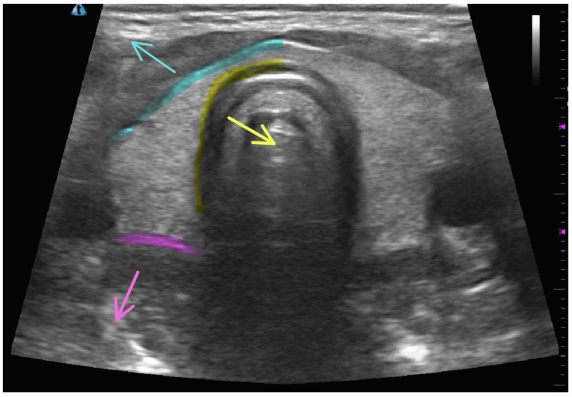

FIGURE 6
Locations of nodule rupture on normal thyroid ultrasonographic imaging with arrows indicating anterior rupture (blue), medial rupture (yellow), and posterolateral rupture (pink).

reduction in pressure exerted on the anterior capsule by the strap muscles compared to the trachea, vasculature, and paraspinal muscles makes the anterior capsule more vulnerable to rupture (6). Nodular contents can result in sinus track formation to the skin, possibly following the artificial track made by the RF needle (Figure 7). Dou et al. hypothesized fistula formation as a consequence of nodule rupture from microwave ablation (MWA) due to necrotic breakdown of the needle tract (7).

Medial nodule ruptures occur due to loss of integrity of the medial aspect of the thyroid capsule with ablated material protruding into the potential space between the thyroid and trachea, potentially leading to mass effect on trachea. One patient with reported medial rupture presented with cough due to tracheal irritation from ruptured nodule contents (2). Posterolateral nodule ruptures occur from disruption of the thyroid capsule posterior to the vascular compartment and occurs at the same frequency (6.5%) as medial ruptures (Table 1).

4.2 Etiology and risk factors

The pathophysiology of nodule rupture is not known; however, several mechanisms have been proposed. Baek et al. described a series of three patients with nodule rupture and proposed acute volume expansion of nodule due to hemorrhage (5). Supporting this theory, Shin et al. in 2011 reported that nodule ruptures

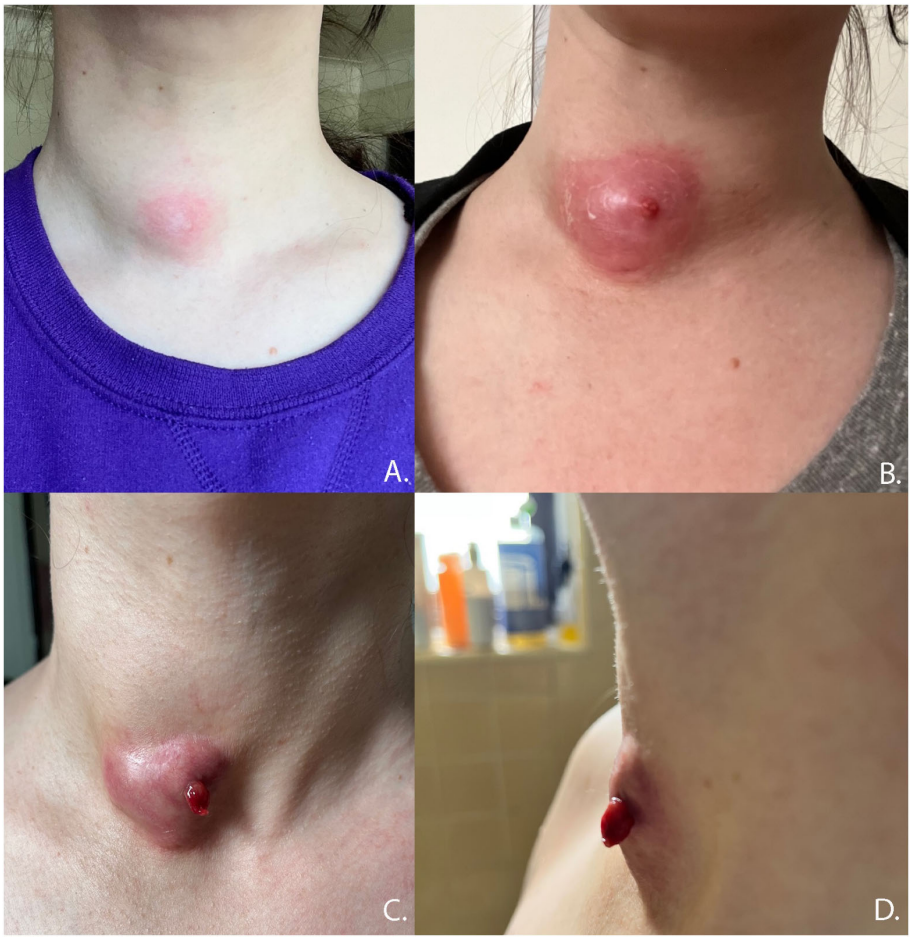

FIGURE 7
Progression of anterior nodule rupture with sinus track development. **(A)** 60 days post-RFA procedure, **(B)** 67 days post RFA, **(C, D)** 82 days post-RFA.

demonstrated hyperechoic areas of high attenuation consistent with intranodular bleeding on CT scan. These authors hypothesized that microvessel leakage within the nodule leads to a delayed volume expansion with subsequent rupture (6).

However, in 2021, Chen et al. reported that aspirated nodule rupture contents consisted of mucus and turbid content without evidence of bleeding most consistent with necrotic fluid collection (1). Dou et al. proposed the concept of symptomatic aseptic necrosis (SAN) in which microwave thermal destruction of nodule vasculature resulted in delayed clearance of necrotic content leading to symptomatic irritation of the nodule capsule and surrounding thyroid tissue, a prodrome of impending rupture (7). We suggest that the currently reported case demonstrated a prodrome consistent with SAN on day 7 post-RFA, with ultimate manifestation in nodule rupture at day 30 post-procedure.

Trauma to the treated nodule is another possible mechanism of nodule rupture (5, 6). Kim et al. reported a case of nodule rupture in a patient who habitually massaged his treated nodule leading to diagnosis of rupture at day 60 post-RFA (9). The patient presented in the current study experienced neck extension during dental procedure, a possible contributing factor to the rupture.

The timing of nodule rupture is not predictive of underlying etiology. Nodules with imaging findings consistent with intranodular bleed presented on days 22, 30, and 60 post-RFA (6). The patient with history of habitual massage of treated nodule presented on day 60 post-RFA. Our patient and the patient reported by Chen et al. both presented with extravasation of poorly absorbed necrotic nodule contents, in a similar time frame of 30 and 21, respectively, demonstrating significant overlap of presentation timing of all suspected etiologies (1).

Clinically relevant risks for nodule rupture after RFA have not been delineated. Dou et al. reported increased risk of rupture in larger nodules and in men after microwave ablation. Initial nodule volume and increasing amount of energy used did not reach significance for nodule rupture risk (7). A systematic review by Chen et al. in 2021 speculates that nodule rupture risk following RFA is associated with greater total energy used, severe tissue edema, and increased volumes of necrotic tissue (1). Expert opinion also postulated higher energy deposition near the affected capsule, trauma from multiple RF needle entry points or repetitive patient swallowing during RFA, overlap of energy deposition at capsule entry of the RF needle, and increasing cystic composition of the treated nodule as risk factors for the development of nodule rupture.

4.3 Management

Reported management ranges from active surveillance to lobectomy with or without use of antibiotics and analgesia (Table 2). Selecting the correct therapy is based on early identification of nodule rupture to prevent unnecessary procedures for diagnosis and management, such as aspiration and empiric antibiotic use (2). Of the currently reported cases, 59.4% were managed with antibiotics, monotherapy, or in combination with additional strategies. However, there are no reported cases of culture-positive rupture fluid collection, suggesting that selective use antibiotics may be the most appropriate management.

Impingement on surrounding structures including tracheal compromise, severe dysphagia, or recurrent laryngeal nerve dysfunction may necessitate invasive management like aspiration, I&D, or lobectomy. Aspiration of necrotic content has also been proposed as a method to reduce patient symptomatology but currently lacks evidence of efficacy. Factors that may predict the need for invasive management after nodule rupture have been proposed and include initial nodule diameter and ablative time. Initial diameter of thyroid nodule >4.5 cm has a reported sensitivity and specificity of 69% and 79%, respectively, for predicting the need for invasive management after rupture (1). Shin et al. found that all patients with nodule rupture with an initial greatest diameter >5 cm required invasive management (6). Chen et al. reports RUP, defined as the ablation duration of the RFA session immediately prior to rupture, >20 min is associated with increased odds of requiring invasive treatment of the management of nodule rupture compared to those that can be conservatively managed (OR 1.11, p=0.025). The authors note this association to be of limited clinical utility as RFA procedures commonly exceed 20 min (1).

4.4 Outcomes

Nodule rupture can be an unsettling complication to providers and patients alike, requiring serial evaluations and patient discomfort and cosmetic defect. However, all current studies suggest that after management, regardless of the treatment method, all patients experience resolution of symptoms without permanent sequalae (1–4, 6, 10). Theoretic concerns for sequalae include the creation of adhesions that complicate subsequent surgical interventions and risk of extrathyroidal extension of subsequently developed thyroid tumors.

The timeline to resolution of nodule rupture clinical symptoms and imaging features is variable and overall underreported. Che et al. reports symptomatic recovery in 2 weeks following rupture with no intervention (4). Baek et al. described spontaneous reabsorption over 3–6 months (5). In the reported case, symptomatic improvement of pain occurred within 3 days with a slow resolution of pressure and cosmetic defect over 4 months,

TABLE 2 Management of nodule rupture after radiofrequency ablation (RFA).

Management Type	% Patients (N=32)
Non-Invasive Management	*56.3% (N=18)*
• Observation (+/– NSAID) Only	31.3% (N=10)
• Antibiotics monotherapy	25.0% (N=8)
• Antibiotics used	59.4% (N=19)
Invasive Management	*43.8% (N=14)*
• Aspiration	9.4% (N=3)
• Incision and Drainage	21.9% (N=7)
• Surgical Debridement	9.4% (N=3)
• Lobectomy	3.1% (N=1)

*Additional treatment modalities include NSAID use, aspiration, I&D, surgical debridement.

correlating with the resolution of ultrasonographic features of rupture (Figure 5).

5 Summary

Thyroid nodule rupture is a major complication following thermal ablation. The available data supports that the majority of nodule rupture patients can be diagnosed with ultrasound and managed conservatively with pain control with serial ultrasounds documenting resolution. Empiric antibiotics in all cases are not necessary and can be reserved for patients with signs of infection or circumstances that increase risk of infectious inoculation, like dental procedures. Patients can be counseled that symptoms of pain resolve before pressure and cosmetic defects over the course of 3–6 months. Fistula formation with cutaneous drainage may occur with anterior nodule rupture. Rare cases will require invasive management such as lobectomy/I&D due to impingement on critical structures of the neck. Improved understanding of nodule rupture and its management is dependent on the accumulation of clinical experience. The adoption of common terminology and collection of proposed data points (Table 3) are necessary to improve our understanding of rupture. The current study is the first, to our knowledge, to summarize the presentation, proposed etiologies, management strategies, and outcomes of thyroid nodule rupture after RFA. Based on the current literature review, we propose a management strategy (Figure 8) to guide clinicians whose patients experience nodule rupture.

TABLE 3 Comprehensive data collection points for future cases of post-RFA thyroid nodule rupture.

Baseline characteristics
Nodule size
Nodule content (% solid component)
Nodule location
Nodule distance from affected capsule
Gender
Age
Procedure data
Thermal modality used
RUP
Number of RF needle punctures
Number of RFA treatments
Total energy deposition from all treatments
Power setting used along anterior capsule
Maximum power
Rupture characteristics
Location of rupture
Anterior
Posterolateral
Medial
History of Trauma or aggravating activity
Symptoms consistent with SAN
Diagnostic imaging technique
Additional methods of diagnosis
Aspiration
Other
Treatment
Antibiotics
Anti-Inflammatory
Analgesia
Aspiration
Cytology
Culture
I&D
Surgical wash out
Lobectomy
Other
Outcomes
Complete resolution without sequalae
Hypothyroidism
Chronic cosmetic deformity
Chronic discomfort/functional limitation
Time to patient reported improvement of symptoms
Time to cosmetic improvement
Time to negative VRR
From rupture diagnosis
From baseline nodule volume
Development of sinus track
Time to resolution
Outcome of culture if performed

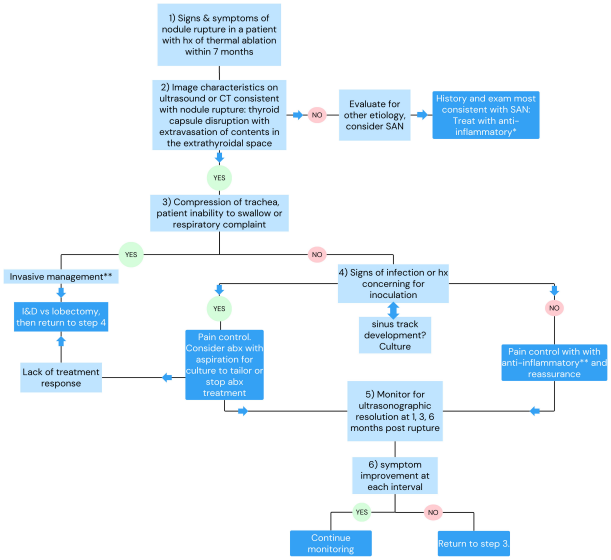

FIGURE 8
Proposed treatment algorithm for nodule rupture post-RFA.

Author contributions

TF: Writing – review & editing, Writing – original draft, Formal analysis, Data curation. SS: Writing – review & editing, Writing – original draft. SH: Writing – review & editing, Writing – original draft. CB: Writing – review & editing, Writing – original draft, Supervision, Methodology, Formal analysis, Data curation, Conceptualization.

Funding

The author(s) declare financial support was received for the research, authorship, and/or publication of this article. For this work, there was no funding utilized for research purposes. The publication fee was covered by our affiliate department, Department of Medicine, Diabetes and Endocrinology Section, New York University.

Acknowledgments

We acknowledge the Department of Medicine, Diabetes and Endocrinology Section, New York University School of Medicine and the Department of Endocrinology at George Washington University for their support in our research endeavors.

Conflict of interest

The authors declare that the research was conducted in the absence of any commercial or financial relationships that could be construed as a potential conflict of interest.

Publisher's note

References

1. Chen WC, Luo SD, Chen WC, Chou CK, Chang YH, Cheng KL, et al. The importance of nodule size in the management of ruptured thyroid nodule after radiofrequency ablation: A retrospective study and literature review. *Front Endocrinol.* (2021) 12:776919. doi: 10.3389/fendo.2021.776919

2. Chung SR, Baek JH, Sung JY, Ryu JH, Jung SL. Revisiting rupture of benign thyroid nodules after radiofrequency ablation: Various types and imaging features. *Endocrinol Metab.* (2019) 34:415. doi: 10.3803/EnM.2019.34.4.415

3. Valcavi R, Tsamatropoulos P. Health-related quality of life after percutaneous radiofrequency ablation of cold, solid, benign thyroid nodules: A 2-year follow-up study in 40 patients. *Endocr Pract.* (2015) 21:887–96. doi: 10.4158/EP15676.OR

4. Che Y, Jin S, Shi C, Wang L, Zhang X, Li Y, et al. Treatment of benign thyroid nodules: comparison of surgery with radiofrequency ablation. *Am J Neuroradiol.* (2015) 36:1321–5. doi: 10.3174/ajnr.A4276

5. Baek JH, Lee JH, Sung JY, Bae JI, Kim KT, Sim J, et al. Complications encountered in the treatment of benign thyroid nodules with US-guided radiofrequency ablation: A multicenter study. *Radiology.* (2012) 262:335–42. doi: 10.1148/radiol.11110416

6. Shin JH, Jung SL, Baek JH, Kim Jh. Rupture of benign thyroid tumors after radiofrequency ablation. *Am J Neuroradiol.* (2011) 32:2165–9. doi: 10.3174/ajnr.A2661

7. Dou Jp, Yu J, Cheng Zg, Liu Fyi, Yu Xl, Hou Qdi, et al. Symptomatic aseptic necrosis of benign thyroid lesions after microwave ablation: risk factors and clinical significance. *Int J Hyperthermia.* (2021) 38:815–22. doi: 10.1080/02656736.2021.1930203

8. Valcavi R, Riganti F, Bertani A, Formisano D, Pacella CM. Percutaneous laser ablation of cold benign thyroid nodules: A 3-year follow-up study in 122 patients. *Thyroid.* (2010) 20:1253–61. doi: 10.1089/thy.2010.0189

9. Kim JH, Baek JH, Lim HK, Ahn HS, Baek SM, Choi YJ, et al. 2017 Thyroid radiofrequency ablation guideline: Korean society of thyroid radiology. *Korean J Radiol.* (2018) 19:632–55. doi: 10.3348/kjr.2018.19.4.632

10. Kim C, Lee JH, Choi YJ, Kim WB, Sung TY, Baek JH. Complications encountered in ultrasonography-guided radiofrequency ablation of benign thyroid nodules and recurrent thyroid cancers. *Eur Radiol.* (2017) 27:3128–37. doi: 10.1007/s00330-016-4690-y

frontiers | Frontiers in Endocrinology

TYPE Clinical Trial
PUBLISHED 15 April 2024
DOI 10.3389/fendo.2024.1327766

OPEN ACCESS

EDITED BY
Pia Pace-Asciak,
University of Toronto, Canada

REVIEWED BY
Barbara Maria Jarzab,
Maria Sklodowska-Curie National Research Institute of Oncology, Poland
David Toro Tobon,
Mayo Clinic, United States

*CORRESPONDENCE
Zhijun Chen
1248414251@qq.com

†These authors share first authorship

RECEIVED 25 October 2023
ACCEPTED 11 March 2024
PUBLISHED 15 April 2024

CITATION
Wan Q, Tan L, Tang X, Wang W, Su Y, Wu Z, Ke M and Chen Z (2024) The clinical value of iodine-125 seed implantation in the treatment of iodine-refractory differentiated thyroid carcinoma.
Front. Endocrinol. 15:1327766.
doi: 10.3389/fendo.2024.1327766

The clinical value of iodine-125 seed implantation in the treatment of iodine-refractory differentiated thyroid carcinoma

Qin Wan[1†], Liling Tan[2†], Xinlan Tang[1], Wenjun Wang[1], Yu Su[1], Zhen Wu[1], Mengmeng Ke[1] and Zhijun Chen[1*]

[1]Department of Nuclear Medicine, Jiangxi Cancer Hospital, Nanchang University, Nanchang, Jiangxi, China, [2]Department of Nuclear Medicine, The Second Affiliated Hospital of Nanchang University, Nanchang University, Nanchang, Jiangxi, China

Objective: To explore the clinical benefits of ^{125}I seed implantation for iodine-refractory differentiated thyroid cancer (RAIR-DTC).

Methods: A retrospective analysis was conducted on 36 patients with RAIR-DTC who underwent radioactive ^{125}I seed implantation from January 2015 to February 2022, involving 73 lesions. Prescription dose: 80~120 Gy. All cases were followed up at 1, 3, and 5 months postoperatively to monitor changes in tumor size, serum thyroglobulin (Tg), and serum anti-thyroglobulin antibody levels in thyrotropin-inhibited states, pain scores, and postoperative adverse reactions. The data were processed and analyzed using IBM SPSS 26.0. LER (Local Effective Rate) and LCR (Local Control Rate) were expressed as n (%), tumor diameter, Tg, and pain scores were represented as Median (Q1, Q3). Pairwise comparisons were conducted using the Wilcoxon signed-rank test, and a p-value of less than 0.05 indicated statistical significance.

Results: Tumor size was significantly reduced after treatment (all $P < 0.001$): tumor length diameters were 32.67 (17.70, 45.72) mm, 27.45 (12.30, 39.98) mm, 20.70 (11.98, 37.58) mm, and 20.39 (10.56, 33.20) mm in the preoperative, 1-, 3-, and 5-months postoperative periods, respectively. Additionally, two consecutive post-treatment results were more minor and statistically significant than the previous results ($P < 0.001$). The LER at 1-, 3-, and 5-months post-surgery was 23.73%, 38.98%, and 52.54%, respectively, while the LCR at the same time points was 98.31%, 96.61%, and 94.92%, respectively. Patients' serum Tg levels decreased significantly after surgery. ($P < 0.001$). Serum Tg levels were measured before surgery and 1-, 3-, and 5-months post-surgery. The results showed that serum Tg levels were 249.45 (79.39, 4718.75) ng/ml, 193.40 (44.53, 2829.00) ng/ml, 192.10 (25.58, 1758.00) ng/ml, and 136.25 (16.57, 1553.25) ng/ml, respectively. Two consecutive post-treatment results were more minor and statistically significant than the previous results ($P < 0.001$). The patients' pain symptoms were significantly relieved after ^{125}I brachytherapy ($P < 0.001$). The pain scores before ^{125}I seed implantation and at 1, 3, and 5 months after the operation were 5.00 (4.00, 6.00), 3.00 (2.25, 4.00), 2.00 (2.00, 3.00), and 2.00 (1.00, 3.00), respectively.

Conclusion: Most lesions treated with ^{125}I seed implantation in RAIR-DTC patients showed shrinkage and improved pain symptoms.

Clinical trial registration: https://www.clinicaltrials.gov, identifier NCT06362772.

KEYWORDS

iodine-refractory differentiated thyroid carcinoma, iodine-125 particles, brachytherapy, iodine radioisotopes, thyroglobulin

1 Introduction

Thyroid cancer (TC) is the most common malignant tumor of the endocrine system, and its incidence is increasing (1). Over 90% of cases are differentiated thyroid cancer (DTC). While the majority of DTC cases have a favorable prognosis, with a 10-year survival rate of 90% (2), a subset of patients experience recurrence or distant metastases even after surgery, ^{131}I therapy, and thyrotropin (TSH) inhibition therapy (3), and progress to radioactive iodine-refractory differentiated thyroid cancer (RAIR-DTC) (4).

Current therapies for RAIR-DTC, including targeted therapy and external beam radiotherapy, have advantages and disadvantages. Although the targeted drugs sorafenib and lenvatinib are approved for treating RAIR-DTC (5), the impact on overall survival is insignificant (6). There are apparent drug resistance and adverse reactions (5), such as hand-foot syndrome, myelosuppression, hypertension, proteinuria, and diarrhea (7), which make it challenging to meet clinical needs. Molecular targeted drugs, such as mitogen-activated protein kinase (MAPK) inhibitors and phosphatidylinositol 3-kinase (PI3K)/AKT inhibitors, have the potential to redifferentiate RAIR-DTC (8). Although the combination of ^{131}I therapy after redifferentiation therapy showed positive effects in RAIR-DTC, long-term follow-up data are lacking. Issues such as population screening, exploration of individualized treatment, and criteria for evaluating therapeutic response remain to be addressed. External beam radiotherapy cannot continuously affect the complete division cycle of the tumor; it damages the surrounding tissue. In addition, TC cells are hypersensitive to external beam radiotherapy (9), limiting local control's effectiveness.

After Whitmore (10) successfully implanted ^{125}I seeds to treat prostate cancer in 1972, ^{125}I seed implantation became increasingly popular after the success of TPS in the 1980s. Over the last three decades, due to its effective local control, minimally invasive nature, low complication rates, and good tolerability, ^{125}I seed implantation has been widely utilized in treating malignant tumors such as prostate and lung cancer (11). This study aims to explore the application of ^{125}I seed implantation in treating bone, lymph node, and lung metastases in RAIR-DTC. Further details are provided below.

2 Materials and methods

2.1 Clinical data

Data from 36 RAIR-DTC patients hospitalized at Jiangxi Cancer Hospital from January 2015 to February 2022 were retrospectively collected. The average age was 57.39 ± 14.76 years, with 14 males and 22 females. A total of 73 lesions were recorded, including four local recurrences and metastases in various parts of the body: 19 in lymph nodes (8 central, three lateral cervical, two supraclavicular, and six mediastinal), 4 in lung (3 in the left lung and 1 in the right lung), 4 in pleura, and 42 in bones (1 in the mandible, 18 in the vertebrae, 4 in the sternum, 6 in the ribs, 2 in the extremities, 11 in the pelvis). Of the bone metastases, 28 had bone destruction and soft tissue formation, while 14 had bone destruction only. The staging of patients is based on the American Joint Committee on Cancer's 8th edition thyroid cancer staging system (12). The Jiangxi Cancer Hospital Ethics Committee approved all treatment plans. In advance of the surgery, patients were informed about their condition, the expected efficacy of ^{125}I seed implantation therapy, alternative treatments such as external beam radiotherapy and chemotherapy, as well as potential side effects and toxic effects. The patient signed an informed consent form after accepting the treatment plan. A total of 1,971 ^{125}I seeds were implanted. The median number of particles injected per lesion was 20 (range 4 to 146) with a median radioactivity of 2.59×10^7 Bq (range 1.85×10^7 to 3.33×10^7 Bq). Table 1 provides detailed baseline data on the patients and foci.

2.1.1 Critical eligibility criteria included

DTC was confirmed by pathology, with local recurrence or distant metastasis of residual thyroid cancer and conforming to any of the following RAIR-DTC criteria: (1) no uptake of ^{131}I in the initial ^{131}I treatment; (2) loss of iodine uptake capacity in previously functional iodine-avid lesions; (3) disease progression after ^{131}I therapy, including gradual enlargement of the lesion and continuously increasing levels of serum thyroglobulin (Tg).

2.1.2 Critical exclusion criteria were as follows

Patients with severe physical diseases, such as severe dysfunction of the cardiac, pulmonary, hepatic, or renal systems, poor compliance, inability to tolerate ^{125}I seed implantation, severe

10.3389/fendo.2024.1327766

TABLE 1 Patient characteristics(n=36).

Characteristics		No	%
Sex			
Male		14	38.89
Female		22	61.11
Age			
≤60		18	50.00
>60		18	50.00
Histopathology			
PTC		24	66.67
FTC		12	33.33
	Cancer Stage		
Age<55Y	I	8	22.22%
	II	6	16.67%
Age≥55Y	I	0	0.00%
	II	2	5.56%
	III	3	8.33%
	IVa	2	5.56%
	IVb	15	41.67%
KPS			
≤80		5	13.89
>80		31	86.11
Previous surgeries			
0		1	2.78
1		16	44.44
2		13	36.11
≥3		6	16.67
Previous radiotherapies			
0		32	88.89
1		1	2.78
2		3	8.33
Previous chemotherapy			
Yes		1	2.78
No		35	97.22
Previous ablation			
Yes		1	2.78
No		35	97.22
Type of lesions			
Local recurrence		4	5.48
Lymph node metastasis		19	26.03
Type of lesions			
Pulmonary metastasis		4	5.48
Bone metastasis		42	57.53
Pleural metastasis		4	5.48
Type of bone metastasis			
Soft tissue formulation		28	66.67
Bone destruction only		14	33.33

PTC, Papillary Thyroid Carcinoma; FTC, Follicular Thyroid Carcinoma; KPS, Karnofsky Performance Scale; Y, years.

acute infectious or chronic infection with acute exacerbation, severe coagulopathy that may lead to serious complications like infection or bleeding, pregnant or lactating women affecting fetal and infant growth and development, patients with cachexia or expected survival of ≤3 months and patients with positive serum anti-thyroglobulin antibodies (TgAb) that may impact the assessment of treatment efficacy.

2.2 Materials

Tianjin Said Biopharmaceutical Co., Ltd. supplies ^{125}I seeds, specifically seed model 6711-99. Physicists verify the quality of seeds by conducting quality control and sampling at least 10% of the seeds (100% if there are fewer than five seeds). They ensure that the seed radioactivity is within a ±5% deviation to meet the required standards for seed quality. Beijing Atomic Hi-Tech Co., Ltd. provided the seed implantation device, and the 18G seed implantation needle was provided by Hakko International Trading (SHANGHAI) Co., Ltd. The CT scan was performed using a SPECT/CT Symbia T2 from Siemens Healthineers, Germany, with a slice thickness of 5 mm, a slice pitch of 2 mm, a current of 48 mA, and a voltage of 130 kV. The KL-SIRPS-3D model from Beijing Astro Technology Ltd. was used as the treatment planning system.

2.3 Method

All patients received ^{125}I brachytherapy treatment and follow-up care at the Department of Nuclear Medicine within Jiangxi Provincial Cancer Hospital. The preoperative evaluation process includes assessments of coagulation function, liver and kidney function, cardiopulmonary function, and local CT scans. A collaborative effort between physicians and physicists was undertaken to establish a treatment regimen with a prescription dose ranging from 80 to 120 Gy. For individuals who have undergone external beam radiotherapy within five months, a dose of 80 Gy is recommended. For individuals with a history of external beam radiotherapy lasting more than five months or those who have

received a cumulative dose of ^{131}I therapy exceeding 2.22*10^{10} Bq, a dose of 100 Gy is recommended. Patients who did not fall into these specific categories were prescribed 120 Gy. There was a difference in the activity level among ^{125}I particles implanted at different locations. The activity level was 1.85 x 10^{7} Bq for near-surface lesions, 3.33 x 10^7 Bq for bone metastases, and 2.22-2.96 x 10^{7} Bq for other metastatic sites. The CT-guided ^{125}I seed implantation procedure was conducted following the prescribed treatment regimen. Subsequent evaluations were scheduled at 1-, 3-, and 5-months post-surgery, focusing on lesion dimensions, serum Tg levels, pain levels, and adverse reactions. Lesion size was determined using CT imaging, with a total of 73 RAIR-DTC metastases from various locations included in the study. Measurements were conducted for 59 metastases, excluding 14 lesions that solely impacted bone tissue without associated soft-tissue hyperplasia. This rendered the assessment of treatment efficacy based on tumor size alterations unfeasible. Lymph nodes were assessed based on their shortest diameter (Figure 1), while other target lesions were evaluated based on their longest diameter (Figure 2). Each measurable lesion underwent an average measurement derived from a minimum of three readings, with all measurements conducted by the same individual to minimize measurement discrepancies.

Response Evaluation Criteria in Solid Tumors (RECIST 1.1) (13) were used to assess treatment response. Local Effective (LE) was defined as a 30% or greater reduction in the longest diameter of the targeted lesion. Progressive Disease (PD) was defined as a 20% or greater increase in the longest diameter of the targeted lesion, while Stable Disease (SD) was defined as being in between. The Local Efficacy Rate (LER) and Local Control Rate (LCR) were calculated by recording the number of lesions classified as LE, SD, and PD at months 1, 3, and 5. (LER = LE/total number of lesions × 100%; LCR = (LE + SD)/total number of lesions × 100%).

Use the Visual Analogue Scale to record patients' pain scores. The scale ranges from 0 to 10 points, with pain increasing incrementally. 0 indicates no pain, 1-3 indicate mild pain that is still tolerable and does not interfere with sleep or normal life, 4-6

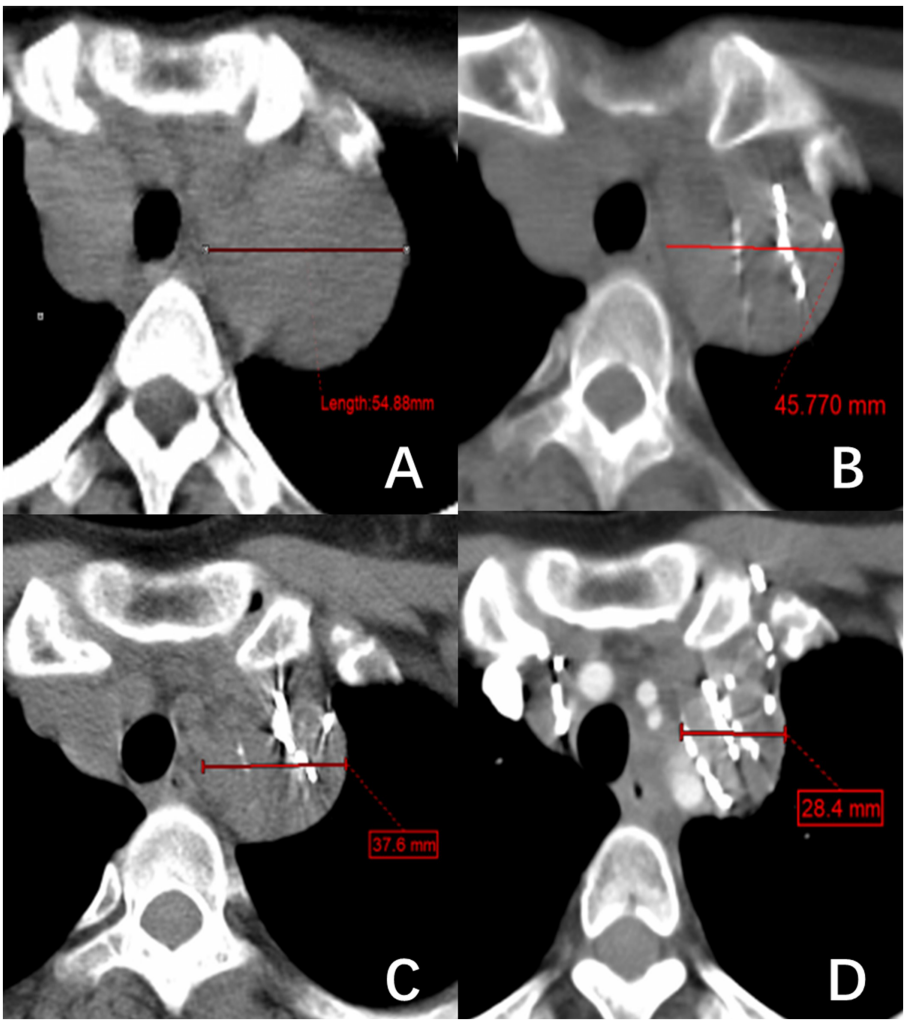

FIGURE 1
A right superior mediastinal lymph node metastasis of thyroid follicular papillary carcinoma. **(A–D)** show the changes in lymph node short diameter before ^{125}I brachytherapy (54.88 mm) and after treatment at one month (45.77 mm), three months (37.6 mm), and five months (28.4 mm), respectively.

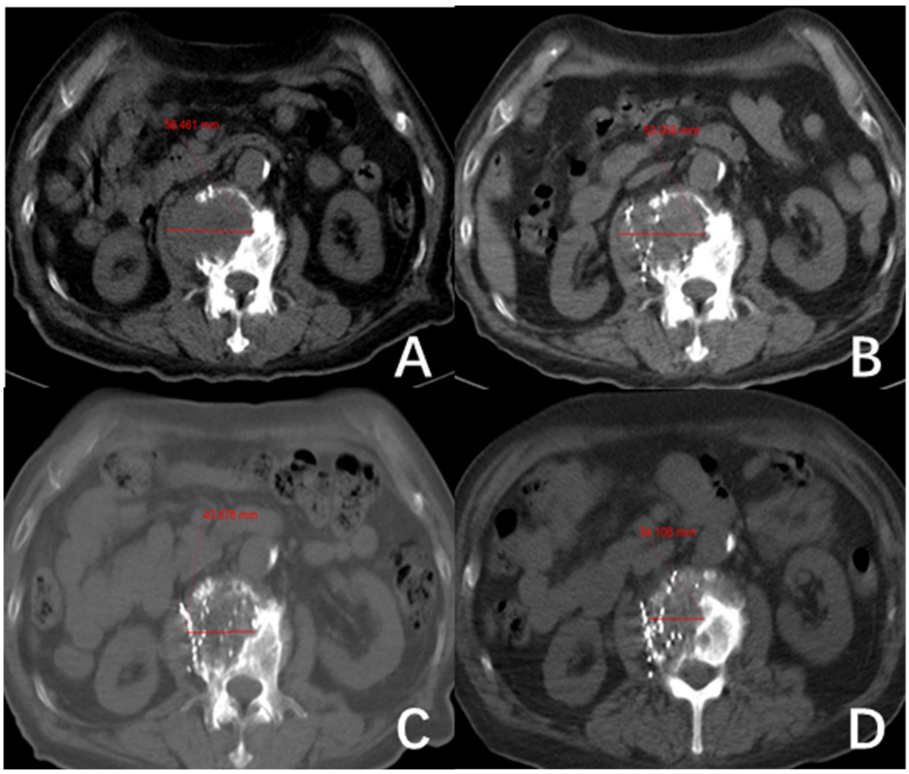

FIGURE 2
The second lumbar vertebra shows metastasis from follicular thyroid carcinoma (FTC). **(A–D)** show the changes in length and diameter of paraspinal soft tissue metastasis before 125I seed implantation (56.46 mm) and after treatment at one month (53.1 mm), three months (40.68 mm) and five months (34.11 mm), respectively.

indicate moderate pain that interferes with sleep and requires analgesic medication to alleviate it, and 7-10 show intense and intolerable pain that seriously interferes with sleep and diet and requires strong analgesic drugs.

Postoperative adverse reactions, including infection, bleeding, pneumothorax, bone marrow suppression, and seed displacement, were recorded. Radiation injury was graded according to the Radiation Therapy Oncology Group (RTOG) and European Organization for Research and Treatment of Cancer (EORTC) toxicity criteria (14).

2.4 Statistical analysis

The data were analyzed using IBM SPSS 26.0. The count data (n %) and skewed measures [Md (Q1, Q3)] are presented. Group comparisons were conducted using the paired Wilcoxon rank-sum test, with statistical significance set at $P < 0.05$.

3 Results

The diameters of the tumor lengths were 27.45 (12.30, 39.98mm), 20.07 (11.98, 37.58mm) and 20.39 (10.56, 33.20mm) at months 1, 3, and 5 after ^{125}I seed implantation, respectively. These values were significantly reduced compared to the initial diameter of 32.67 (17.70, 45.72mm) before treatment (Z= -6.227, -6.272, -6.189; all $P < 0.001$). Two consecutive post-treatment results were more minor and statistically significant than the previous results ($P < 0.001$). At one month postoperatively, there were 14 cases of LE, 44 cases of SD, and 1 case of PD. At three months postoperatively, there were 23 cases of LE, 34 cases of SD, and 2 cases of PD. At five months postoperatively, there were 31 cases of LE, 25 cases of SD, and 3 cases of PD. The LER at 1, 3, and 5 months postoperatively was 23.73% (14/59), 38.98% (23/59), and 52.54% (31/59), respectively. The LCR was 98.31% (58/59) at one month, 96.61% (57/59) at three months, and 94.92% (56/59) at five months postoperatively. The interquartile range includes the data [Md(Q1, Q3)]. Please refer to Table 2 for further details.

The serum Tg levels of 36 patients were measured before and after ^{125}I seed implantation. The levels were measured in the 1st, 3rd, and 5th postoperative months. Specifically, the serum Tg levels were 249.45 (79.39, 4718.75) ng/ml before treatment, 193.40 (44.53, 2829.00) ng/ml in the 1st month, 192.10 (25.58, 1758.00) ng/ml in the 3rd month, and 136.25 (16.57, 1553.25) ng/ml in the 5th month. The results showed that the serum Tg level decreased significantly after treatment (Z = -3.881, -4.587, -4.823, all $P < 0.001$). Furthermore, serum Tg levels had returned to normal or were approaching normal in some patients. Two consecutive post-treatment results were more minor and statistically significant than the previous ones (Z = -3.661, -3.931, and $P < 0.001$). Please refer to Table 3 for further details.

TABLE 2 The efficacy of radioactive ^{125}I seed implantation.

Follow-up time	LE	SD	PD	LER(%)	LCR(%)
One month	14(23.73)	44(74.58)	1(1.69)	23.73	98.31
Three months	23(38.98)	34(57.63)	2(3.39)	38.98	96.61
Five months	31(52.54)	25(42.37)	3(5.08)	52.54	94.92

The number of lesions is expressed as n(%); LE: Local Effective; SD: Stable Disease; PD: Progressive Disease; LER: Local Effective Rate (LER = LE/total number of lesions × 100%); LCR: Local Control Rate (LCR = (LE + SD)/total number of lesions × 100%).

The pain scores of 36 patients were recorded at months 1, 3, and 5 after treatment. The scores were 3.00 (2.25, 4.00), 2.00 (2.00, 3.00), and 2.00 (1.00, 3.00), respectively. These scores were significantly lower than the score of 5.00 (4.00, 6.00) recorded before treatment ($Z = -5.339, -5.330, -5.278$; all $P < 0.001$). Statistically significant differences were observed between month one and month 3 ($Z = -4.914$, $P < 0.001$) and between month three and month 5 ($Z = -4.104$, $P < 0.001$). Please refer to Table 4 for more information on this.

All 36 patients remained infection-free following ^{125}I seed implantation. Two cases of radiation injury were reported: one case of Grade I radiation dermatitis, which gradually improved after treatment with anti-inflammatory drugs, and one case of Grade I radiation pneumonitis, which resolved without specific treatment. Puncture-related complications occurred in two cases. One minor bleeding was controlled by applying local pressure to stop it. In the other case, a small pneumothorax was detected by CT after a few days and resolved spontaneously. Mild myelosuppression was observed in three cases, which was managed with leukocyte-boosting medications and later determined. Five instances of seed displacement were reported, with one involving the left ventricle, one affecting the left upper lung, and three affecting the chest cavity. Radiological toxicity did not occur in these cases, affecting adjacent vital organs. Further details are provided in Table 5.

4 Discussion

The available studies on the clinical benefit of ^{125}I seed implantation for treating RAIR-DTC are limited, and most studies only focus on single types of metastatic cancer, such as lymph nodes or bone metastases (15, 16). This study aims to comprehensively evaluate the clinical improvement of ^{125}I seed implantation for RAIR-DTC across a wide range of metastatic sites, including locally recurrent foci in the thyroid surgical bed, metastatic lymph nodes in the neck and mediastinum, lung metastases, bone metastases, and pleural metastases.

This study included a total of 73 RAIR-DTC metastases from various sites. However, 14 lesions that only destroyed bone without soft tissue hyperplasia were excluded because their efficacy could not be evaluated based on tumor size changes. The LER of the remaining 59 metastases was 23.73%, 38.98%, and 52.54% at postoperative months 1, 3, and 5, respectively. The LCR was 98.31%, 96.61%, and 94.92% at postoperative months 1, 3, and 5, respectively. The study's results align with Chen et al.'s (15) report of a 95% LCR for RAIR-DTC bone metastases in 9 cases. Additionally, the results are superior to Chen et al.'s (16) report of over a 90% shrinkage rate of metastatic lymph nodes in the neck of RAIR-DTC through ultrasound-guided ^{125}I seed implantation. The data show that ^{125}I seed implantation effectively reduces the tumor size and achieves local tumor control (refer to Figures 1, 2). The physical properties of ^{125}I seeds, such as their low energy (27~35 keV) and long half-life (59.5 days), strongly correlate with these results. Due to its low energy and long half-life, the radiation emitted by the ^{125}I seeds implanted in the tumor causes minimal damage to surrounding normal tissues while delivering a lethal dose of radiation to the tumor cells. Liyuan Zhang (17) reports that small doses of radiation can stimulate the immune system to suppress tumor growth. Due to the necessity of considering the tolerated dose of surrounding normal tissues, external beam radiotherapy cannot administer a radical dose to tumors. Furthermore, ^{125}I particles emit rays continuously over an extended period, impacting the entire cycle of tumor cell division for an extended duration. In contrast, conventional external beam radiotherapy involves multiple split irradiations, which make tumor cells in the interphase of division insensitive to the rays. This is the primary reason why ^{125}I seeds can effectively treat cases that have failed conventional external beam radiotherapy, chemotherapy, and ^{131}I therapy. Proton and heavy ion radiotherapy can induce double-strand breaks in the chromosomes of tumor cells (18), resulting in a

TABLE 3 The serum Tg level is associated with radioactive ^{125}I seed implantation.

Follow-up time	Tg(ng/ml)	Z	P
Preoperative	249.45(79.39,4718.75)	–	–
One month	193.40(44.53,2829.00)	-3.881	<0.001*
Three months	192.10(25.58,1758.00)	-4.587	<0.001*
Five months	136.25(16.57,1553.25)	-4.823	<0.001*

*Compared with preoperative.

TABLE 4 Pain score related to radioactive ^{125}I seed implantation.

Follow-up time	Pain score	Z	P
Preoperative	5.00(4.00,6.00)	–	–
One month	3.00(2.25,4.00)	-5.339	<0.001*
Three months	2.00(2.00,3.00)	-5.330	<0.001*
Five months	2.00(1.00,3.00)	-5.278	<0.001*

*Compared with preoperative.

10.3389/fendo.2024.1327766

TABLE 5 Complications related to radioactive ^{125}I seed implantation (n=36).

Complications	No.	%
Infection	0	0.00
Bleeding	1	2.78
Myelosuppression	3	8.33
Seed migration	5	13.89
Pneumothorax	1	2.78
Radiodermatitis	1	2.78
Radiation pneumonitis	1	2.78

loss of their ability to increase. Due to its unique Bragg peak effect, this effect is achieved with minimal damage to surrounding normal tissues. However, proton and heavy ion therapy are costly and require highly qualified personnel. It is mainly used in clinical research and is still being developed for routine tumor treatment.

The study identified three progressive lesions that may have been caused by the presence of poorly differentiated tumor tissue. These cells have a short doubling time, and the initial dose rate of ^{125}I seed is low (approximately 0.07-0.09 Gy/h) (17), which may result in tumor progression before the ^{125}I seed has had a chance to take effect. ^{125}I seeds can treat tumors by slowly releasing radiation and gradually increasing the cumulative dose in the tumor cells. In this study, most RAIR-DTC tumor cells were relatively inactive and slow-growing. Thus, although the LCR at 1 and 3 months postoperatively were low and most lesions showed SD, the treatment's effectiveness became more apparent as the cumulative tumor dose increased, consistent with a progressive increase in LCR and LER over time.

Serum Tg is a crucial indicator of postoperative relapse and metastasis in patients with DTC (19). A decrease in serum Tg levels may indicate the effectiveness of DTC treatment if a patient tests negative for TgAb. The study found that the serum Tg levels of the patients decreased after treatment compared to before treatment (both $P < 0.001$). Additionally, the serum Tg levels of some patients had returned to normal. These findings suggest that ^{125}I seeds can effectively inhibit and kill RAIR-DTC tumor cells.

The progression of RAIR-DTC may cause severe pain and a significant reduction in patients' quality of life, mainly when metastatic lesions occur in the bone and pleura (20). The results of this study indicate that ^{125}I seed implantation can effectively relieve and reduce patient pain, resulting in significantly lower pain scores post-treatment compared to pre-treatment.

While ^{125}I seed implantation is minimally invasive, it is still considered an invasive treatment. Therefore, it may lead to complications related to puncture, such as bleeding, pain, and pneumothorax. As tumor volume and metastases increase, the number and activity of ^{125}I seeds required for implantation also increase, leading to higher radiation exposure and an increased risk of complications. In addition, adverse reactions related to radiation, such as radioactive damage and necrosis, may be experienced (21). Three patients experienced mild bone marrow suppression after ^{125}I seed implantation. Patient 1 had 146 particles implanted with an activity of $2.22*10^7$ Bq in an extensive mediastinal lymph node metastasis. In contrast, patients 2 and 3 had 57 and 88 seeds planted with an activity of $2.59*10^7$ Bq in bone metastases with soft tissue formation, respectively. A small number of adverse events were reported in this study, including pneumothorax, bleeding, radiation pneumonitis, dermatitis, and mild myelosuppression. These issues were resolved through observation or symptom management, indicating the relative safety of ^{125}I brachytherapy.

5 Conclusions

^{125}I seed brachytherapy has demonstrated reasonable local tumor control, effective pain relief, and minimal side effects in RAIR-DTC. However, this study has several limitations compared to similar research efforts. These limitations include a small sample size, the absence of a control group, and insufficient reliability in data analysis. These limitations hinder a comprehensive depiction of the actual scenario in particle therapy. Furthermore, the follow-up period is relatively short, which limits a thorough evaluation of the medium- and long-term effectiveness of ^{125}I brachytherapy (22). This is especially true regarding potential toxic side effects resulting from dose accumulation. The therapy effectiveness evaluation is based solely on changes in tumor dimensions observed through CT

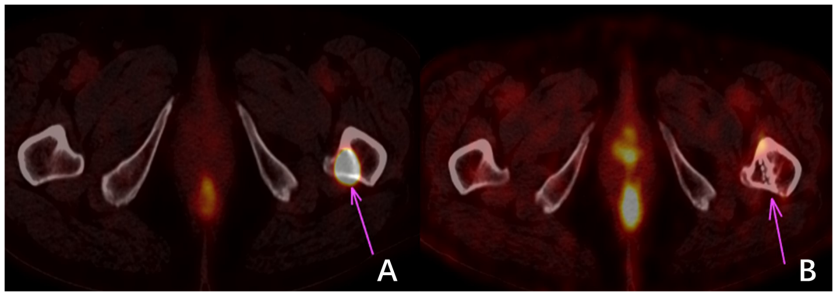

FIGURE 3
^{18}F-FDG imaging of bone metastasis in the left proximal femur of thyroid carcinoma. **(A)** shows a high uptake of 18F-FDG in the metastatic focus before treatment. In contrast, **(B)** shows no significant change in the size of the metastatic focus and bone destruction three months after treatment. However, no 18F-FDG uptake indicates that the tumor cells were inactivated.

scans. However, this approach neglects the consideration of the tumor's functional metabolism at the treatment site post-implantation (refer to Figure 3) or alterations in other tumor sites induced by treatment that may enhance immune responses (23). It is essential to conduct further comprehensive clinical investigations to explore these aspects.

Data availability statement

The raw data supporting the conclusions of this article will be made available by the authors, without undue reservation.

Ethics statement

The studies involving humans were approved by Jiangxi Cancer Hospital Ethics Committee. The studies were conducted in accordance with the local legislation and institutional requirements. The participants provided their written informed consent to participate in this study. Written informed consent was obtained from the individual(s) for the publication of any potentially identifiable images or data included in this article.

Author contributions

QW: Conceptualization, Data curation, Formal analysis, Investigation, Methodology, Software, Writing – original draft. LT: Project administration, Supervision, Validation, Writing – review & editing. XT: Data curation, Investigation, Visualization, Writing – original draft. WW: Funding acquisition, Project administration, Writing – original draft. YS: Investigation, Writing – original draft. ZW: Investigation, Writing – original draft. MK: Investigation, Writing – review & editing. ZC: Funding acquisition, Project administration, Resources, Supervision, Validation, Visualization, Writing – review & editing.

Funding

The author(s) declare that no financial support was received for the research, authorship, and/or publication of this article.

Conflict of interest

The authors declare that the research was conducted in the absence of any commercial or financial relationships that could be construed as a potential conflict of interest.

Publisher's note

All claims expressed in this article are solely those of the authors and do not necessarily represent those of their affiliated organizations, or those of the publisher, the editors and the reviewers. Any product that may be evaluated in this article, or claim that may be made by its manufacturer, is not guaranteed or endorsed by the publisher.

References

1. Chinese Society of Clinical Oncology Guidelines Working Committee. Chinese Society of Clinical Oncology (CSCO) diagnosis and treatment guidelines for differentiated thyroid cancer 2021. *J Cancer Control Treat*. (2021) 34:1164–200. doi: 10.3969/i.issn.1674-0904.2021.12.013

2. Ganly I, Nixon IJ, Wang LY, Palmer FL, Migliacci JC, Aniss A, et al. Survival from differentiated thyroid cancer: what has age got to do with it? *Thyroid*. (2015) 25:1106–14. doi: 10.1089/thy.2015.0104

3. Berdelou A, Lamartina L, Klain M, Leboulleux S, Schlumberger M. Treatment of refractory thyroid cancer. *Endocr Relat Cancer*. (2018) 25:R209–23. doi: 10.1530/ERC-17-0542

4. Chinese Society of Nuclear Medicine. Clinical guidelines for 131I therapy of differentiated thyroid cancer. *Chin J Nucl Med Mol Imaging*. (2021) 41:218–41. doi: 10.3760/cma.j.cn321828-20201113-00412[5

5. Teng LS, Xu ZH, Wang WB. Advances in targeted therapy for refractory differentiated thyroid cancer. *Tumor Prev Treat Res*. (2023) 5:452–7. doi: 10.3971/i.issn.1000-8578.2023.23.0009

6. Tang XW, Shi L, Bu T, Wang F. Current status and latest advances in targeted therapy for refractory thyroid cancer. *J Immunoassay Clin Chem*. (2020) 7:1255–60. doi: 10.11748/bimy.issn.1006 -1703.2020.07.035

7. Hong CM, Ahn BC. Redifferentiation of radioiodine refractory differentiated thyroid cancer for reapplication of I-131 therapy. *Front Endocrinol (Lausanne)*. (2017) 8:260. doi: 10.3389/fendo.2017.00260

8. Laha D, Nilubol N, Boufraqech M. New therapies for advanced thyroid cancer. *Front Endocrinol (Lausanne)*. (2020) 11:82. doi: 10.3389/fendo.2020.00082

9. Huang NS, Wei WJ, Xiang J, Chen JY, Guan Q, Lu ZW, et al. The efficacy and safety of anlotinib in neoadjuvant treatment of locally advanced thyroid cancer: A single-arm phase II clinical trial. *Thyroid*. (2021) 31:1808–13. doi: 10.1089/thy.2021.0307

10. Di X, Zhang H, Liu X, Zhao J, Gao Z, Yu H, et al. A new technique for trans-perirectal iodine-125 seed implantation in prostatic cancer guided by CT and 3D printed template: Two case reports. *Front Oncol*. (2022) 12:1031970. doi: 10.3389/fonc.2022.1031970

11. Li P, Fan J, Zhang K, Wang J, Hu M, Yang S, et al. Interstitial 125I brachytherapy as a salvage treatment for refractory cervical lymph node metastasis of thoracic esophageal squamous cell carcinoma after external irradiation with a CT-guided coplanar template-assisted technique: A retrospective study. *Technol Cancer Res Treat*. (2022) 21. doi: 10.1177/15330338221103102

12. Lamartina L, Grani G, Arvat E, Nervo A, Zatelli MC, Rossi R, et al. 8th edition of the AJCC/TNM staging system of thyroid cancer: what to expect (ITCO#2). *Endocr Relat Cancer*. (2018) 25:L7–L11. doi: 10.1530/ERC-17-0453

13. Watanabe H, Okada M, Kaji Y, Satouchi M, Sato Y, Yamabe Y, et al. [New response evaluation criteria in solid tumours-revised RECIST guideline (version 1.1)]. *Gan To Kagaku Ryoho*. (2009) 36:2495–501. doi: 10.1016/j.ejca.2008.10.026

14. Cox JD, Stetz J, Pajak TF. Toxicity criteria of the radiation therapy oncology group (RTOG) and the european organization for research and treatment of cancer (EORTC). *Int J Radiat Oncol Biol Phys*. (1995) 31:1341–6. doi: 10.1016/0360-3016(95)00060-C

15. Chen Z, Tan L, Su Y, Xie J, Zhou A, Zou W, et al. Clinical application of 125I seed implantation in the treatment of refractory thyroid cancer bone metastasis. *Chin J Nucl Med Mol Imaging*. (2018) 38:14–6. doi: 10.3760/cma.j.issn.2095-2848.2018.01.004

16. Chen W, Luo YK, Zhang Y, Song Q, Tang J. Ultrasound-guided implantation of radioactive 125I seed in radioiodine refractory differentiated thyroid carcinoma. *BMC Cancer*. (2021) 21:834. doi: 10.1186/s12885-021-08500-5

17. Kong Y, Ma Y, Zhao X, Zhang L. Research progress on the sensitization of radiotherapy to the efficacy of PD-1/PD-L1 inhibitors. *Chin J Radiat Oncol*. (2021) 30 (9):984–8. doi: 10.3760/cma.j.cn113030-20201119-00559

18. Hughes JR, Parsons JL. FLASH radiotherapy: current knowledge and future insights using proton-beam therapy. *Int J Mol Sci*. (2020) 21:6492. doi: 10.3390/ijms21186492

19. Yuan MX, Zhao HN, Yu ZW, Zhang J. Clinical significance of monitoring the change in TGAb levels when serum Tg values are disturbed in patients with differentiated thyroid cancer. *Clin Med Prog*. (2022) 6:5236–44. doi: 10.12677/ACM.2022.126758

20. Jiao D, Wu G, Ren J, Han X. Radiofrequency ablation versus 125I-seed brachytherapy for painful metastases involving the bone. *Oncotarget*. (2016) 7:87523–31. doi: 10.18632/oncotarget.11983

21. Li Rf, Wang YD, Yan Y, Yang P, Sha F, Li W, et al. Implantation of 125I seeds for the treatment of non-small cell lung cancer: evaluation of short-term effect. *J interventional Radiol*. (2014) 23(1):65–8. doi: 10.3969/j.issn.1008-794X.2014.01.018

22. Su Y, Wang J, Huang L, Xie L, Yu X, Zha J. Clinical efficacy of iodine-125 (125I) seed implantation in patients with iodine-refractory differentiated thyroid cancer. *Am J Cancer Res*. (2023) 13:4794–802.

23. Wang C, Sun B, Wang H, Shi H. Research progress in the molecular biological mechanism of 125I seed in the treatment of Malignant tumors. *J interventional Radiol*. (2023) 32:1263–8. doi: 10.3969/j.issn.1008-794X.2023.12.020

frontiers | Frontiers in Endocrinology

TYPE Original Research
PUBLISHED 12 June 2024
DOI 10.3389/fendo.2024.1399912

OPEN ACCESS

EDITED BY
Pia Pace-Asciak,
University of Toronto, Canada

REVIEWED BY
Giorgio Radetti,
Ospedale di Bolzano, Italy
Emrah Karatay,
Marmara University Istanbul Pendik Education and Research Hospital, Türkiye

*CORRESPONDENCE
Mario Rotondi
mario.rotondi@icsmaugeri.it

RECEIVED 12 March 2024
ACCEPTED 30 May 2024
PUBLISHED 12 June 2024

CITATION
Chytiris S, Teliti M, Croce L, Coperchini F, Grillini B, Cerutti M, Fonte R, Magri F and Rotondi M (2024) Proficiency in performing radiofrequency ablation procedure for non-functioning benign thyroid nodules: a qualitative rather than quantitative matter. *Front. Endocrinol.* 15:1399912. doi: 10.3389/fendo.2024.1399912

Proficiency in performing radiofrequency ablation procedure for non-functioning benign thyroid nodules: a qualitative rather than quantitative matter

Spyridon Chytiris[1], Marsida Teliti[1,2], Laura Croce[1,2], Francesca Coperchini[2], Beatrice Grillini[2], Matteo Cerutti[2], Rodolfo Fonte[1], Flavia Magri[1,2] and Mario Rotondi[1,2]*

[1]Unit of Endocrinology and Metabolism, Laboratory for Endocrine Disruptors, Istituti Clinici Scientifici Maugeri IRCCS, Pavia, Italy, [2]Department of Internal Medicine and Therapeutics, University of Pavia, Pavia, Italy

Objective: Radiofrequency ablation (RFA) is an emerging non-surgical treatment for benign thyroid nodules (BTN). Despite its proven safety profile, data on the learning curve (LC) required to achieve proficiency are still lacking.

Materials and methods: The first 179 RFA procedures performed by a single operator in patients with non-functioning BTN were retrospectively analyzed. Six-month nodule volume reduction rate (VRR) ≥ 50% was regarded as reflection of proficiency. Multiple linear regression analysis has been performed to determine the relationship between the VRR and clinical variables. Cumulative sum (CUSUM) charts were plotted to assess LCs for all consecutive procedures and in relation to basal nodule size. In details, Group 1 (G1): 57 patients with small nodules (<10 ml); Group 2 (G2): 87 patients with intermediate nodules (10 – 25 ml); Group 3 (G3): 35 patients with large size (> 25 ml).

Results: LC of all 179 procedures showed 3 phases: initial learning (1–39 procedures); consolidation (40–145 procedures); and experienced period (146–179 procedures). For G1 and G2 proficiency is achieved starting from the 10th procedure within the group (or 37th considering consecutively all procedures) and from the 59th procedure within the group (or 116th considering consecutively all procedures), respectively. LC of G3 did not detect operator proficiency.

Conclusion: Specific LCs exist concerning the basal size of the nodule treated with RFA. In nodules with baseline volume > 25 ml suboptimal VRR has to be

expected. Previously achieved experience on small-intermediate nodules does not seem to provide advantages in terms of higher VRR in the treatment of large nodules. Other potential and non-modifiable factors likely play a key role in the final volume reduction independently from the increased skill of the operator.

KEYWORDS

thyroid nodules, benign, non-functioning, radiofrequency ablation, learning curve

Introduction

Thermal ablation for benign thyroid nodules is an effective and safe non-surgical treatment for benign thyroid nodules (BTN) (1, 2). Radiofrequency ablation (RFA), is a procedure performed through a trans-isthmic approach and a moving-shot technique, reported to display a high efficacy together with a low complication rate (3). In this regard, a recent interdisciplinary consensus statement of the American Thyroid Association aimed to provide a framework for the safe adoption and implementation of non-surgical ablation technologies for BTN, including data on the learning curve (LC) and necessary prior skillset (4).

LC is defined as the time taken and/or the number of cases required by an average operator to become proficient to be able to perform a procedure independently and obtaining a satisfactory outcome (5). The concept of the LC is often employed in surgery, where a constant stream of new skills must be acquired safely and effectively (6). Similarly, some Authors have addressed the issue of how many RFA procedures an operator may have to carry out before reaching a safe and competent level of performance.

Up to now, only three reports with an overall number of 291 patients have focused on LCs for thyroid RFA (7–9). Two of the three studies focused on the LC for a single operator (7, 8), and the other involved a team of two radiologists (9). According to these previous studies, physicians with prior expertise in thyroid ultrasound (US) and fine-needle aspiration (FNA) biopsy may have to carry out at least 20–30 RFA procedures before reaching a safe and competent level of performance. Although these previous experiences have provided a first and meaningful insight into the role of the operator experience on clinical efficacy in RFA for benign nodules, some additional aspects require further investigation. Just to give an example, the baseline nodule volume was consistently reported to be related to RFA treatment outcomes (10, 11), but the role of basal volume of the treated nodule was not fully characterized when LC is considered.

Thus, the primary outcome of this study will be to assess the LC for thyroid RFA of a single operator in treating non-functioning BTN, using volume reduction rate (VRR) as a proficiency marker. The secondary goal will be to identify both baseline patient-related as well as technical aspects of the ablation procedure potentially related to the therapeutic outcome as assessed by VRR.

Patients and methods

This cohort study enrolled the first 179 consecutive patients with non-functioning BTN receiving RFA treatment at the Endocrinology and Metabolism Unit of the ICS Maugeri, Pavia. The reasons for performing RFA included: 1) subjective compressive symptoms such as difficulty in swallowing or the feeling of local pressure and/or cosmetic concerns; 2) increase in the volume of the nodules over an ultrasound follow-up in the last years; 3) patient's preference for RFA rather than surgery. Inclusion criteria were: 1) serum TSH, FT4, and FT3 levels within the normal range; (3) at least one benign cytological result at fine-needle aspiration (FNA). All patients signed an informed consent concerning the future use of their clinic data for research purposes and data collected remained strictly confidential and anonymous, according to the ethical rules of our Hospital institutions and to the Declaration of Helsinki.

Procedure

All patients referred for RFA treatment underwent a complete thyroid work-up, including a measurement of serum FT4, FT3, and TSH. A baseline US of the neck was performed by the same endocrinologist (S.C) who performed the RFA procedures. The thyroid nodule's location, volume, and characteristics were collected, and all nodules were classified based on EU-TIRADS criteria (12). Thyroid nodule volume was calculated using the ellipsoid volume formula as follows: volume = 0.525 × length × width × depth. US-guided FNA was performed at least once in all patients, and cytological results were provided according to the Italian Thyroid Cytology Classification System 2014 (13). The procedures were performed in a sterile setting. Local anesthesia with Lidocaine 2% was administered at the skin puncture site and the perithyroidal space. No hydro dissection or anesthetic infusion was made in the peri- or under-capsular layer. The operator (S.C.), an endocrinologist with more than two decades of expertise in thyroid imaging, fine-needle aspirations, core-needle biopsies, and percutaneous ethanol therapy, initiated RFA treatment with the first patient enrolled. All RFA procedures were performed using a 18-gauge internally cooled electrode, 7 or 10 cm length with a 10 mm active tip (RF AMICA PROBE, Hs Hospital Service S.p.A, Italy). The US-guided moving-shot technique with a trans-isthmic

10.3389/fendo.2024.1399912

approach was applied (14). During the procedure, patients remained in a supine position with mild neck extension. They were advised to report pain, and voice testing was performed at regular intervals. The starting level of energy delivered per second was 30 W. The energy output was progressively increased if no response was visible on the US within 60 seconds. At the end of the procedure, the patient applied mild compression of the treated thyroid lobe for 20 min. If necessary, an icepack was applied to relieve pain. After 2 h of post-procedural observation, a neck US was performed. Standard follow-up included outpatient visits with FT4, FT3, and TSH after 6 and 12 months. Nodule volumes were measured by the US after 1, 6, and 12 months. Nodal volume reduction was expressed as volume reduction ratio, calculated as follows: VRR = ((initial volume − final volume)/(initial volume)) × 100. Technique efficacy was defined as a volumetric reduction ≥50% of the initial nodule volume.

Data analysis

The statistical analyses were performed using the SPSS software (SPSS, Inc., Evanston, IL) and JMP (version 17, SAS Institute Inc., Cary, NC).

The LCs of the technical efficacy were analyzed using the calculated cumulative sum (CUSUM), a graphics-based analysis approach typically used for monitoring change detection. The CUSUM of the deviations of each sample value from the target value is plotted in the y-axis and the case number is plotted on the x-axis. The target value is set to VRR 50%. The cumulative sum of the deviations upper and below the target value is indicated by the black dots. The upper and lower control limits are determined as ± 20 standard deviations (SD) from the target value and are drawn as red horizontal lines. Results are reported as mean values with S.D., medians with ranges, or as proportions. A multiple linear regression model was constructed by entering VRR as a dependent variable while chronological order, age, nodule composition, nodule location, nodule baseline volume, and applied energy served as covariates. A p-value <0.05 was considered statistically significant.

Results

Basic characteristics of all patients

Throughout the study-span, 179 benign thyroid nodules (178 patients) were treated by RFA. In one patient, two separate nodules were treated. The mean age of the patients was 58,10 ± 13,17 years (range, 23 to 92). The mean baseline nodule volume was 17,73 ± 13.29 ml (range, 2.39 to 80.58). In all, 80 were solid-predominantly solid; 92 were mixed; and 5 were cystic-predominantly cystic. At 6 -month post-RFA the mean VRR of 179 nodules was 58,38 ± 17.28% and volumetric reduction ≥50% of the initial nodule volume was achieved in 78.13% of patients. The treatments were performed by using a mean total estimated energy of 19337,80 ± 11517,67 J and a mean energy per volume of 1361,86 ± 883,28 J/ml. Table 1 shows the patient's demographic and clinical characteristics.

Learning curve analyses

Based on the CUSUM analysis of the 179 consecutive procedures, changes in the slope could be observed after 39 and 145 procedures, allowing to divide the LC into 3 distinct phases. Indeed, the vertical line on the CUSUM Chart indicates that a positive shift in the VRR values started around sample 39 (end of the initial LC), "plateaus" between cases 40–145 with higher variability in the CUSUM trend (consolidation phase), subsequently a new shift is recorded from case 146 (proficiency phase). Figure 1 shows the CUSUM analysis of the LC of the 179 RFA procedures.

To identify baseline and procedural parameters that correlate with VRR values, a multiple linear regression analysis was performed including chronological order, age, nodule composition, nodule location, nodule baseline volume, and applied energy (Table 2). The only independent predictor of 6-month VRR was nodule baseline volume (β = -0,31, 95% confidence interval = -0,501, -0,123, p = 0,001).

Based on the above results, to explore the possibility that differences in nodule baseline volume might influence proficiency, patients were stratified into three groups according to nodule volume. In detail, Group I encompassed 57 patients with small nodules (<10 ml); Group 2 encompassed 87 patients with intermediate nodules (volume 10 – 25 ml); Group 3 encompassed 35 patients with large size (volume > 25 ml). As a further step, a single CUSUM chart for each group was drawn.

TABLE 1 Patient's demographic and clinical characteristics.

Age (years)	58,10 ± 13,17
Male/Female (n°)	28/151
TSH (mUI/mL)	1,96 ± 4.18
Nodule location	
Right Isthmus Left	86 3 90
Nodule composition	
Solid- predominantly solid Mixed Cystic-Predominantly cystic	82 92 5
Nodule baseline volume (ml)	17,73 ± 13,29
Depth (mm)	23,84 ± 6,27
Width (mm)	30,37 ± 8,50
Length (mm)	40,77 ± 10,23
VRR at 6 mo (%)	58,38 ± 17.28
VRR ≥ 50% at 6-month (yes/no)	131/48
RFA time (sec)	643,12 ± 308,3
Applied energy (J)	19337,80 ± 11517,67
Applied energy (J/ml)	1361,86 ± 883,28

Results are expressed as mean ± standard deviation or numbers. TSH, thyroid-stimulating hormone; VRR, volume reduction rate; RFA, radiofrequency ablation.

10.3389/fendo.2024.1399912

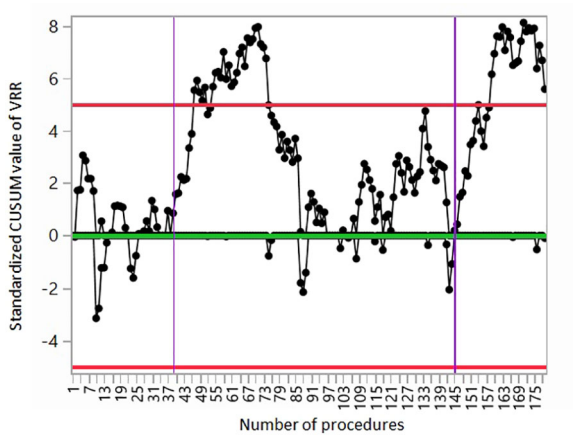

FIGURE 1
CUSUM analysis of the LC of the 179 RFA procedures. The CUSUM of the deviations of each sample value from the target value of VRR 50% is plotted in the y-axis. The case number plotted on the x-axis shows consecutively all 179 procedures. VRR, volume reduction rate.

TABLE 2 Multivariate analysis of factors predicting VRR.

Independent variables	Coefficient (β)	Lower limit 95% CI	Upper limit 95% CI	*p-value*
Chronological order	0,01	-0,14	0,16	0,899
Age (years)	-0,088	-0,241	0,066	0,262
Nodule location	0,064	-0,078	0,207	0,372
Nodule composition	0,035	-0,109	0,179	0,632
Nodule baseline volume (ml)	-0,31	-0,501	-0,123	0,001
Applied energy (J)	-0,002	-0,18	0,176	0,981

VRR, volume reduction rate, CI, confidence interval.

Figures 2A, B show the CUSUM analysis of the LC of G1. The vertical line on the CUSUM Chart indicates that a positive shift in the VRR values started around sample 10 when taking into account only the patients with small nodules; and "moves" to sample 37 when we consider consecutively all patients treated.

Figures 3A, B show the CUSUM analysis of the LC of G2. The vertical line on the CUSUM Chart indicates that a positive shift in the VRR values started around sample 59 when taking into account only the patients with intermediate nodules; and moves to sample 116 when we consider consecutively all patients treated.

Figures 4A, B show the CUSUM analysis of the LC of G3. There is no positive or negative shift in the VRR values.

Discussion

The present study follows some previous ones, clearly indicating that a 6-month VRR of 50% represents a realistic and rapidly achieved goal in most patients treated by RFA for benign thyroid nodules. According to a large body of evidence, demonstrating that RFA-associated complications are rather rare, the main outcome measure to determine RFA proficiency has become the rate of volume reduction (15). Thus, three previous studies have conventionally focused on a minimum threshold for procedural volume in order to achieve a higher 6-month VRR (7–9). Bom et al. demonstrated that about 40 procedures are required to achieve a VRR >50% and of 79% in the following 63 patients (9). Russ et al, in their experience with the first 90 patients treated, showed that a LC existed regarding technical efficacy, VRR, and ablation ratio, a relatively new objective parameter to assess the percentage of the successfully ablated nodule. However, after 60 procedures, improvement only persisted in the latter and for small to medium nodules. Recently, Kuo et al, using the CUSUM chart, identified two inflection points of the LC at the 20th and 65th cases, respectively (8).

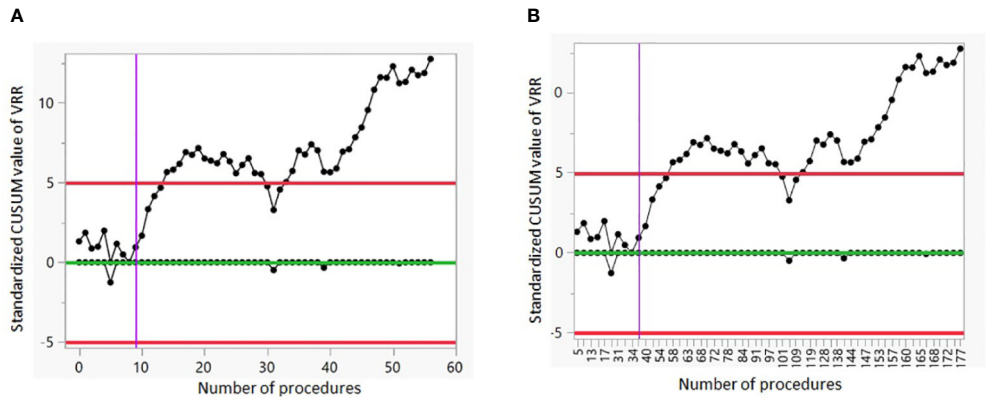

FIGURE 2
CUSUM analysis of the LC of G1. **(A)** The CUSUM of the deviations of each sample value from the target value of VRR 50% is plotted in the y-axis. The case number plotted on the x-axis shows the 57 procedures performed on patients with small nodules. **(B)** The CUSUM of the deviations of each sample value from the target value of VRR 50% is plotted in the y-axis. The case number plotted on the x-axis shows consecutively all 179 procedures. VRR, volume reduction rate.

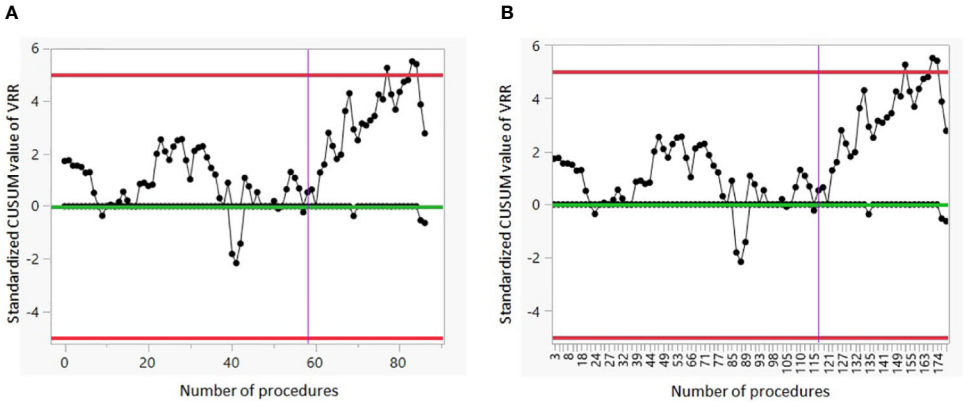

FIGURE 3
CUSUM analysis of the LC of G2. **(A)** The CUSUM of the deviations of each sample value from the target value of VRR 50% is plotted in the y-axis. The case number plotted on the x-axis shows the 87 procedures performed on patients with intermediate nodules. **(B)** The CUSUM of the deviations of each sample value from the target value of VRR 50% is plotted in the y-axis. The case number plotted on the x-axis shows consecutively all 179 procedures. VRR, volume reduction rate.

Thus, a certain degree of amelioration in the skilled operator was reported after a minimum of ablation procedures ranging from 40 to 60. However, it is rather disappointing to find that, although a rather limited number of procedures is sufficient to achieve a VRR >50% in most patients, further increasing the numbers of procedures performed, leads to limited additional increase in VRR. This appears in agreement with the findings by De Andrea et al. who, in an international prospective randomized controlled trial, compared the volume reduction obtained in patients treated in two centers (Italy and Korea) with different experience of the moving-shot technique (respectively 50 vs 3000 procedures). The results in terms of volume reduction were impressive in the treated group, both in Italy and Korea, with a slightly greater efficacy in the latter group where experience in the moving-shot technique is consolidated, but without a significant difference between the two countries. To note, the baseline volume was larger in the Italian series (16.4 ± 2.5 mL vs. 13.9 ± 3.3 mL, p=0.009) (16).

The results of our study demonstrate that single-operator LC patterns in achieving higher 6-month VRR are profoundly different according to the baseline volume of the nodule treated. Indeed, as assessed by CUSUM charts, it is evident that while for small volume nodules (< 10 ml) a relevant increase in VRR is observed starting from the 10th procedure, for intermediate volume nodules (10–25 ml), ~60 RFA procedures were required to obtain a comparable amelioration in the VRR. Consistently, when treating large volume nodules (> 25 ml), even when performed by an operator who has simultaneously demonstrated optimal volume reduction rate in the treatment of lower volume nodules, ~ 35 previous procedures do not warrant a mean 6-month VRR > 50%. Furthermore, according to our result, it could be stated that an experienced proceduralist (~180 procedures performed) may fail to achieve a 6-month VRR > 50% when large nodules are taken into account.

The above evidence would support the concept that specific LCs exist concerning the size of the nodule treated and, more importantly and surprisingly, that previously achieved experience (as assessed by the number of total procedures performed) on small-intermediate nodules does not provide advantages (at least in terms of higher VRR) when the same operator faces large nodules.

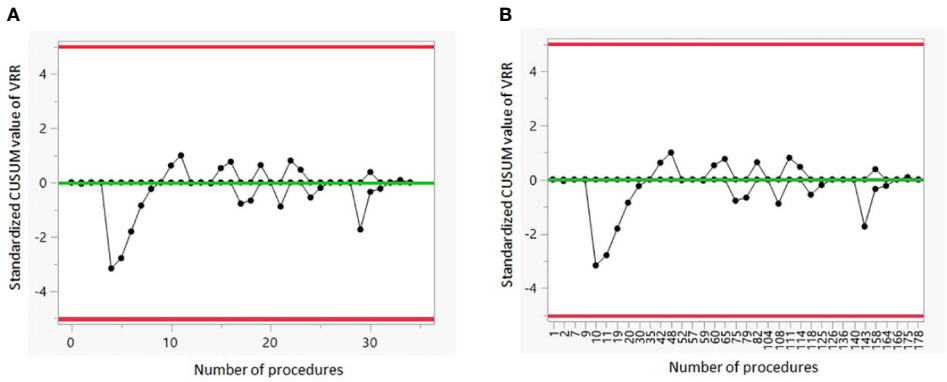

FIGURE 4
CUSUM analysis of the LC of G3. **(A)** The CUSUM of the deviations of each sample value from the target value of VRR 50% is plotted in the y-axis. The case number plotted on the x-axis shows the 35 procedures performed on patients with large nodules. **(B)** The CUSUM of the deviations of each sample value from the target value of VRR 50% is plotted in the y-axis. The case number plotted on the x-axis shows consecutively all 179 procedures. VRR, volume reduction rate.

Although the here reported LCs outcome in relation to baseline thyroid volume may result from a lower efficacy and efficiency of the moving-shot technique on large nodules, other potentially relevant variables should be taken into account and discussed.

Beyond the operator's mastery, the patient's characteristics (i.e. age and ability to maintain neck hyperextension for increasing amount of time) and nodule's characteristics (large thyroid nodules and particular anatomical site and/or surrounding critical structures) may all contribute to the final outcome when assessed by the degree of VRR (17).

The above considerations suggest a further aspect that might be important to highlight which is related to the desired therapeutic goal. Indeed, in treating nodules with small and medium sizes, it is desirable to achieve the highest possible volume reduction. In patients with large nodule sizes, we should look at RFA as a technique providing personalized treatment, in that, we may actually fix a given end-point for each patient. Thus, it is reasonable to assume that the final aim of the procedure is to provide relief of symptoms which is not always observed in parallel with greater VRR. In line with this statement, Papini et al. reported that a 50% volume reduction is most often sufficient to improve patients' symptoms (18).

The current problem is that we should distinguish between the technical efficacy of RFA (i.e. VRR) and the clinical efficacy of RFA (i.e. therapeutic success).

Our data suggest that in nodules with baseline volume > 25 ml suboptimal VRR has to be expected and the concept of LC may not be applicable. Potential and non-modifiable factors such as nodule vascularization, composition, anatomical site and biological characteristics as well as patients' compliance likely play a key role in the final volume reduction independently from the increased skill of the operator. Consistent with this, Bernardi et al, investigated the outcomes of re-treatment on symptomatic BTN with a VRR <50% after the initial thermal ablation treatment (19). The RFA re-treatment led to greater VRR as compared to the first treatment only in small and medium nodules (<30 mL) but not in large nodules (>30 mL).

The current study has several strengths. The cohort size is roughly double compared to other studies on LC, increasing our results' representativeness and accuracy. Secondly, the cases included were consecutive and inclusive of all RFA procedures performed by the operator, unraveling a realistic picture of daily clinical practice. Thirdly we used a specific statistical approach for LC evaluation (CUSUM analysis).

Potential limitations of the present study include the single-center and the retrospective design, which inherently restricts external generalizability, even though the here reported results are in overall agreement with those provided by previous studies. Furthermore, this study lacks an evaluation of the initial ablation ratio (IAR), calculated as the ratio between the ablated volume and the total nodule volume before RFA (20). Its potential value as a parameter to document operator skills was recently demonstrated by Russ et al., showing that a single-operator LC for achieving an IAR >90% was substantially longer than required for a VRR >50% and exceeded 90 procedures when large nodes are involved (7). However, the accuracy of IAR for long-term volume reduction and regrowth prediction remains to be established (21, 22).

In conclusion, the results of the present study demonstrate that: i) RFA is a safe and rapidly acquired procedure at least for small to medium size nodules; ii) the therapeutic efficacy of RFA should not be exclusively assessed by VRR as relevant clinical benefits may be obtained also for sub-optimal VRR; iii) RFA treatment should be regarded as an additional therapeutic tool for personalized treatment of patients bearing thyroid nodule.

Future prospective longitudinal studies, specifically aimed to evaluate the long-term outcome as well as the role of 6 month VRR to predict final size of the nodules will be required to further characterize the relationship between technical efficacy and clinical efficacy of the RFA procedure.

Data availability statement

The raw data supporting the conclusions of this article will be made available by the authors, without undue reservation.

Ethics statement

Ethical approval was not required for the studies involving humans because Formal approval by the ethical committee was not required in accordance with the Italian regulation for non-interventional (observational) retrospective studies concerning human beings (AIFA Guidelines for Observational Studies, see www.AIFA.gov). The studies were conducted in accordance with the local legislation and institutional requirements. The participants provided their written informed consent to participate in this study.

Author contributions

SC: Conceptualization, Data curation, Writing – original draft. MT: Writing – review & editing, Data curation, Writing – original draft. LC: Writing – review & editing. FC: Writing – review & editing. BG: Data curation, Writing – review & editing. MC: Data curation, Writing – review & editing. RF: Writing – review & editing. FM: Writing – review & editing. MR: Conceptualization, Writing – review & editing.

Funding

The author(s) declare financial support was received for the research, authorship, and/or publication of this article. This research was partially funded under the National Recovery and Resilience Plan (NRRP), Mission 4 Component 2 Investment 1.4 - Call for tender No. 3138 of 16 December 2021, rectified by Decree n.3175 of 18 December 2021 of Italian Ministry of University and Research funded by the European Union – NextGenerationEU. This research was partially supported through the Ricerca Corrente funding of the Italian Ministry of Health.

Conflict of interest

The authors declare that the research was conducted in the absence of any commercial or financial relationships that could be construed as a potential conflict of interest.

Publisher's note

References

1. Cesareo R, Egiddi S, Naciu AM, Tabacco G, Leoncini A, Napoli N, et al. Efficacy of radiofrequency and laser thermal ablation in solving thyroid nodule-related symptoms and cosmetic concerns. A systematic review and meta-analysis. *Rev Endocr Metab Disord*. (2022) 23:1051–61. doi: 10.1007/s11154–022-09743–8

2. Chung SR, Suh CH, Baek JH, Park HS, Choi YJ, Lee JH. Safety of radiofrequency ablation of benign thyroid nodules and recurrent thyroid cancers: a systematic review and meta-analysis. *Int J Hyperthermia*. (2017) 33:920–30. doi: 10.1080/02656736.2017.1337936

3. Jung SL, Baek JH, Lee JH, Shong YK, Sung JY, Kim KS, et al. Efficacy and safety of radiofrequency ablation for benign thyroid nodules: A prospective multicenter study. *Korean J Radiol*. (2018) 19:167–74. doi: 10.3348/kjr.2018.19.1.167

4. Sinclair CF, Baek JH, Hands KE, Hodak SP, Huber TC, Hussain I, et al. General principles for the safe performance, training, and adoption of ablation techniques for benign thyroid nodules: an American thyroid association statement. *Thyroid*. (2023) 33:1150–70. doi: 10.1089/thy.2023.0281

5. Khan N, Abboudi H, Khan MS, Dasgupta P, Ahmed K. Measuring the surgical "learning curve": Methods, variables and competency. *BJU Int*. (2014) 113:504–8. doi: 10.1111/bju.12197

6. Lin PL, Zheng F, Shin M, Liu X, Oh D, D'Attilio D. CUSUM learning curves: what they can and can't tell us. *Surg Endosc*. (2023) 37:7991–9. doi: 10.1007/s00464–023-10252–1

7. Russ G, Ben Hamou A, Poirée S, Ghander C, Ménégaux F, Leenhardt L, et al. Learning curve for radiofrequency ablation of benign thyroid nodules. *Int J Hyperthermia*. (2021) 38:55–64. doi: 10.1080/02656736.2021.1871974

8. Kuo CY, Liu CL, Tsai CH, Cheng SP. Learning curve analysis of radiofrequency ablation for benign thyroid nodules. *Int J Hyperthermia*. (2021) 38:1536–40. doi: 10.1080/02656736.2021.1993358

9. Bom WJ, Joosten FBM, van Borren MMGJ, Bom EP, van Eekeren RRJP, de Boer H. Radiofrequency ablation for symptomatic, non-functioning, thyroid nodules: a single-center learning curve. *Endocr Connect*. (2022) 11:e210304. doi: 10.1530/EC-21–0304

10. Russell JO, Desai DD, Noel JE, Hussein M, Toraih E, Seo S, et al. Radiofrequency ablation of benign thyroid nodules: A prospective, multi-institutional North American experience. *Surg (United States)*. (2024) 175:139–45. doi: 10.1016/j.surg.2023.07.046

11. Bisceglia A, Rossetto R, Garberoglio S, Franzin A, Cerato A, Maletta F, et al. Predictor analysis in radiofrequency ablation of benign thyroid nodules: A single center experience. *Front Endocrinol (Lausanne)*. (2021) 12:638880. doi: 10.3389/fendo.2021.638880

12. Russ G, Bonnema SJ, Erdogan MF, Durante C, Ngu R, Leenhardt L. European thyroid association guidelines for ultrasound Malignancy risk stratification of thyroid nodules in adults: the EU-TIRADS. *Eur Thyroid J*. (2017) 6:225–37. doi: 10.1159/000478927

13. Nardi F, Basolo F, Crescenzi A, Fadda G, Frasoldati A, Orlandi F, et al. Italian consensus for the classification and reporting of thyroid cytology. *J Endocrinol Invest*. (2014) 37:593–9. doi: 10.1007/s40618–014-0062–0

14. Shin JH, Baek JH, Ha EJ, Lee JH. Radiofrequency ablation of thyroid nodules: Basic principles and clinical application. *Int J Endocrinol*. (2012) 2012:919650. doi: 10.1155/2012/919650

15. Noel JE, Sinclair CF. Radiofrequency ablation for benign thyroid nodules. *J Clin Endocrinol Metab*. (2023) 109:e12–7. doi: 10.1210/clinem/dgad357

16. Deandrea M, Sung JY, Limone P, Mormile A, Garino F, Ragazzoni F, et al. Efficacy and safety of radiofrequency ablation versus observation for nonfunctioning benign thyroid nodules: A randomized controlled international collaborative trial. *Thyroid*. (2015) 25:890–6. doi: 10.1089/thy.2015.0133

17. Lin Y, Shi YP, Tang XY, Ding M, He Y, Li P, et al. Significance of radiofrequency ablation in large solid benign thyroid nodules. *Front Endocrinol (Lausanne)*. (2022) 13:902484. doi: 10.3389/fendo.2022.902484

18. Papini E, Rago T, Gambelunghe G, Valcavi R, Bizzarri G, Vitti P, et al. Long-term efficacy of ultrasound-guided laser ablation for benign solid thyroid nodules. Results of a three-year multicenter prospective randomized trial. *J Clin Endocrinol Metab*. (2014) 99:3653–9. doi: 10.1210/jc.2014–1826

19. Bernardi S, Rosolen V, Barbone F, Borgato S, Deandrea M, De Feo P, et al. Clinical outcomes of thermal ablation re-treatment of benign thyroid nodules: A multicenter study from the Italian minimally invasive treatments of the thyroid group. *Thyroid*. (2024) 34:360–70. doi: 10.1089/thy.2023.0501

20. Sim JS, Baek JH, Lee J, Cho W, Jung S. Il. Radiofrequency ablation of benign thyroid nodules: depicting early sign of regrowth by calculating vital volume. *Int J Hyperthermia*. (2017) 33:905–10. doi: 10.1080/02656736.2017.1309083

21. Bernardi S, Cavallaro M, Colombin G, Giudici F, Zuolo G, Zdjelar A, et al. Initial ablation ratio predicts volume reduction and retreatment after 5 years from radiofrequency ablation of benign thyroid nodules. *Front Endocrinol (Lausanne)*. (2021) 11:582550. doi: 10.3389/fendo.2020.582550

22. Yan L, Luo Y, Xie F, Zhang M, Xiao J. Residual vital ratio: predicting regrowth after radiofrequency ablation for benign thyroid nodules. *Int J Hyperthermia*. (2020) 37:1139–48. doi: 10.1080/02656736.2020.1825835

frontiers | Frontiers in Endocrinology

TYPE Original Research
PUBLISHED 25 June 2024
DOI 10.3389/fendo.2024.1402380

OPEN ACCESS

EDITED BY
Pia Pace-Asciak,
University of Toronto, Canada

REVIEWED BY
Kyriakos Vamvakidis,
Henry Dunant Hospital, Greece
Giorgio Radetti,
Ospedale di Bolzano, Italy

*CORRESPONDENCE
Liu Huan
cmuliuhuan@outlook.com

RECEIVED 17 March 2024
ACCEPTED 10 June 2024
PUBLISHED 25 June 2024

CITATION
Chuanke S, Ming L, Zhideng Y and Huan L (2024) A 6-year single-center prospective follow-up study of the efficacy of radiofrequency ablation for thyroid nodules. *Front. Endocrinol.* 15:1402380. doi: 10.3389/fendo.2024.1402380

A 6-year single-center prospective follow-up study of the efficacy of radiofrequency ablation for thyroid nodules

Shi Chuanke, Luo Ming, Yan Zhideng and Liu Huan*

Department of General Surgery, Zhongshan Hospital of Traditional Chinese Medicine, Zhongshan, Guangdong, China

Background: Radiofrequency ablation (RFA) is an alternative modality for thyroid nodules (TNs) and many studies have also confirmed its favorable efficacy and safety. The scope of RFA increases in clinical practice and the aim of our study was to evaluate the efficacy of RFA.

Methods: We conducted a prospective study to evaluate the efficacy of RFA for thyroid nodules between January 2017 and December 2022 at our institution. We assessed the change in nodal volume, volume reduction ratio (VRR), technique effective (TE) rate, complete ablation (CA) rate, and nodal regrowth rate and time after RFA.

Results: We performed RFA for 1703 patients with TNs between January 2017 and December 2022, of which a total of 970 eligible patients were enrolled in the study. The preoperative volume of TNs was 6.23 ± 8.11ml, with 821 benign and 149 malignant nodules. The post-RFA TE and adjusted TE rate were 80% and 88.8%, respectively. CA was achieved in 145 (14.9%) patients with a mean time of 18.32± 12.98 months; nodal regrowth occurred in 15 (1.5%) patients with a mean time of 29.80 ± 12.47 months. TNs volume and VRR changed significantly at years 1 and 2 after RFA and stabilized after 5 years. A serious postoperative adverse event occurred in one patient with cervical sympathetic chain injury resulting in Horner's syndrome. A transient or permanent damage of the recurrent laryngeal nerve could not be evaluated due to the lack of postoperative laryngoscopy, and this is a significant limitation of the study.

Conclusion: The expanded RFA indications were also effective for TNs, with no significant change in long-term efficacy.

KEYWORDS

radiofrequency ablation (RFA), volume reduction ratio (VRR), technique effective, regrowth, efficacy

1 Introduction

Thyroid nodules (TNs) are very common in the general population up to 68% (1) and their incidence is also gradually increasing attributed to incidental nodule findings. It includes both benign and malignant nodules, however, benign nodules are more than 90%. Most of these benign nodules are clinically asymptomatic requiring only follow-up observation (2), and treatment is indicated for those with symptoms of compression (including important structures such as the trachea, recurrent laryngeal nerve, esophagus, etc.) or aesthetic concerns. More than 90% of malignant nodules are papillary thyroid carcinomas, which are indolent tumors. Surgery is the standard treatment for thyroid nodules; however, it leads to scar formation and, there are adverse events such as recurrent laryngeal nerve, hypothyroidism, and hypoparathyroidism after surgery (3, 4). Long-term hormone replacement therapy may be required for postoperative hypothyroidism, which may have adverse effects on the bone and cardiac system (5). Moreover, thyroid nodules are becoming more common among young people; therefore, more and more patients prefer minimally invasive treatments without surgical scars. Thermal ablation has emerged as an alternative minimally invasive treatment for thyroid nodules, including radiofrequency ablation (RFA), laser ablation (LA), microwave ablation (MA), and high-frequency focused ultrasound (HIFU).

RFA is the most commonly used thermal ablation technique, and many previous studies have confirmed that RFA has no significant difference in efficacy compared with surgery (6, 7). However, the risk of adverse events such as postoperative voice changes, hypothyroidism, and hypoparathyroid function was significantly lower (6–9). Currently, the indications for RFA in multiple guidelines are benign thyroid nodules, thyroid micropapillary carcinoma, recurrent lymph nodes in the neck, those who refuse thyroid surgery, or those who are ineligible for surgery due to systemic disease (5, 10, 11). However, due to the indolent characteristics of malignant nodules and aesthetic concerns, many studies have attempted to perform RFA for low-risk papillary thyroid carcinoma (12, 13). Moreover, the RFA threshold for benign nodules has not been clearly defined, and many studies have also applied RFA to larger nodules, like Deandrea M et al. for volumes >20 ml (14). Many previous studies have evaluated RFA separately for benign and malignant nodules (4, 11–14) and our study evaluated its efficacy for both. At the same time, these studies had small sample sizes, and we conducted a 6-year continuous prospective study with a larger sample size.

The aim of our study was to conduct a large sample size, consecutive prospective study to evaluate the efficacy of RFA for thyroid nodules, both benign and malignant.

2 Materials and methods

2.1 Patients

Our study was a single-center prospective study, which was approved by our Institutional Ethics Committee (No. 2022ZSY-LLK-456), and all subjects obtained informed consent prior to surgery. Patients with TNs who underwent RFA at Zhongshan Hospital of Traditional Chinese Medicine between January 2017 and December 2022 were enrolled. All thyroid nodules were evaluated for malignant risk by experienced sonographers based on the ACR TI-RADS grading system (15) prior to RFA. All patients also underwent fine-needle aspiration biopsy (FNA) of the TNs to clarify their nature prior to RFA.

The inclusion criteria for eligible patients were as follows: 1) RFA performed at our institution between January 2017 and December 2022; 2) TNs with TI-RADS grading; and 3) TNs with definitive FNA pathology results, including benign nodules and malignant nodules (papillary thyroid carcinoma). The exclusion criteria were as follows: 1) those who refused to participate in this study; 2) patients who were lost to follow-up; 3) incomplete data; and 4) those who received other RF treatments before RFA (LA, MA, HIFU).

2.2 RFA preoperative preparation and postoperative follow-up

All patients completed routine blood, biochemical tests, coagulation, thyroid function, electrocardiogram (ECG), and chest X-ray to exclude contraindications before RFA. The demographic characteristics of the patients included age, gender, and history of previous surgeries and diseases, especially thyroid surgery and treatment. All thyroid nodules were scored and risk stratified according to the ACR TI-RADS grading system.

After RFA, ultrasound(US) was performed at months 1, 3, 6, 12, and every 6 or 12 months thereafter. Thyroid function was assessed again 1 month after RFA. We followed up to assess whether there were events requiring emergency surgery or prolonged hospitalization after RFA.

2.3 RFA procedure

All RFAs were performed by experienced surgeons and sonographers in an outpatient setting applying a bipolar RFA generator and an 18-gauge bipolar radiofrequency electrode with a 0.9 cm active tip (CelonProSurge, Olympus Surgical Technologies, Germany). The patient was placed in the supine position with full neck extension, and local anesthesia with lidocaine was applied for pain control. The RFA was performed under real-time ultrasound guidance with hydro dissection, trans-isthmic approach, and the moving shot technique (16). Appropriate length electrodes were selected for the RFA procedure based on the size and location of the TNs, and contrast-enhanced ultrasonography (CEUS) was performed before and after RFA. During the RFA procedure, we assessed the patients for changes in voice, dyspnea, and other discomforts, and discharged them after 12 hours of postoperative observation without significant discomfort.

2.4 Variables

The variables in this study were general demographic characteristics and post-RFA efficacy indicators. Demographic

characteristics included age, gender, underlying disease, thyroid-related disease and their treatment history. Post-RFA indicators included TNs volume, volume reduction ratio (VRR), technical effectiveness (TE), TNs regrowth, new onset, period of stabilization of TNs after RFA and re-intervention rate.

The three-dimensional size of the TNs was measured in ultrasound and its volume was calculated: Volume equation= [length(sagittal,cm)×depth(anteroposterior, cm)×width(transverse, cm)]×0.524. Volume Reduction Rate (VRR) is an important indicator for assessing the effectiveness of RFA and is calculated as follows:VRR = [(Initial Volume - Final Volume)×100%]/Initial Volume. Technical effectiveness (TE) was a >50% reduction in TNs volume at 12 months after RFA; TNs regeneration was defined as a 50% increase in total volume over the previous minimum volume (17).

2.5 statistical analysis

In our study, continuous variables were described by mean ± standard deviation (SD) and statistically analyzed by Students t test or Mann Whitney U test according to their distribution. Categorical variables are expressed in frequency (percentage), and statistical analysis is performed using Chi-square tests or Fisher exact tests when appropriate. We used multivariate logistic regression analysis to find the factors that affected the RFA effect, expressed by the adjusted Odds ratio (OR) and 95% confidence interval (CI). $P < 0.05$ was considered statistically significant. All data were analyzed using SPSS 25.0 version.

3 Results

The flow of our study was shown in Figure 1. A total of 1703 patients with TNs underwent RFA between January 2017 and December 2022. After excluding 733 ineligible patients, a total of 970 eligible patients were included in our study. The demographic characteristics of all eligible patients are shown in Table 1. There were 803 females and 167 males, with minimum and maximum ages of 5 and 78 years, and a mean age of 43.63 ± 12.36 years. Of these patients, 654 (67.4%) had multiple TNs, and, 201 (20.7%) of those with multiple nodes underwent multiple node ablation treatments during a single RFA. 18 (1.9%) patients had previous RFA and 15 (1.5%) patients were postoperative nodules of residual glands for RFA. Preoperative FNA in RFA for TNs has confirmed 821 (84.6%) as benign and 149 (15.4%) as malignant.

The post-RFA follow-up and efficacy assessments were shown in Table 2. Of the 970 patients who were eligible for consecutive follow-up, the mean follow-up time was 17.60 ± 13.66 months, with the shortest and longest follow-up times being 1 month and 66 months, respectively. Technically effective (TE) was achieved in 776 patients after RFA, and their overall TE rate was 80%. However, because some patients were followed up for less than 12 months, their adjusted TE rate was 88.8% (776/874) after excluding the 96 unsuccessful TEs in these patients. Of these 970 patients, 145 patients achieved complete ablation (CA) with a CA rate of 14.9%, and the mean time to achieve CA was 18.32 ± 12.98 months. Regrowth of TNs occurred in 15 patients with a rate of 1.5% and its mean regrowth time was 29.80 ± 12.47 months.

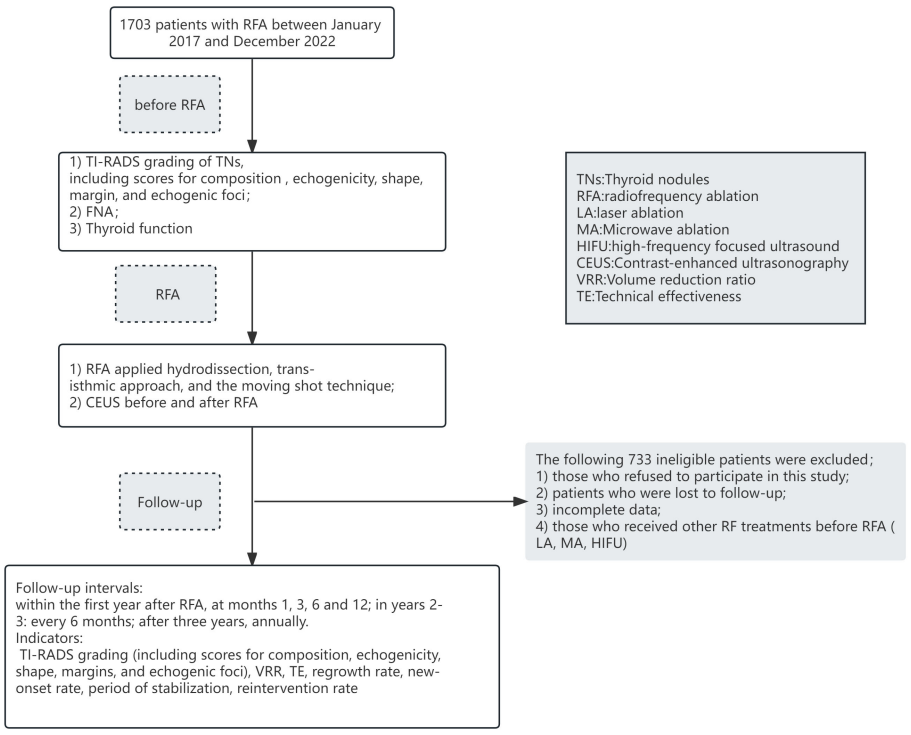

FIGURE 1
Flow chart of the study.

TABLE 1 Clinical characteristics of the study.

Characteristic	n (%)
Genders	
Female/male n (%)	803/167(82.8%/17.2%)
Age, years,	
(min,max;mean ± SD)	(5,78; 43.63 ± 12.36)
Number of TNs	
1/>1 n (%)	(316/654) (32.6%/67.4%)
The number of TNs for RFA	
1/>1 n (%)	(769/201) (79.3%/20.7%)
History of prior RFA	
Yes/no n (%)	(952/18) (98.1%/1.9%)
Postoperative residual thyroid	
Yes/no n (%)	(15/955) (1.5%/98.5%)
Pathologic results of TNs	
Benign/Malignant n (%)	(821/149) (84.6%/15.4%)

SD, Standard deviation; TNs, Thyroid nodules; RFA, radiofrequency ablation.

The changes in the volume of TNs after RFA were shown in Table 3; Figures 2A, B. The mean volume of TNs before RFA was 6.23 ± 8.11 ml. There was a gradual decrease in the volume of TNs after RFA, which was most significant at months 3 (2.60 ± 3.06 ml, $p < 0.001 < 0.05$) and months 12 (1.60 ± 2.30 ml, $p = 0.004 < 0.05$). The volume reduction rate (VRR) of TNs did not decrease at month 3 after RFA; on the contrary, an increase occurred (-70.36 ± 402.64%). The VRR gradually increased after months 3 and was most significant at postoperative 1 year (58.18 ± 76.86%, $p < 0.001 < 0.05$) and 2 years (68.98 ± 59.91%, $p = 0.019 < 0.05$). The complete ablation and re-growth rates of TNs after RFA were shown in Table 4; Figure 2C. The CR rates were 7.11%, 11.13%, 13.51%, 14.54%, 14.85%, and 14.95% at 1, 2, 3, 4, 5, and 6 years after RFA, respectively. Re-growth rates at 1, 2, 3, 4, 5, and 6 years after RFA were 0.21%, 0.52%, 1.03%, 1.44%, 1.55%, and 1.55%, respectively.

TABLE 2 Follow up and efficacy of RFA.

Characteristic	n (%)
Patients (n)	970
Follow-up time, months	
(min,max)	(1,66)
(mean ± SD)	17.60 ± 13.66
TE rate n (%)	776/970, 80
TE* rate n (%)	776/874,88.8
CA rate, n (%)	145/970, 14.9
CA time, months	
(mean ± SD)	18.32 ± 12.98
Regrowth rate	15/970, 1.5
Regrowth time, months	
(mean ± SD)	29.80 ± 12.47

SD, Standard deviation; TE, Technical effectiveness; TE*, The adjusted technical effectiveness; CA, Complete ablation.

4 Discussion

Thyroid nodules (TNs) are extremely common in the general population, and their incidence is increasing due to the popularity of high-resolution ultrasound and the emphasis on health issues. Many previous studies have confirmed that RFA is an optional safe and effective treatment for TNs. The majority of TNs are benign nodules and more than 90% of malignant nodules are papillary thyroid carcinomas with a biological predisposition to indolence; similarly, patients have aesthetic concerns, all of which contribute to a higher incidence of RFA. As a result, the scope of RFA has gradually expanded from benign nodules to micropapillary thyroid cancer and even to recurrent thyroid cancer and low-risk papillary thyroid cancer.

Surgery is still the mainstay of treatment for TNs, and its postoperative risk of adverse events such as hypothyroidism, hypoparathyroidism, and recurrent laryngeal nerve injury is significantly higher than that of RFA (4, 18, 19). Surgery involves removal of the thyroid gland with nodules, whereas RFA involves coagulative necrosis of the nodules into biologically inactive scar tissue by thermal ablation; therefore, TNs do not immediately decrease or disappear in apparent physical size after RFA, and may even show enlargement in the short-term. TNs volume and volume reduction rate (VRR) are important indicators for assessing the efficacy of RFA. In our study, the volume of TNs decreased from 6.23 ml preoperatively to 1.6 ml, 1.34 ml, 1.27 ml, 1.57 ml, 0.97 ml, and 0.90 ml at postoperative 1, 2, 3, 4, 5, and 6 years, respectively and its VRR was 58.18%, 68.98%, 73.76%, 75.92%, 84.56% and 85.44% at postoperative 1, 2, 3, 4, 5 and 6 years, respectively. Volume reductions in TNs were most significant at years 1 and 2 after RFA, and it stabilized after 2 years. A meta-analysis showed that benign TNs had a VRR of 75% and 87% at years 1 and 2 after RFA, respectively (4). In another meta-analysis including 24 studies of ablation of benign TNs showed a VRR of 66% and 62% at years 1 and 2 after RFA, respectively; these are consistent with our study (20). Kim MK et al. found that the VRR of malignant nodules was lower than that of benign ones at 12 months after RFA (51.4% versus 83.8%, $P = 0.01 < 0.05$) (21). A study of 74 patients with thyroid micropapillary carcinoma (PTMC) followed for more than 5 years found that RFA resulted in complete disappearance of the tumor lesions without local tumor progression, lymph node or distant metastasis (22). In our study, we saw complete ablation of TNs lesions in 145 (4.9%) patients, which occurred with a mean follow-up time of 18.32 ± 12.98 months.

RFA treatment is not the removal of glands with clinically significant nodules; therefore, patients are more anxious and concerned about the recurrence of nodules after RFA. Many studies have demonstrated that incomplete ablation resulting in residual nodules at the margins is an important factor in regeneration (23, 24). It has been also noted that incomplete ablation of benign nodules may promote nodule growth to some

10.3389/fendo.2024.1402380

TABLE 3 Volume and VRR of TNs.

	Volume (mean ± SD,ml)	P-value	VRR (mean± SD,%)	P-value
preoperative	6.23 ± 8.11		–	–
Post-operative			–	–
1–3 months	2.60 ± 3.06	<0.001	-70.36 ± 402.64	–
3–6 months	2.10 ± 3.01	0.297	32.42 ± 137.36	<0.001
6–12 months	1.60 ± 2.30	0.004	58.18 ± 76.86	<0.001
12–24months	1.34 ± 2.08	0.077	68.98 ± 59.91	0.019
24–36months	1.27 ± 2.00	0.670	73.76 ± 33.58	0.321
36–48months	1.57 ± 2.39	0.259	75.92 ± 33.60	0.607
48–60months	0.97 ± 1.52	0.089	84.56 ± 19.34	0.151
>60months	0.90 ± 0.97	0.930	85.44 ± 15.59	0.601

TNs, Thyroid nodules; VRR, Volume reduction rate; SD, Standard deviation.

extent (25). However, many studies indicated that the initial ablation ratio (IAR) did not correlate with nodal regrowth, but rather with VRR and the likelihood of retreatment (25–28). Performing CEUS before and after RFA for more complete ablation reduces the possibility of residual nodules; however, factors such as large nodules, restricted anatomical locations V (29), and large calcified foci (30) affect ablation efficacy, and identification of accurate borders leads to residual nodules after initial ablation. Although previous studies have indicated that the primary purpose of RFA for benign nodules is to alleviate compression symptoms rather than complete ablation (31), many studies have confirmed its favorable safety and efficacy, allowing it to treat PTMC, recurrent thyroid cancer, and even low-risk papillary thyroid cancer. Therefore, the current aims of RFA are not only to improve symptoms, but also to eliminate tumor lesions (12, 13, 22). Those puncture-proven benign nodules that do not achieve satisfactory regression or regeneration after RFA may actually be malignant. Many studies have also confirmed its and found that regenerating nodules after RFA were confirmed to be malignant during subsequent surgeries (32, 33). Therefore, for these nodules that do not significantly regress or regenerate after RFA, a puncture biopsy is recommended to exclude the possibility of malignancy and guide subsequent treatment.

In our study, we saw a significant reduction in the volume of TNs after RFA at 1 and 2 years, and its stabilization at 2 years. A meta-analysis also showed that the volume of benign nodules decreased rapidly within 12 months after ablation, with a plateau at months 12 - 36 (34). The change in VRR was consistent with the change in nodal volume, which also stabilized at 2 years. The VRR showed a negative increase in 3 months after RFA, which is consistent with previous studies; it is due to the ablation area exceeding the boundaries of the nodule (especially small nodules), and changes such as peripheral edema and inflammation affecting the definition of the boundaries in the early post-RFA period. Regrowth of the nodules predominantly started in the 2nd year after RFA and stabilized in the 4th year. Previous studies have also confirmed that regrowth occurs after 2 and 3 years (35–37). However, Sim JS et al. found that its regrowth shows a peak during the 2nd-3rd year after RFA and another peak after the 5th year (23). Valcavi R et al. found that regrowth is rare after the 4th year (38), which is consistent with our findings. These differences may be due to inconsistencies in follow-up times, leading to different definitions of minimum volume; therefore, Mauri, G et al. suggested that regrowth be defined as a 50% increase in the minimum recorded volume compared to that measured at a given follow-up time point (17).

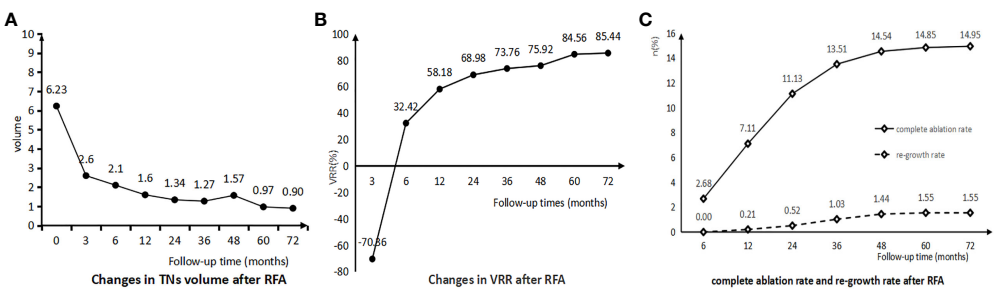

FIGURE 2
(A) Changes in TNs Volume after RFA. **(B)** Changes in TNs VRR after RFA. **(C)** Complete ablation rate and re-growth rate after RFA.

TABLE 4 Complete ablation rate and re-growth rate after RFA.

	Complete ablation rate n(%)	P-value	Regrowth rate n(%)	P-value
Post-operative				
0–6 months	6(2.68)	–	0(0)	–
6–12 months	69(7.11)	<0.001	2(0.21)	0.949
12–24months	108(11.13)	<0.001	5(0.52)	0.452
24–36months	131(13.51)	0.128	10(1.03)	0.300
36–48months	141(14.54)	0.556	14(1.44)	0.539
48–60months	144(14.85)	0.898	15(1.55)	0.999
>60months	145(14.95)	0.949	15(1.55)	0.999

RFA, radiofrequency ablation.

Parameters regarding the prediction of regrowth after RFA have not been clarified (37). Yan et al. found that residual active nodule rate, initial volume, location, and vascular distribution were all independent risk factors associated with regrowth (28). Negro R et al. found that VRR at 12 months after RFA was associated with regrowth (35). An increase in the volume of the residual active nodule may be an early sign of nodule regrowth (27, 39). Many studies also indicated that margin re-expansion is an important cause of recurrence after RFA (23, 29, 40). There is currently no consensus on the timing and indications for reintervention in these regrowing nodules. Some studies have indicated that a single treatment for benign nodules treated to relieve compression symptoms or improve cosmetic problems is sufficient, even if nodule regrowth occurs (31). Kim HJ et al. demonstrated that single RFA is effective for small nodules without initial regrowth or symptomatic recurrence. However, additional treatments improved the VRR for nodules with regrowth, increased Vv, or symptomatic recurrence (41). One study found that a VRR of <66% at 1 year after RFA was a better predictor of nodal retreatment, whereas young age and large initial volume may also be associated with its retreatment (37). Another study found that an IAR >73% was a good predictor of no retreatment within 5 years after RFA (26). The study showed that the energy delivered during RFA is also a reliable predictor of retreatment (37). Therefore, avoiding residual active nodules after RFA reduces the likelihood of nodule regrowth or retreatment. Preoperative CEUS identified the targeting area and postoperative CEUS confirmed complete ablation of the targeting area. Additional RFA is indicated for patients with larger nodules, unresolved clinical problems, or regrowth or increased Vv after initial ablation. Some studies have also confirmed that subsequent RFA for large benign nodules improves VRR and efficacy. However, the optimal timing and indications for reintervention, including RFA and invasive procedures, need to be further explored.

Our study has its own limitations as follows: 1. We followed up only for major complications of E and F classifications as defined by the Society of Interventional Radiology (SIR) (42). A serious postoperative adverse event occurred in one patient with cervical sympathetic chain injury resulting in Horner's syndrome. A transient or permanent damage of the recurrent laryngeal nerve could not be evaluated due to the lack of postoperative laryngoscopy, and this is a significant limitation of the study. 2. Most thyroids are multiple nodules, and many patients had multiple nodules ablated during a single RFA; however, we only evaluated large nodules. Therefore, whether there is a difference between ablation of multiple nodules versus single nodules during the same RFA, and whether ablation has an effect on untreated nodules (both ipsilateral and contralateral); none of the above were involved in this study and will be explored in our subsequent studies.

Data availability statement

The original contributions presented in the study are included in the article/supplementary material. Further inquiries can be directed to the corresponding author.

Author contributions

SC: Supervision, Writing – review & editing, Project administration, Methodology, Investigation, Data curation, Conceptualization. LM: Writing – review & editing, Supervision, Methodology. YZ: Investigation, Writing – review & editing, Supervision, Methodology. LH: Writing – original draft, Project administration, Formal Analysis, Data curation, Conceptualization, Writing – review & editing, Methodology, Investigation.

Funding

The author(s) declare that no financial support was received for the research, authorship, and/or publication of this article.

Conflict of interest

The authors declare that the research was conducted in the absence of any commercial or financial relationships that could be construed as a potential conflict of interest.

Publisher's note

References

1. Kant R, Davis A, Verma V. Thyroid nodules: advances in evaluation and management. *Am Fam Physician*. (2020) 102:298–304.

2. Durante C, Costante G, Lucisano G, Bruno R, Meringolo D, Paciaroni A, et al. The natural history of benign thyroid nodules. *JAMA*. (2015) 313:926–35. doi: 10.1001/jama.2015.0956

3. Weiss A, Parina RP, Tang JAB, Brumund KT, Chang DC, Bouvet M. Outcomes of thyroidectomy from a large California State database. *Am J Surg*. (2015) 210:1170–7. doi: 10.1016/j.amjsurg.2015.08.011

4. Trimboli P, Castellana M, Sconfenza LM, Virili C, Pescatori LC, Cesareo R, et al. Efcacy of thermal ablation in benign non-functioning solid thyroid nodule: a systematic review and meta-analysis. *Endocrine*. (2020) 67:35–43. doi: 10.1007/s12020-019-02019-3

5. Haugen BR, Alexander EK, Bible KC, Doherty GM, Mandel SJ, Nikiforov YE, et al. 2015 American Thyroid Association Management guidelines for adult patients with thyroid nodules and diferentiated thyroid cancer: The American Thyroid Association Guidelines Task force on thyroid nodules and diferentiated thyroid cancer. *Thyroid*. (2015) 26:1–133. doi: 10.1089/thy.2015.0020

6. Kim JH, Yoo WS, Park YJ, Park DJ, Yun TJ, Choi SH, et al. Efficacy and Safety of Radiofrequency Ablation for Treatment of Locally Recurrent Thyroid Cancers Smaller than 2 cm. *Radiology*. (2015) 276:909–18. doi: 10.1148/radiol.15140079

7. Choi Y, Jung SL, Bae JS, Lee SH, Jung CK, Jang J, et al. Comparison of efficacy and complications between radiofrequency ablation and repeat surgery in the treatment of locally recurrent thyroid cancers: A single-center propensity score matching study. *Int J Hyperth*. (2019) 36:359–67. doi: 10.1080/02656736.2019.1571248

8. Bernardi S, Palermo A, Grasso RF, Fabris B, Stacul F, Cesareo R. Current status and challenges of US-guided radiofrequency ablation of thyroid nodules in the long term: A systematic review. *Cancers (Basel)*. (2021) 13:27–46. doi: 10.3390/cancers13112746

9. Kim C, Lee JH, Choi YJ, Kim WB, Sung TY, Baek JH. Complications encountered in ultrasonography-guided radiofrequency ablation of benign thyroid nodules and recurrent thyroid cancers. *Eur Radiol*. (2017) 27:3128–37. doi: 10.1007/s00330-016-4690-y

10. Ahmad S, Aljammal J, Orozco I, Raashid S, Zulfiqar F, Nikravan SP, et al. Radiofrequency ablation of cervical thyroid cancer metastases-experience of endocrinology practices in the United States. *J Endocr Soc*. (2023) 7:bvad066. doi: 10.1210/jendso/bvad066

11. Van Dijk SP, Coerts HI, Gunput ST, van Velsen EFS, Medici M, Moelker A, et al. Assessment of radiofrequency ablation for papillary microcarcinoma of the thyroid: A systematic review and meta-analysis. *JAMA Otolaryngol Neck Surg*. (2022) 148:317–25. doi: 10.1001/jamaoto.2021.4381

12. Lim HK, Cho SJ, Baek JH, Lee KD, Son CW, Son JM, et al. US-guided radiofrequency ablation for low-risk papillary thyroid microcarcinoma: efficacy and safety in a large population. *Korean J Radiol*. (2019) 20:1653–61. doi: 10.3348/kjr.2019.0192

13. Yan L, Lan Y, Xiao J, Lin L, Jiang B, Luo Y. Long-term outcomes of radiofrequency ablation for unifocal low-risk papillary thyroid microcarcinoma: A large cohort study of 414 patients. *Eur Radiol*. (2021) 31:685–94. doi: 10.1007/s00330-020-07128-6

14. Deandrea M, Trimboli P, Garino F, Mormile A, Magliona G, Ramunni MJ, et al. Long-term efficacy of a single session of RFA for benign thyroid nodules: A longitudinal 5-year observational study. *J Clin Endocrinol Metab*. (2019) 104:3751–6. doi: 10.1210/jc.2018-02808

15. Tessler FN, Middleton WD, Grant EG, Hoang JK, Berland LL, Teefey SA, et al. ACR thyroid imaging, reporting and data system (TI-RADS): white paper of the ACR TI-RADS committee. *J Am Coll Radiol*. (2017) 14:587–95. doi: 10.1016/j.jacr.2017.01.046

16. Kim JH, Baek JH, Lim HK, Ahn HS, Baek SM, Choi YJ, et al. 2017 Thyroid radiofrequency ablation guideline: Korean society of thyroid radiology. *Korean J Radiol*. (2018) 19:632–55. doi: 10.3348/kjr.2018.19.4.632

17. Mauri G, Pacella CM, Papini E, Solbiati L, Goldberg SN, Ahmed M, et al. Image-guided thyroid ablation: proposal for standardization of terminology and reporting criteria. *Thyroid*. (2019) 29:611–8. doi: 10.1089/thy.2018.0604

18. Che Y, Jin S, Shi C, Wang L, Zhang X, Li Y, et al. Treatment of benign thyroid nodules: comparison of surgery with radiofrequency ablation. *AJNR Am J Neuroradiol*. (2015) 36:1321–5. doi: 10.3174/ajnr.A4276

19. Wu R, Luo Y, Tang J, Yang M, Li J, Zhang Y, et al. Ultrasound-guided radiofrequency ablation for papillary thyroid microcarcinoma: A retrospective analysis of 198 patients. *Int J Hyperth*. (2020) 37:168–74. doi: 10.1080/02656736.2019.1708480

20. Chung SR, Suh CH, Baek JH, Park HS, Choi YJ, Lee JH. Safety of radiofrequency ablation of benign thyroid nodules and recurrent thyroid cancers: A systematic review and meta-analysis. *Int J Hyperthermia*. (2017) 33:920–30. doi: 10.1080/02656736.2017.1337936

21. Kim MK, Shin JH, Hahn SY, Kim H. Delayed cancer diagnosis in thyroid nodules initially treated as benign with radiofrequency ablation: ultrasound characteristics and predictors for cancer. *Korean J Radiol*. (2023) 24:903–11. doi: 10.3348/kjr.2023.0386

22. Cho SJ, Baek SM, Lim HK, Lee KD, Son JM, Baek JH. Long-term follow-up results of ultrasound-guided radiofrequency ablation for low-risk papillary thyroid microcarcinoma: more than 5-year follow-up for 84 tumors. *Thyroid*. (2020) 30:1745–51. doi: 10.1089/thy.2020.0106

23. Sim JS, Baek JH, Lee J, Cho W, Jung SI. Radiofrequency ablation of benign thyroid nodules: depicting early sign of regrowth by calculating vital volume. *Int J hyperthermia: Off J Eur Soc Hyperthermic Oncol North Am Hyperthermia Group*. (2017) 33:905–10. doi: 10.1080/02656736.2017.1309083

24. Sung JY, Baek JH, Jung SL, Kim JH, Kim KS, Lee D, et al. Radiofrequency ablation for autonomously functioning thyroid nodules: a multicenter study. *Thyroid: Off J Am Thyroid Assoc*. (2015) 25:11–27. doi: 10.1089/thy.2014.0100

25. Issa PP, Omar M, Issa CP, Buti Y, Hussein M, Aboueisha M, et al. Radiofrequency ablation of indeterminate thyroid nodules: the first north american comparative analysis. *Int J Mol Sci*. (2022) 23:11493. doi: 10.3390/ijms231911493

26. Bernardi S, Cavallaro M, Colombin G, Giudici F, Zuolo G, Zdjelar A, et al. Initial ablation ratio predicts volume reduction and retreatment after 5 years from radiofrequency ablation of benign thyroid nodules. *Front Endocrinol*. (2021) 11:582550. doi: 10.3389/fendo.2020.582550

27. Chen MH, Lin WC, Luo SD, Chiang PL, Chen YS, Chen WC, et al. Residual, regrowth, and new growth of radiofrequency ablation for benign thyroid nodules of different volumes: two-year follow-up results. *Int J Hyperthermia*. (2022) 39:1172–8. doi: 10.1080/02656736.2022.2112305

28. Yan L, Luo Y, Xie F, Zhang M, Xiao J. Residual vital ratio: predicting regrowth after radiofrequency ablation for benign thyroid nodules. *Int J Hyperthermia*. (2020) 37:1139 48. doi: 10.1080/02656736.2020.1825835

29. Yan L, Zhang M, Li X, Li Y, Luo Y. A nomogram to predict regrowth after ultrasound-guided radiofrequency ablation for benign thyroid nodules. *Front Endocrinol*. (2022) 12:774228. doi: 10.3389/fendo.2021.774228

30. Park KW, Shin JH, Han BK, Ko EY, Chung JH. Inoperable symptomatic recurrent thyroid cancers: preliminary result of radiofrequency ablation. *Ann Surg Oncol*. (2011) 18:2564 8. doi: 10.1245/s10434-011-1619-1

31. Deandrea M, Limone P, Basso E, Mormile A, Ragazzoni F, Gamarra E, et al. US-Guided percutaneous radiofrequency thermal ablation for the treatment of solid benign hyperfunctioning or compressive thyroid nodules. *Ultrasound Med Biol*. (2008) 34:784–91. doi: 10.1016/j.ultrasmedbio.2007.10.018

32. Bernardi S, Dobrinja C, Fabris B, Bazzocchi G, Sabata N, Ulcigrai V, et al. Radiofrequency ablation compared to surgery for the treatment of benign thyroid nodules. *Int J Endocrinol*. (2014) 2014:934595. doi: 10.1155/2014/934595

33. Oddo S, Spina B, Vellone VG, Giusti M. A case of thyroid cancer on the track of the radiofrequency electrode 30 months after percutaneous ablation. *J Endocrinol Invest*. (2017) 40:101–102. doi: 10.1007/s40618-016-0527-4

34. Cho SJ, Baek JH, Chung SR, Choi YJ, Lee JH. Long-term results of thermal ablation of benign thyroid nodules: A systematic review and meta-analysis. *Endocrinol Metab*. (2020) 35:339–50. doi: 10.3803/EnM.2020.35.2.339

35. Negro R, Greco G, Deandrea M, Rucco M, Trimboli P. Twelve-month volume reduction ratio predicts regrowth and time to regrowth in thyroid nodules submitted to laser ablation: A 5-year follow-up retrospective study. *Korean J Radiol*. (2020) 21:764 72. doi: 10.3348/kjr.2019.0798

36. Lim HK, Lee JH, Ha EJ, Sung JY, Kim JK, Baek JH. Radiofrequency ablation of benign non-functioning thyroid nodules: 4-year follow-up results for 111 patients. *Eur Radiol*. (2013) 23:1044 9. doi: 10.1007/s00330-012-2671-3

37. Bernardi S, Giudici F, Cesareo R, Antonelli G, Cavallaro M, Deandrea M, et al. Five-year results of radiofrequency and laser ablation of benign thyroid nodules: A

multicenter study from the Italian minimally invasive treatments of the thyroid group. *Thyroid*. (2020) 30:1759–70. doi: 10.1089/thy.2020.0202

38. Valcavi R, Riganti F, Bertani A, Formisano D, Pacella CM. Percutaneous laser ablation of cold benign thyroid nodules: a 3-year follow-up study in 122 patients. *Thyroid*. (2010) 20:1253–61. doi: 10.1089/thy.2010.0189

39. Baek JH, Ha EJ, Choi YJ, Sung JY, Kim JK, Shong YK. Radiofrequency versus ethanol ablation for treating predominantly cystic thyroid nodules: A randomized clinical trial. *Korean J Radiol*. (2015) 16:1332–40. doi: 10.3348/kjr.2015.16.6.1332

40. Baek JH, Moon WJ, Kim YS, Lee JH, Lee D. Radiofrequency ablation for the treatment of autonomously functioning thyroid nodules. *World J surgery*. (2009) 33:1971–7. doi: 10.1007/s00268-009-0130-3

41. Kim HJ, Baek JH, Cho W, Sim JS. Long-term follow-up of the radiofrequency ablation of benign thyroid nodules: the value of additional treatment. *Ultrasonography*. (2022) 41:661–9. doi: 10.14366/usg.21231

42. Sacks D, McClenny TE, Cardella JF, Lewis CA. Society of interventional radiology clinical practice guidelines. *J Vasc Interv. Radiol*. (2003) 14 Pt 2:S199 S202. doi: 10.1097/01.RVI.0000094584.83406.3e

frontiers | Frontiers in Endocrinology

TYPE Original Research
PUBLISHED 24 July 2024
DOI 10.3389/fendo.2024.1402605

OPEN ACCESS

EDITED BY
Pia Pace-Asciak,
Department of Otolaryngology – Head and Neck Surgery, University of Toronto, Canada

REVIEWED BY
Marco Stefano Demarchi,
Hôpitaux Universitaires de Genève (HUG), Switzerland
Emrah Karatay,
Marmara University Istanbul Pendik Education and Research Hospital, Türkiye

*CORRESPONDENCE
Antoine Eskander
antoine.eskander@sunnybrook.ca

†These authors have contributed equally to this work

RECEIVED 17 March 2024
ACCEPTED 10 July 2024
PUBLISHED 24 July 2024

CITATION
Sarkis LM, Higgins K, Enepekides D and Eskander A (2024) A novel guided approach to radiofrequency ablation of thyroid nodules: the Toronto Sunnybrook experience. *Front. Endocrinol.* 15:1402605. doi: 10.3389/fendo.2024.1402605

A novel guided approach to radiofrequency ablation of thyroid nodules: the Toronto Sunnybrook experience

Leba Michael Sarkis[1,2†], Kevin Higgins[1†], Danny Enepekides[1†] and Antoine Eskander[1,3,4*†]

[1]Department of Otolaryngology-Head and Neck Surgery, Sunnybrook Health Sciences Centre, Toronto, ON, Canada, [2]Sydney Medical School, University of Sydney, Sydney, NSW, Australia, [3]Department of Otolaryngology – Head & Neck Surgery, Michael Garron Hospital, Toronto, ON, Canada, [4]Institute of Health Policy, Management, and Evaluation, University of Toronto, Toronto, ON, Canada

Introduction: Thyroid nodules are extremely common being detected by ultrasonography in up to 67% of the population, with current surgical tenet maintaining that lobectomy is required for large symptomatic benign nodules or autonomously functionally nodules resulting in a risk of hypothyroidism or recurrent laryngeal nerve injury even in high volume centres. The introduction of radiofrequency ablation (RFA) has allowed thermal ablation of both benign and autonomously functioning thyroid nodules with minimal morbidity. The moving shot technique is the most well-established technique in performing RFA of thyroid nodules, and has proven to be safe, efficacious, accurate and successful amongst experienced clinicians. The purpose of this article to propose the use of a novel guide when performing RFA of thyroid nodules in clinical practice utilizing the moving shot technique.

Methods: The technique proposed of RFA involves the use of a 10MHz linear ultrasound probe attached to an 18G guide which provides robust in line visualisation of a 7cm or 10cm radiofrequency probe tip (STARmed, Seoul, Korea) utilizing the trans isthmic moving shot technique. A geometric analysis of the guide has been illustrated diagrammatically.

Results: The use of an 18G radiofrequency probe guide (CIVCO Infiniti Plus™ Needle Guide) maintains in line visualisation of the radiofrequency probe over a cross-sectional area up to 28cm^2, facilitating efficient and complete ablation of conceptual subunits during RFA of thyroid nodules.

Discussion: Radiofrequency ablation of thyroid nodules can be performed safely and effectively using the novel radiofrequency probe guide proposed which we believe potentially improves both accuracy and overall efficiency, along with operator confidence in maintaining visualisation of the probe tip, and hence we believe provides a valuable addition to the armamentarium of clinicians wishing to embark on performing RFA of thyroid nodules.

KEYWORDS

thyroid, nodule, radiofrequency ablation, guide, benign, autonomous

Introduction

Thyroid nodules are common and detectable by ultrasonography in up to 13-67% of individuals (1), with higher frequencies in women and the elderly even when the gland is normal on palpation. The initial work up of thyroid nodules has been well established and includes a thorough clinical history to determine risk factors for malignancy, clinical examination and an assessment of thyroid function followed by ultrasonography of both the thyroid bed and lateral neck. The vast majority do not require treatment, and current treatment paradigm maintains that surgery is required for nodules to confirm either suspicious lesions on fine needle aspiration biopsy (FNA) or on nodules that are confirmed to be malignant. However following FNA confirmation of benign nodules, or in isolated autonomously functioning thyroid nodules (AFTN), the risk of malignancy is low in the order of 2-6%. The majority of solitary toxic nodules represent follicular adenomas with a high prevalence of activating mutations in the TSH receptor and their risk of malignancy is less than 3% (2, 3).

Non-malignant (large benign or autonomously functioning) nodules sometimes, however, do require surgical intervention in the form of partial thyroidectomy (4). This leaves the patient with a small cervical scar and renders up to 22% of patients with hypothyroidism for life (5). Despite advances in surgical training, thyroidectomy still carries with it a 2-5% complication rate, even when performed by high volume surgeons (6), resulting in many patients delaying or avoiding surgery entirely.

With the increasing use of clinician-initiated point of care ultrasonography, ultrasound-guided thermal ablative techniques have been introduced by interventional thyroidologists (surgeons, endocrinologists, and interventional radiologists) to effectively treat and manage benign or AFTN. Radiofrequency ablation (RFA) of the thyroid gland was first introduced in human studies in 2006 (7) and multiple international guidelines (8–13) have since been developed including those most recently released by the American Thyroid Association (ATA) (14). The basic principle of RFA involves using a high-frequency alternating electric current that oscillates resulting in formation of a closed electrical circuit (15). The subsequent activation of radiofrequency power via a probe activates positively charged sodium and potassium ions and negatively charged chloride ions within the adjacent tissue and as they attempt to align with the polarity established by the high frequency electrical current, generate either frictional or resistive heat which is then transmitted and conducted to adjacent tissue (16). This generates heat between 60-100 degrees Celsius around the electrode tip that induces near instantaneous induction of protein coagulation with additional thermal injury via conduction that irreversibly damages cellular enzymes resulting in cell death by coagulative necrosis (15, 16). Perhaps the most established technique in implementing RFA in the thyroid is the moving-shot technique, proposed by Baek et al (17) as a means of maximising the efficiency of frictional heat generated at the electrode tip resulting in a more predictable ablation zone and minimizing risk of damages to adjacent visceral organs and nerves induced by thermal conduction. With this technique, the deepest portion of the nodule is targeted first using a trans-isthmic long-axis technique with a slow withdrawal before the next portion of the nodule is targeted, again from a deep to superficial approach. This technique has a well-established safety profile.

The purpose of this paper is to provide our approach to safely performing RFA for both benign and AFTN using a moving shot trans-isthmic long-axis technique. More specifically, we provide a pictorial and geometric analysis of the benefits and limitations of a novel ultrasound probe needle guide (CIVCO Infiniti Plus™).

Methods

Indications

RFA at Sunnybrook Health Sciences Centre is performed under ultrasound guidance by a clinician with experience in performing ultrasonography, FNA biopsies of the thyroid gland as well as core biopsies of neck masses. Indications for RFA are in keeping with the most recent ATA consensus statement, namely two thyroid FNA confirmed benign biopsies or AFTN (14).

Procedure preparation

The patient is placed in a supine position with the head elevated at approximately 30 degrees. Grounding pads are then applied to the patient's upper thigh to establish a complete grounded electrical circuit by also connecting them to the radiofrequency device. The generator is subsequently connected to a straight monopolar RF electrode with an active tip length between 5, 7 or 10mm, depending on the size of the nodule (STARmed Seoul, Korea), and a 7cm RF probe is most commonly employed. A cooling pump is used to circulate saline through the electrode and lower the temperature around the active tip to maximize ablative margin whilst minimizing tissue charring. Local anaesthetic being lidocaine with 1:100,000 adrenaline is injected around the skin at the site of entry of the probe for the trans-isthmic approach followed by a superficial cervical plexus block. Additional anaesthetic and 5% dextrose is then injected under ultrasound guidance using a spinal needle in a pericapsular plane producing a visualised anechoic band that hydrodissects and separates the nodule from the infrahyoid musculature and laterally away from the carotid sheath and a potentially medialized vagus nerve.

Guide technique

A high resolution 10Mhz linear ultrasound probe is then attached to a GE Edwards ultrasound probe guide which on its lateral aspect is directly connected to an 18G fitting guide (CIVCO Infiniti Plus™ Needle Guide) for the RF probe (STARMed Seoul, Korea). (Figures 1, 2) The purpose of the guide is to maintain constant inline visualisation during the procedure, removing the margin of error associated with freely holding the probe. In the results, we will demonstrate the use of this guided technique using a pictorial and geometric analysis of the probe within this guide. This

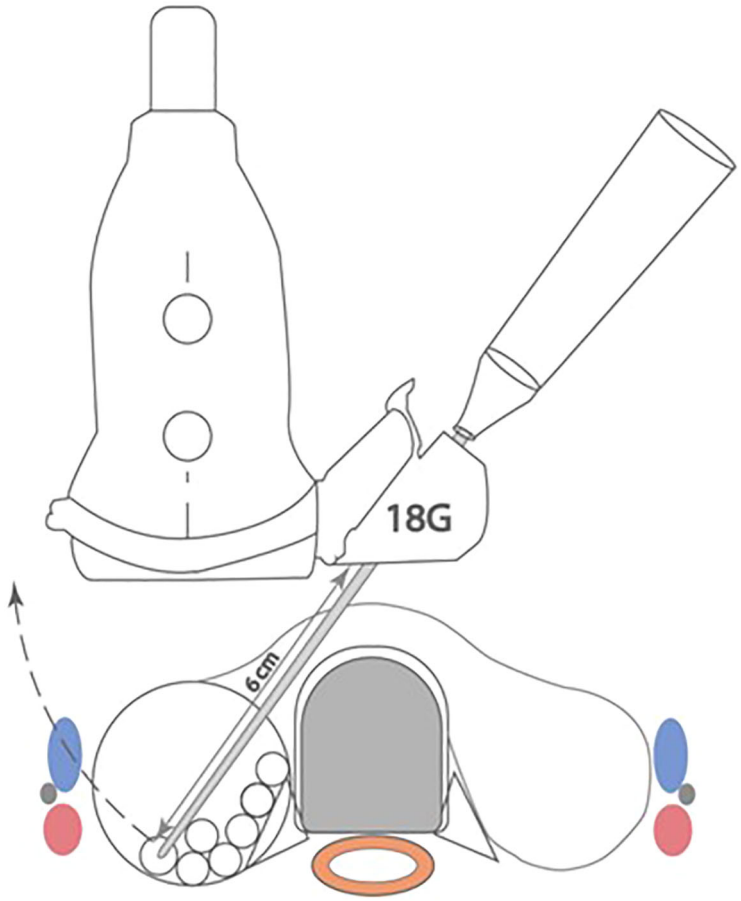

FIGURE 1
Radiofrequency probe with guide attached demonstrating in line stabilization and visualization during procedure.

will allow a greater understanding of the pros and cons of using such a guide. Research ethics board approval was not required as patients were not required for this analysis.

Ablative technique

The moving shot technique is then implemented by the clinician whereby the nodule is divided into a series of conceptual subunits with smaller subunits at the periphery, paying close attention to the danger triangle as has been previously described (7). The radiofrequency active tip probe (STARMed Seoul, Korea) is percutaneously inserted under direct vision using the guide (Figure 1) via a transisthmic approach beginning at the most posterior and deepest aspect of the nodule. The primary treatment endpoint is a combination of hyperechogenic change including echogenic microbubbles on the ultrasound screen and objective monitoring of tissue impedance level. The clinician then retracts the probe along the guide, consistently visualising the probe tip, and proceeds to ablation of the next conceptual subunit until all units have developed a visualised hyperechogenic focus with high tissue impedance proceeding from deep to superficial, and sparing the subunits contained within the danger triangle.

The patient is then monitored for at least one hour following the procedure to ensure there are no complications encountered and subsequently followed up by phone call within 24 hours of the procedure to monitor for any symptom change.

Results

Using the guided technique, a 7cm probe allows a maximum usable length of 3cm and cross-sectional area of 7.1cm^2. Trimming of the guide, facilitates a further 1cm of length, resulting in a cross-sectional area of 13cm^2. A 10cm probe provides a usable length of 6cm using the guide with a cross-sectional area attainable of 28.3cm^2, that can be increased to 38.5cm^2 once the guide is trimmed. Accounting for the thickness of the overlying subcutaneous tissue and skin, the guided technique can be safely used to ablate a 3cm nodule with a 7cm probe and up to a 6cm nodule with the 10cm probe once the guide is trimmed. A summary of the geometric analysis of both guides has been provided in Table 1. Figures 3, 4 provide a schematic geometric analysis using the 10cm RF probe (STARMed Seoul, Korea) length of a potential arc of treatment using a 4cm right thyroid nodule as an example with the ability to ablate a total area of 28cm^2 using the guide with

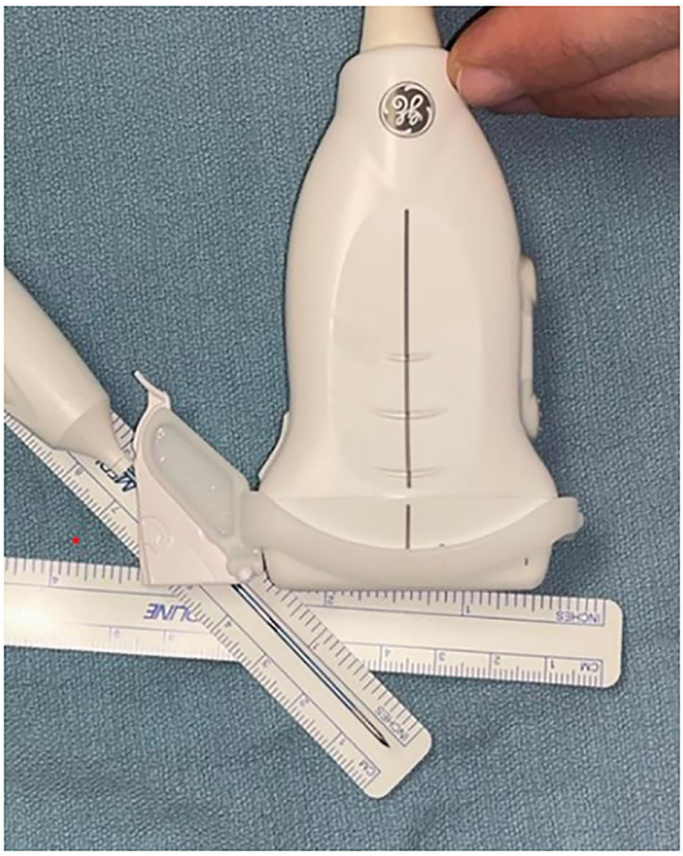

FIGURE 2
Equipment set-up The linear transducer probe guide is attached directly to an 18G radiofrequency probe guide to produce fixed translatory bodily movements with the electrode tip consistently centred in the long axis, minimizing angulation error during ablation.

constant probe tip visualisation. The advantages and disadvantages of such an approach have been summarized in Table 2 below.

Discussion

Radiofrequency ablation of the thyroid gland provides the thyroid interventionalist with a minimally invasive technique to ablate benign thyroid and AFTN in an outpatient setting, without a general anaesthetic, leaving them without a scar and most importantly, avoiding the risk of hypothyroidism. The efficacy of RFA in benign thyroid disease has been previously well established. Most recently, Russell et al. in a multi-institutional prospective collection of 620 patients from a North American population with benign thyroid nodules and a baseline nodule volume of 5.6mL, followed with serial ultrasound and TSH levels for 12 months, demonstrated a median volume reduction rate of 71% at 12 months, with 78% of patients achieving treatment success defined as a volume reduction greater than 50% at 1 year. On multivariate analysis, small nodules (with a treatment volume <10mls) and medium nodules (10-20mls) achieved a success rate of 81% and 87% at 12 months respectively (18). A similar muti-institutional prospective Korean study consisting of 276 patients demonstrated a mean volume reduction of 80% at 12 months with a mean preoperative volume of 14mls and largest diameter of 3.8cm, however, one quarter of these patients also had another ablative procedure (19). When followed by serial ultrasound for 6 years, the mean volume reductions at 24, 36, 48 and 60 months were 84%, 89%, 92% and 95% respectively. Deandrea et al. in their randomized control international collaborative trial across two centres in Italy and Korea demonstrated a mean volume rate reduction of 71% at 6 months (20), and a recent systematic review demonstrated a mean

TABLE 1 Geometric analysis comparing the 7cm RF probe to the 10cm RF probe.

	7cm RF Probe	10cm RF Probe
Cost	$	$$
Maximum usable length (without trim)	3cm	6cm
Maximal usable length (with trim)	4cm	7cm
Cross sectional area	7.1cm^2	28.3cm^2
Cross sectional area with trimmed guide	13cm^2	38.5cm^2
Nodule diameter (maximum)	3cm	6cm

10.3389/fendo.2024.1402605

A

B

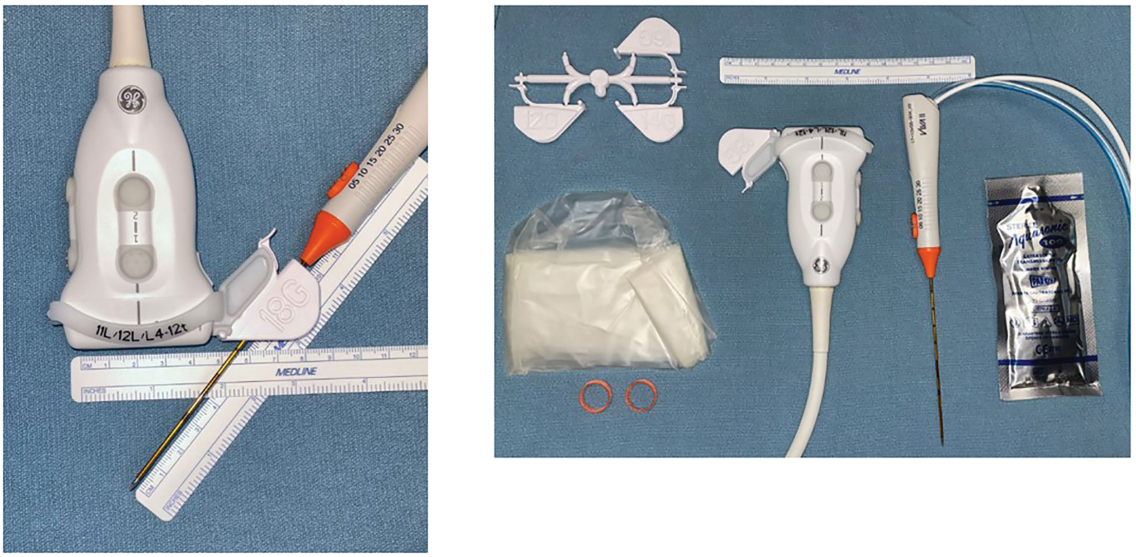

FIGURE 3
The combination of an 18G guide to maintain in line visualisation combined with a 10cm length RF probe **(A)** provides a working field of approximately 28cm^2 whilst applying the moving shot technique. Using a 7cm RF probe, the cross-sectional area achieved is approximately 7cm^2 but can be increased to 13cm^2 by trimming the guide using sterile scissors as shown in **(B)**.

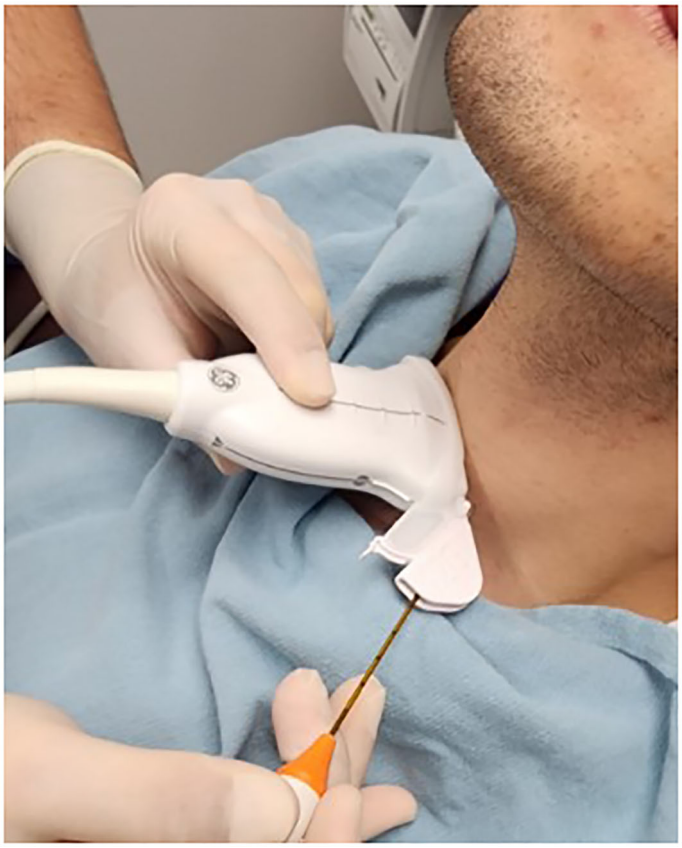

FIGURE 4
Schematic representation of the use of the RF probe guide in ablation of a 4cm thyroid nodule. A total cross sectional of 28cm^2 can be ablated through a single puncture site whilst maintaining in line visualisation of the tip at all times.

TABLE 2 Summary of the advantages and disadvantages of guided RF ablation.

	Advantages	Disadvantages
Guided	• Easier long axis visualisation of the electrode tip at all times • Low cost and user friendly • Attaches to almost any 10MHz ultrasound probe • Simplifies electrode tip control in the long axis for the novel interventionalist	• Obscures the site of puncture and therefore potentially increases the chance and need of multiple puncture sites • Limits the depth of the electrode tip for large or deep nodules >5cm • Additional cost to treatment • May need modification for use with 7 cm probe
Non-guided	• Has been used for several years with a proven safety profile • Doesn't require the additional purchase of a guide • Allows direct visualisation of the puncture site	• Susceptible to movement artefact associated with deglutition, talking and reactions to discomfort • Can be difficult to maintain in-line visualisation of the probe tip at all times • More challenging than the use of a guide for novel interventionalists

volume reduction of 67-75% at 12 months in patients treated with a single procedure, which increased to 94% in patients with repeated ablations consistent with previous findings (21). Thus, the clinical outcome of volume reduction in benign thyroid nodules has previously well documented.

RFA has also recently expanded its use in achieving not only volume reduction of thyroid nodules, but biochemical euthyroidism of patients with AFTN, where the risk of malignancy is exceedingly low. In a systematic review and meta-analysis conducted by Cesareo et al, the pooled rate of patients with TSH normalization was 57% with a pooled volume reduction rate of 79% at one year (22). The rate of success of RFA in AFTN has been significantly correlated not only with volume rate reduction but also with size of nodule, with nodules more likely to respond to treatment when baseline volume is <12mls (23). This has been postulated to relate to the ability to achieve complete ablation of conceptual subunits in smaller volume nodules, minimizing the risk of untreated autonomously hyperfunctioning residual tissue. Therefore, RFA has now been recommended as a treatment option in the majority of internationally established guidelines.8-14 Our practice is currently limited to patients with biopsy confirmed benign nodules or toxic adenomas that are less than 20mls in volume and located away from the danger triangle given the potential for undertreating hyperfunctioning ablation subunits to avoid risk of thermal injury.

Current consensus guidelines have established there is a significant learning curve for thyroid ablation required prior to providing optimal treatment for patients (8). Complete ablation of all conceptual subunits optimizes patient outcomes by increasing the success of the procedure and decreasing the need for additional treatment. The most recent ATA consensus statement indicates that clinical efficacy requires approximately 30 cases based on the results of three previously published series (24–26). We agree with the aforementioned studies and all our procedures are currently performed by two Otolaryngology Head and Neck Surgeons with significant previous expertise in both US and FNA. In addition to this, Improvements in volume rate reduction in benign thyroid nodules has also been attributed to expertise in electrode manoeuvrability, the amount of energy applied to each conceptual subunit and the use of colour doppler during the procedure to identify viable thyroid tissue (22). We feel that our novel guided technique proposed has several advantages. Firstly, the use of a radiofrequency probe guide attached to a high frequency linear ultrasound transducer ensures visualisation of the needle under direct vision for the entirety of the procedure. The probe can then be angled to target separate subunits of varying depth through the same puncture site. We have found the stability gained by the guide improves operator confidence in ablation of smaller conceptual subunits in close proximity to the recurrent laryngeal nerve and the carotid artery, areas often left unattended due to risk of injury. Secondly, the placement of a fixed guide negates the human error in movement often unavoidable during both talking and swallowing which we have found to be a significant advantage. It also facilitates ablation of multiple subunits through a single-entry site by rotating the probe in a counterclockwise fashion, commencing inferiorly and moving superiorly, yet maintaining direct vision. Further to this, the restraint of a guide facilitates the need for a systematic approach to ablation requiring the clinician to subdivide the outlined nodule into horizontal tracts spaced approximately 1cm apart, ensuring a more complete ablation. One of the challenges we recognise in the implementation of a novel interventional technique, pertains to not only familiarity with instrumentation but also the ability to consistently replicate the same result under varied conditions in patients with variable anatomy and we feel the use of a guide aids in achieving this. Further to this, we feel that in the infancy of clinicians adopting radiofrequency into their practice, such an approach facilitates consistency, adaptability and accounts for potential movement artefact otherwise experienced during deglutition, speech or as a reaction to discomfort experienced by the patient during the procedure. This is further enhanced by the use of a 10cm radiofrequency probe allowing an arc of rotation of 6cm, not otherwise achieved with shorter probes, highlighting its use in large benign nodules. However, the 7cm radiofrequency probe can also be used with modifications made to the needle guide. Of course, an individualized approach is required based on the patient's body habitus, the size and depth of the nodule and the clinician needs to remain cognizant of potential complications including nodule rupture, hematoma, nerve and tracheal injury which remain of paramount importance.

There is a currently a large amount of literature supporting radiofrequency ablation of thyroid nodules, however this is only amongst high volume thyroid interventionalists. As the use of RFA becomes more widespread amongst surgeons, a guided approach with the electrode tip fixed within the centre of the long axis field consistently, produces translatory bodily movement of both transducer and RF probe endorsing confidence in achieving accurate subunit ablation. This will allow the thyroid interventionalists to consistently ablate more conceptual subunits and potentially improve the efficiency of RFA in the management of

both benign and AFTN. Further prospective studies will aid in elucidating this as the technology increases in adoption rates across North America.

Conclusion

We present a novel radiofrequency probe guide which is simple and easy to attach to an ultrasound probe that provides a valuable addition to the head and neck surgeons armamentarium in RFA of thyroid nodule.

Data availability statement

The original contributions presented in the study are included in the article/supplementary material. Further inquiries can be directed to the corresponding author.

Author contributions

LS: Writing – review & editing, Writing – original draft, Formal analysis, Data curation, Conceptualization. KH: Writing – review & editing, Writing – original draft, Validation, Methodology, Investigation, Formal analysis, Data curation, Conceptualization. DE: Writing – review & editing, Writing – original draft, Methodology, Investigation, Formal analysis, Conceptualization. AE: Writing – review & editing, Writing – original draft, Visualization, Validation, Supervision, Software, Resources, Project administration, Methodology, Investigation, Funding acquisition, Formal analysis, Data curation, Conceptualization.

Funding

The author(s) declare that no financial support was received for the research, authorship, and/or publication of this article.

Conflict of interest

The authors declare that the research was conducted in the absence of any commercial or financial relationships that could be construed as a potential conflict of interest.

The handling editor PP-A declared a shared parent affiliation with all authors at the time of review.

Publisher's note

References

1. Yeung MJ, Serpell JW. Management of the solitary thyroid nodule. *Oncologist*. (2008) 13:105–12. doi: 10.1634/theoncologist.2007-0212

2. Boelaert K, Horacek J, Holder RL, Watkinson JC, Sheppard MC, Franklyn JA. Serum thyrotropin concentration as a novel predictor of Malignancy in thyroid nodules investigated by fine-needle aspiration. *J Clin Endocrinol Metab*. (2006) 91:4295–301. doi: 10.1210/jc.2006-0527

3. Erdoğan MF, Anil C, Ozer D, Kamel N, Erdoğan G. Is it useful to routinely biopsy hot nodules in iodine deficient areas? *J Endocrinol Invest*. (2003) 26:128–31.

4. Sarkis LM, Norlen O, Sywak M, Delbridge L. Minimally invasive thyroid nodulectomy reduces post-operative hypothyroidism when compared with thyroid lobectomy. *ANZ J Surg*. (2017) 87:360–3. doi: 10.1111/ans.12904

5. Verloop H, Louwerens M, Schoones JW, Kievit J, Smit JW, Dekkers OM. Risk of hypothyroidism following hemithyroidectomy: systematic review and meta-analysis of prognostic studies. *J Clin Endocrinol Metab*. (2012) 97:2243–55. doi: 10.1210/jc.2012-1063

6. Bergenfelz A, Jansson S, Kristoffersson A, Mårtensson H, Reihnér E, Wallin G, et al. Complications to thyroid surgery: results as reported in a database from a multicenter audit comprising 3,660 patients. *Langenbecks Arch Surg*. (2008) 393:667–73. doi: 10.1007/s00423-008-0366-7

7. Kim YS, Rhim H, Tae K, Park DW, Kim ST. Radiofrequency ablation of benign cold thyroid nodules: initial clinical experience. *Thyroid*. (2006) 16:361–7. doi: 10.1089/thy.2006.16.361

8. Kim JH, Baek JH, Lim HK, Ahn HS, Baek SM, Choi YJ, et al. Guideline committee for the Korean society of thyroid radiology (KSThR) and Korean society of radiology. 2017 thyroid radiofrequency ablation guideline: Korean society of thyroid radiology. *Korean J Radiol*. (2018) 19:632–55. doi: 10.3348/kjr.2018.19.4.632

9. Papini E, Crescenzi A, D'Amore A, Deandrea M, De Benedictis A, Frasoldati A, et al. Italian guidelines for the management of non-functioning benign and locally symptomatic thyroid nodules. *Endocr Metab Immune Disord Drug Targets*. (2023) 23:876–85.

10. Gharib H, Papini E, Garber JR, Duick DS, Harrell RM, Hegedüs L, et al. AACE/ACE/AME task force on thyroid nodules. American association of clinical endocrinologists, american college of endocrinology, and associazione medici endocrinologi medical guidelines for clinical practice for the diagnosis and management of thyroid nodules–2016 update. *Endocr Pract*. (2016) 22:622–39. doi: 10.4158/EP161208.GL

11. Dobnig H, Zechmann W, Hermann M, Lehner M, Heute D, Mirzaei S, et al. Radiofrequency ablation of thyroid nodules: "Good Clinical Practice Recommendations" for Austria : An interdisciplinary statement from the following professional associations: Austrian Thyroid Association (ÖSDG), Austrian Society for Nuclear Medicine and Molecular Imaging (OGNMB), Austrian Society for Endocrinology and Metabolism (ÖGES), Surgical Endocrinology Working Group (ACE) of the Austrian Surgical Society (OEGCH). *Wien Med Wochenschr*. (2020) 170:6–14. doi: 10.1007/s10354-019-0682-2

12. Orloff LA, Noel JE, Stack BC Jr, Russell MD, Angelos P, Baek JH, et al. Radiofrequency ablation and related ultrasound-guided ablation technologies for treatment of benign and Malignant thyroid disease: an international multidisciplinary consensus statement of the American Head and Neck Society Endocrine Surgery Section with the Asia Pacific Society of Thyroid Surgery, Associazione Medici Endocrinologi, British Association of Endocrine and Thyroid Surgeons, European Thyroid Association, Italian Society of Endocrine Surgery Units, Korean Society of Thyroid Radiology, Latin American Thyroid Society, and Thyroid Nodules Therapies Association. *Head Neck*. (2021) 44:633–60.

13. Papini E, Monpeyssen H, Frasoldati A, Hegedüs L. 2020 European Thyroid Association clinical practice guideline for the use of image-guided ablation in benign thyroid nodules. *Eur Thyroid J*. (2020) 9:172–85. doi: 10.1159/000508484

14. Sinclair CF, Baek JH, Hands KE, Hodak SP, Huber TC, Hussain I, et al. General principles for the safe performance, training, and adoption of ablation techniques for benign thyroid nodules: an American thyroid association statement. *Thyroid*. (2023) 33:1150–70. doi: 10.1089/thy.2023.0281

15. Shin JH, Baek JH, Ha EJ, Lee JH. Radiofrequency ablation of thyroid nodules: basic principles and clinical application. *Int J Endocrinol*. (2012) 2012:919650. doi: 10.1155/2012/919650

16. Goldberg SN. Radiofrequency tumor ablation: principles and techniques. *Eur J Ultrasound*. (2001) 13:129–47. doi: 10.1016/S0929-8266(01)00126-4

17. Baek JH, Moon WJ, Kim YS, Lee JH, Lee D. Radiofrequency ablation for the treatment of autonomously functioning thyroid nodules. *World J Surg*. (2009) 33:1971–7. doi: 10.1007/s00268-009-0130-3

18. Russell JO, Desai DD, Noel JE, Hussein M, Toraih E, Seo S, et al. Radiofrequency ablation of benign thyroid nodules: A prospective, multi-institutional North American experience. *Surgery*. (2024) 175:139–45. doi: 10.1016/j.surg.2023.07.046

19. Jung SL, Baek JH, Lee JH, Shong YK, Sung JY, Kim KS, et al. Efficacy and safety of radiofrequency ablation for benign thyroid nodules: A prospective multicenter study. *Korean J Radiol*. (2018) 19:167–74. doi: 10.3348/kjr.2018.19.1.167

20. Deandrea M, Sung JY, Limone P, Mormile A, Garino F, Ragazzoni F, et al. Efficacy and safety of radiofrequency ablation versus observation for nonfunctioning benign thyroid nodules: A randomized controlled international collaborative trial. *Thyroid*. (2015) 25:890–6. doi: 10.1089/thy.2015.0133

21. Monpeyssen H, Alamri A, Ben Hamou A. Long-term results of ultrasound-guided radiofrequency ablation of benign thyroid nodules: state of the art and future perspectives-A systematic review. *Front Endocrinol (Lausanne)*. (2021) 12:622996. doi: 10.3389/fendo.2021.622996

22. Cesareo R, Palermo A, Benvenuto D, Cella E, Pasqualini V, Bernardi S, et al. Efficacy of radiofrequency ablation in autonomous functioning thyroid nodules. A systematic review and meta-analysis. *Rev Endocr Metab Disord*. (2019) 20:37–44. doi: 10.1007/s11154-019-09487-y

23. Cesareo R, Naciu AM, Iozzino M, Pasqualini V, Simeoni C, Casini A, et al. Nodule size as predictive factor of efficacy of radiofrequency ablation in treating autonomously functioning thyroid nodules. *Int J Hyperthermia*. (2018) 34:617–23. doi: 10.1080/02656736.2018.1430868

24. Kuo CY, Liu CL, Tsai CH, Cheng SP. Learning curve analysis of radiofrequency ablation for benign thyroid nodules. *Int J Hyperthermia*. (2021) 38:1536–40. doi: 10.1080/02656736.2021.1993358

25. Bom WJ, Joosten FBM, van Borren MMGJ, Bom EP, van Eekeren RRJP, de Boer H. Radiofrequency ablation for symptomatic, non-functioning, thyroid nodules: A single center learning curve. *Endocr Connect*. (2022) 11:e210304. doi: 10.1530/EC-21-0304

26. Clark JE, Stan MN. The learning curve for radiofrequency ablation of benign thyroid nodules. *Clin Thyroidol*. (2021) 33:529–31. doi: 10.1089/ct.2021;33.529-531

frontiers | Frontiers in Endocrinology

TYPE Original Research
PUBLISHED 01 August 2024
DOI 10.3389/fendo.2024.1398208

OPEN ACCESS

EDITED BY
Pia Pace-Asciak,
University of Toronto, Canada

REVIEWED BY
Mojtaba Akbari,
Isfahan University of Medical Sciences, Iran
Yu Lan,
China Medical University, China

*CORRESPONDENCE
Songtao Zhang
zhst143@126.com

RECEIVED 09 March 2024
ACCEPTED 22 July 2024
PUBLISHED 01 August 2024

CITATION
Gong W, Zhang R, Zhang S, Zhai Y, Zheng C and Zhang D (2024) Comparison between thermal ablation and surgery in low risk papillary thyroid carcinoma: a prospective study.
Front. Endocrinol. 15:1398208.
doi: 10.3389/fendo.2024.1398208

Comparison between thermal ablation and surgery in low risk papillary thyroid carcinoma: a prospective study

Wenbo Gong, Runfang Zhang, Songtao Zhang*, Yifei Zhai, Chen Zheng and Dongyan Zhang

Department of Thyroid and Head & Neck Surgery, The Affiliated Cancer Hospital of Zhengzhou University & Henan Cancer Hospital, Zhengzhou, China

Objective: To conduct a comparative analysis of the efficacy, safety, and impact on quality of life outcomes between thermal ablation and surgical interventions in patients diagnosed with papillary thyroid carcinoma (PTC).

Methods: A prospective study was undertaken, enrolling patients with PTC ≤5mm who underwent radiofrequency ablation (RFA), laser ablation (LA), or surgery, for analysis of efficacy and safety outcomes. The Thyroid Cancer-Specific Quality of Life questionnaire was administered to all patients before treatment and at 3, 6, and 12 months post-treatment.

Results: A total of 162 eligible patients were included in the study. Major complications were not observed in the RFA and LA groups, while five cases were reported in the surgery group, although no statistically significant differences were observed. Minor complications were documented in two, three, and 14 patients in the RFA, LA, and surgery groups, respectively, with no significant variances noted. Surgical duration and hospitalization time were notably shorter in the thermal ablation groups. At the final follow-up, complete disappearance of nodules was seen in 71.4% of cases treated with RFA and 71.0% of cases managed with LA, with no significant disparities between the groups. Both RFA and LA exhibited similar effects on quality of life, with thermal ablation techniques showing better functional outcomes in comparison to surgery. Across all groups, adverse effects were most pronounced at the 3-month post-treatment mark but gradually reverted to baseline levels in the thermal ablation group, contrasting with the surgery group.

Conclusions: For PTC ≤5mm, both RFA and LA exhibited similar cancer control outcomes and superior quality of life on par with surgery, while minimizing complications. These findings underscore the promise of RFA and LA as potential standard treatments for small PTCs, subject to further confirmation in future studies.

KEYWORDS

radiofrequency ablation, laser ablation, quality of life, papillary thyroid carcinoma, thermal ablation

Introduction

Papillary thyroid carcinoma (PTC) stands as the most predominant form of endocrine malignancy (1). Advances in health consciousness and the utilization of high-resolution ultrasound have led to the identification of an increasing number of PTC cases with a primary tumor diameter ≤1.0 cm and no discernible cervical lymph node enlargement (2). While surgery has historically been the favored treatment modality, the swift progression of thermal techniques, in which radiofrequency ablation (RFA) and laser ablation (LA) is the most frequently used, offers an alternative approach, especially for patients at risk of anesthesia complications or adverse to visible scarring (3).

Various investigations have explored the efficacy and safety of thermal ablation in PTC, highlighting its high feasibility, favorable rate of tumor resolution, effective local disease management, and minimal complications (4–6). Additionally, multiple meta-analyses have revealed that, in comparison to surgery, thermal ablation yields comparable quality of life (QoL) outcomes and non-inferior prognoses at a reduced cost (7–11). Despite these encouraging results, many of these studies are constrained by their retrospective nature, and the comparison of QoL between thermal ablation and endoscopic surgery remains equivocal. Furthermore, occult metastasis plays a crucial role in determining treatment strategies, as delayed detection of occult metastasis can lead to increased surgical complications. Unfortunately, this aspect has often been overlooked in previous studies. It is worth noting that occult metastasis can develop in over 50% of cases of cT1N0 PTC (12), with tumor size playing a significant role. Current evidence indicates that compared to PTC ≤5mm, the risk of lymph node metastasis is nearly five times higher in cases of PTC >5mm (13).

Henceforth, our aim is to undertake a prospective assessment of the effectiveness, safety, and QoL outcomes of thermal ablation and endoscopic surgery in individuals diagnosed with cN0 PTC ≤5mm.

Patients and methods

Ethical considerations

This study was approved by the Institutional Research Committee of Henan Cancer Hospital (No.2020-LC156), and all patients provided written informed consent for participation in medical research prior to undergoing treatment. All methods and procedures adhered to relevant guidelines and regulations.

Study design

A prospective investigation was carried out from January 2021 to January 2022 to explore the favored therapeutic approach among individuals with cN0 solitary PTC ≤5mm. Prior to treatment, all patients underwent preoperative fine needle aspiration biopsy and genetic mutation profiling encompassing BRAF, RAS, RET, CTNNB1, TERT, PAX8-PPARγ, and PTEN. The findings were evaluated in accordance with the Bethesda classification system (14), with only patients exhibiting thyroid nodules categorized as Bethesda category V or VI being included in the study. In instances where two or more gene mutations were identified, surgery was recommended over thermal ablation. The selection of treatment modality predominantly hinged upon patient preference and the proficiency of the surgical team.

Patients who opted for thermal ablation or surgery were included, while those with a history of prior cancer or other specific characteristics were excluded (Figure 1). Participants completed the Thyroid Cancer-Specific Quality of Life (THYCA-QoL) questionnaire both before and at 3, 6, and 12 months postoperatively.

Variable definitions

The absence of clinically positive lymph nodes was defined as cN0 (4). Tumor size was determined by the largest diameter measured via ultrasound (5). Major complications were characterized as those with the potential to be life-threatening, cause significant morbidity or disability, and included complications such as prolonged vocal paralysis (lasting>6 months), neck hematoma necessitating surgical intervention, surgical site infection, lymphatic fistula, and permanent hypoparathyroidism (lasting >6 months) (15). Minor complications encompassed transient voice or vocal dysfunction, transient hypoparathyroidism (lasting<6 months), bleeding managed with local compression, and moderate pain requiring medication (15). Mild side effects such as transient post-procedural pain, heat sensation, and neck discomfort that did not necessitate intervention or prescription medications were not included in the analysis (15). Operation time was defined as the duration between the onset of local anesthesia and completion of ablation in the RFA/LA group, and the duration between skin incision and wound closure in the surgery group (6). Hospitalization period was considered as the time from completion of thermal ablation or surgery to discharge (10). Recurrence was identified as lymph node or distant metastasis (16).

Sonographic characteristics of the nodules were meticulously evaluated, with three orthogonal dimensions of the nodule measured, including the largest diameter and the other two perpendicular dimensions. The volume was calculated using the formula: $\pi * L * W * H/6$, where L represents the largest diameter, and W and H are the perpendicular dimensions. The volume reduction ratio (VRR) was calculated as follows: [(initial volume - final volume) * 100]/initial volume. The initial volume was defined as the tumor volume measured on conventional ultrasound before treatment, while the final volume was defined as the volume of the ablated area measured on conventional ultrasound during each follow-up (6).

Quality of life

The THYCA-QoL questionnaire, primarily designed to assess quality of life post-thyroidectomy, was employed in this study (11, 17). Comprising 24 items evaluating seven scales

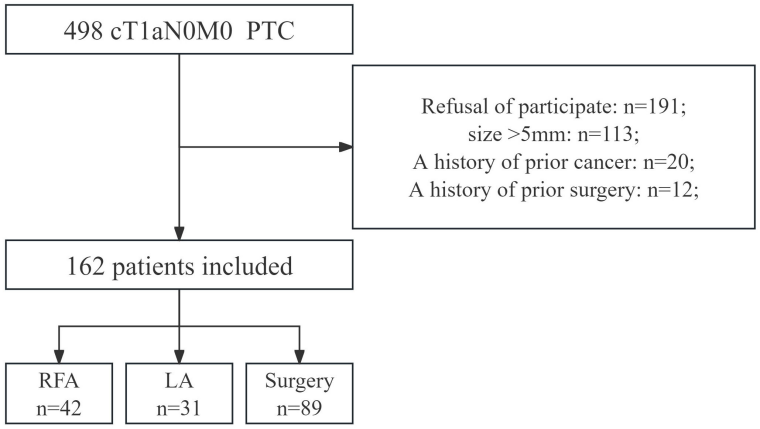

FIGURE 1
Flow chart of patients enrolled for this research.

(neuromuscular, voice, concentration, sympathetic, throat/mouth, psychological, and sensory problems) and six single items (scar, chilly, tingling, weight gain, headache, and anxiety) over the past week. Each item was rated on a four-point response scale from 1 = "not at all" to 4 = "very much". Scores were linearly transformed to a 0-100 scale, with higher scores indicating greater complaints.

Treatment

Thermal ablation encompassed RFA and LA procedures, both conducted by the same two physicians (YZ and WG) with 5 years' experience under local anesthesia. RFA utilized a generator and an 18-gauge internally cooled electrode with 5mm or 7mm active tips (Minimax Medical, China), according to tumor size and surgeon preference. The LA system (Esaote, Italy) included an optical beam-splitting device and a plane-cut optic fiber measuring 1.5 m in length and 300 μm in diameter. During LA, the fiber was connected to a continuous-wave neodymium yttrium-aluminum-garnet (Nd: YAG) laser source operating at a wavelength of 1064 nm with an output power of 3-4 W.

Endoscopic surgery was performed via axilla approaches, while open surgery was conducted through an anterior cervical median incision, involving unilateral thyroidectomy with central lymph node dissection. All surgeries were performed by a professor (SZ) with 20 years' experience.

Statistical analysis

During the baseline data comparison, the Chi-square test was employed for categorical variables, while the Student's t-test was utilized for continuous variables. The primary outcome variables assessed across various groups encompassed efficacy, safety, and QoL. For the evaluation of efficacy and safety, continuous and categorical outcomes were compared using independent-samples t-tests and Chi-square tests, respectively. In the examination of QoL, the outcomes were scrutinized through Two-way repeated-measures ANOVA with the Bonferroni correction method. The threshold for statistical significance was established at $p < 0.05$.

Results

Baseline data

A total of 162 participants were included in the analysis, with a mean age of 50.9 ± 12.5 years, comprising 68 (42.0%) men and 94 (58.0%) women. The average volume of malignant nodules measured 32.3 ± 13.4 mm^3. Hashimoto's thyroiditis was present in 17 (10.5%) patients, whereas hypothyroidism was observed in two (1.2%) patients. Central lymph node metastasis was identified in three (3.3%) patients undergoing surgery. These clinicopathologic variables were evenly distributed across all three groups (all $p>0.05$) (Table 1).

Efficacy

The mean operation time for the RFA and LA groups was 5.5 ± 4.3 minutes and 6.1 ± 3.9 minutes, respectively, which were significantly shorter than the average operation time of 58.6 ± 23.5 minutes in the surgery group ($p<0.001$). Patients treated with RFA or LA had an average hospital stay of approximately one day, while those in the surgery group stayed for an average of 4.2 ± 1.3 days, indicating a significant difference ($p<0.001$). At the last follow-up, complete disappearance was noted in 71.4% of nodules treated with RFA and 71.0% of those subjected to LA. The difference was not statistically significant ($p=0.966$). There were no instances of cervical lymph node or distant metastasis, nor occurrences of hypothyroidism in the RFA and LA groups (Table 2).

Over the follow-up period, variations in VRR were observed. In the RFA group, the mean VRR was 26.6% ± 9.4%, 76.4% ± 14.3%, and 93.1% ± 14.2% at 3, 6, and 12 months postoperatively. In the LA group, the mean VRR was 25.8% ± 7.6%, 81.0% ± 10.5%, and 94.0% ± 11.3% at 3, 6, and 12 months postoperatively. Both techniques exhibited comparable changes in VRR.

TABLE 1 Baseline data of T1aN0M0 patients treated by radiofrequency ablation (RFA), laser ablation (LA) and surgery.

Variable	RFA (n=42)	LA (n=31)	Surgery (n=89)	p
Age	51.4 ± 10.5	52.6 ± 9.3	50.0 ± 14.6	0.286
Sex				
Male	16 (38.1%)	13 (41.9%)	39 (43.8%)	
Female	26 (61.9%)	18 (58.1%)	50 (56.2%)	0.825
Volume (mm^3)	30.5 ± 10.2	31.8 ± 12.0	33.3 ± 15.4	0.400
Hashimoto's thyroiditis				
Yes	5 (11.9%)	3 (9.7%)	9 (10.1%)	0.940
Hypothyroidism				
Yes	0	0	2 (2.2%)	0.502
Lymph node metastasis	–	–	3	

The symbol "-" represents "no data".

Safety

No major complications occurred in the RFA or LA groups; however, four complications were reported in the surgery group (vocal paralysis: n=1; voice change: n=1; hematoma: n=1; surgical site infection: n=1). The difference was not significant among the three groups (p=0.179). Minor complications were more prevalent, with a total of 13 cases. In the RFA group, one patient experienced vocal paralysis and bleeding. Similarly, in the LA group, one patient each reported voice change, bleeding, and pain. Among the surgery group, bleeding (n=3) was the most common issue, while vocal paralysis (n=1) was the least frequent. Nonetheless, the differences were not statistically significant (p=0.733) (Table 3).

TABLE 3 Safety of radiofrequency ablation (RFA), laser ablation (LA), and surgery in T1aN0M0 papillary thyroid carcinoma patients.

Complication	RFA (n=42)	LA (n=31)	Surgery (n=89)	p
Major				
Vocal paralysis	0	0	1 (1.1%)	
Voice change	0	0	1 (1.1%)	
Hematoma	0	0	1 (1.1%)	
Infection	0	0	1 (1.1%)	
Fistula	0	0	0	
Total	0	0	4 (4.4%)	0.179
Minor				
Vocal paralysis	1 (2.4%)	0	1 (1.1%)	
Voice change	0	1 (3.2%)	2 (2.2%)	
Bleeding	1(2.4%)	1 (3.2%)	3 (3.3%)	
Pain	0	1 (3.2%)	2 (2.2%)	
Total	2 (4.8%)	3 (9.7%)	8 (9.0%)	0.733

Quality of life

All participants completed the questionnaire, resulting in a response rate of 100%. Baseline quality of life scores were 3.0 ± 2.1 for the RFA group, 2.2 ± 2.0 for the LA group, and 3.2 ± 3.0 for the surgery group, with no significant differences observed. At 3 months postoperatively, the mean quality of life score increased to 17.3 ± 10.2 in the surgery group, significantly higher (both p<0.001) than those of the other two groups. By 6 months postoperatively, overall quality of life began to improve, with patients treated with surgery achieving a mean score of 12.2 ± 8.6, still higher (both p<0.001) than the scores of 6.2 ± 4.2 in the RFA group and 5.5 ± 4.3 in the LA group. After 12 months, quality of life tended to return to baseline levels, but patients managed with surgery had higher mean scores compared to those treated with RFA (p=0.005) or LA (p=0.004) (Figure 2).

TABLE 2 Efficacy of radiofrequency ablation (RFA), laser ablation (LA), and surgery in T1aN0M0 papillary thyroid carcinoma patients at last follow-up.

Variable	RFA (n=42)	LA (n=31)	Surgery (n=89)	p
Operation time (minute)	5.5 ± 4.3	6.1 ± 3.9	58.6 ± 23.5	<0.001
Hospitalization (day)	1.0 ± 0.3	1.0 ± 0.3	4.2 ± 1.3	<0.001
Complete disappearance	30 (71.4%)	22 (71.0%)	–	0.966
Recurrence	0	0	2 (2.2%)	0.502
Hypothyroidism	0	0	–	1.000

The symbol "-" represents "no data".

Post-ablation evaluation

At the 12-month follow-up, residual lesions were identified in ultrasound scans for 12 patients treated with RFA and nine patients managed with LA. Fine needle aspiration biopsies were performed

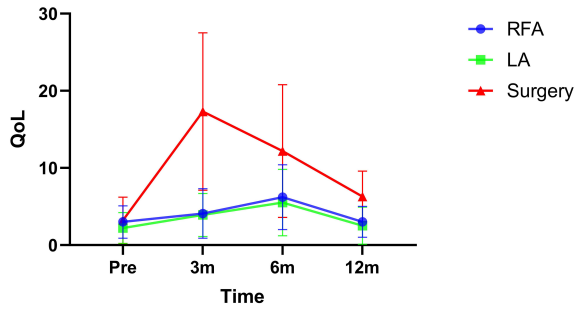

FIGURE 2
Quality of life (QoL) in radiofrequency ablation (RFA), laser ablation (LA), or surgery groups at different time points.

on all these cases, confirming the absence of cancer cells, with findings indicating fibrous connective tissue or necrotic cells.

Discussion

The paramount discovery of our study lies in the establishment of the safety and efficacy of both RFA and LA as treatments for patients with PTC ≤5mm, yielding comparable outcomes with minimal complications. In comparison to surgery, RFA and LA demonstrated equivalent cancer control while posing fewer risks. While the QoL experienced a decline in all three groups following treatment, this decline was less pronounced in thermal ablation procedures than in surgery. Moreover, QoL showed a tendency towards restoration to baseline levels within a year. These results underscore the effectiveness, safety, and advantages of RFA and LA in the management of PTC, providing valuable insights for individualized treatment decision-making.

The issue of safety has been a paramount concern and has undergone meticulous examination. In an extensive review conducted by Ming et al. (18), it was highlighted that a small fraction of patients exhibited symptoms linked to thermal damage. Common complications post thermal ablation in previous studies included transient hoarseness and a burning sensation, with the majority of these symptoms spontaneously resolving within a brief timeframe. Tong et al. (19) also compiled the cumulative incidence of complications observed in RFA and LA, reporting rates of 4.0% for the former and 2.0% for the latter, with no occurrences of life-threatening events. To some extent, our study corroborated these findings, unveiling a complication rate of 4.7% for RFA and 9.7% for LA, slightly surpassing previous documentation. Various factors may contribute to these disparities. Primarily, unlike the studies mentioned, we classified complications as major and minor, with no major complications identified in our analysis. Secondly, the safety of the thermal ablation procedure is intricately linked to the tumor's location. Tumors situated in close proximity to the trachea or within the posterior thyroid region adjacent to the capsule, where the recurrent laryngeal nerve travels, present a relatively higher risk of recurrent laryngeal nerve injury during ablation. Thirdly, variations in operator expertise and procedural techniques may lead to incidental complications like bleeding and neck swelling. Lastly, inconsistent definitions of complications and our relatively modest sample size may have influenced the outcomes. In the comparison with surgical interventions, while a greater number of adverse events were noted in patients undergoing surgery, the difference lacked statistical significance. This discovery aligns with findings from other reviews (15, 20). Both RFA and LA are minimally invasive methods that induce tissue necrosis through thermal energy, eliminating the necessity for anatomical dissection.

The evaluation of VRR stands as a crucial parameter for assessing the effectiveness of thermal ablation. In a comprehensive analysis by Choi et al. (15), it was reported that the rates of complete disappearance were 48.7% for the LA group and 65.2% for the RFA group. Remarkably, these rates surged to 93% for LA and 81% for RFA in subsequent investigations by Gao et al. (21). These outcomes, including our own, can be attributed to various factors. Initially, the timing of assessing complete disappearance status is pivotal, highlighting the prolonged immune-mediated absorption process of residual tumors within the body. Discrepancies in follow-up durations across available literature may not allow ample time for the complete absorption of certain tumors. Teng et al. (22) showcased a substantial reduction in volume from a median of 55.78 mm^3 to 0 mm^3 ($p < 0.001$) at 60 months post-treatment. Our study aligns with this observation, indicating persistent reduction in tumor size, particularly notable at three to six months post-surgery. Additionally, residual calcification and fibrous scarring within the tumor may impede the complete disappearance of tumor volume. These remnants manifest as non-enhancing zones on contrast-enhanced ultrasound and are confirmed as necrotic material through fine-needle aspiration biopsies (6).

The consideration of QoL emerges as a pivotal aspect that has been relatively understudied in comparative analyses between thermal ablation and surgery. In a prospective study conducted by Zheng et al. (10), wherein 92 patients with PTC underwent thermal ablation and 106 patients opted for surgical excision, both cohorts were monitored for approximately 12 months. Significantly, the surgical group exhibited elevated scores indicative of scar-related issues and heightened anxiety. In the investigation by Li et al. (23), a comparison between the thermal ablation and surgical groups revealed that the former showcased superior ratings in global health, physical well-being, and emotional stability. Notably, except for headaches, the thermal ablation group attained lower scores across other domains in the THYCA-QoL questionnaire when juxtaposed with the surgery cohort. These studies collectively brought to light that thermal ablation was associated with an enhanced QoL relative to surgery, notwithstanding the use of microwave technology in the thermal ablation approach as opposed to RFA and LA. Studies by Lan et al. (24, 25) further reinforced that RFA engendered better QoL outcomes compared to surgery, although their investigations were delimited by a retrospective design. Significantly, the exploration of the correlation between LA and QoL in PTC has been limited in the extant literature. Thus, our study potentially forges ahead by delving into this domain, revealing that both RFA and LA evoke similar effects on QoL, showcasing superior functional outcomes in contrast to surgery. Furthermore, across all groups, the nadir of adverse effects was most pronounced at the 3-month post-treatment juncture, gradually improving towards baseline levels in the thermal ablation cohort as opposed to the surgery cohort. This intriguing finding could potentially be ascribed to the inherently minimally invasive nature of RFA and LA, whereas endoscopic thyroid surgery, while more aesthetically pleasing, triggers the formation of scar tissue within the cavity, a process that initiates healing from the third month onwards.

Previous evidence has validated the favorable outcomes delivered by thermal ablation (1, 3–6). However, all these studies encompassed a large cohort of patients with PTC >5mm in size and overlooked the presence of occult metastasis, a factor significantly influenced by tumor size. In comparison to PTC ≤5mm, PTC >5mm conferred an additional 4-fold risk of lymph node metastasis (13). Although these researchers noted similar cancer control outcomes between thermal ablation and surgery, the detection of metastasized lymph nodes clinically required considerable time, thus limiting the scope of many studies due to relatively short follow-up durations. In our oncology

center, the utilization of RFA and LA for PTC was meticulously regulated based on tumor size and other pertinent characteristics. PTC ≤5mm presented an exceedingly low risk of occult metastasis.

There is a divergence in the management of small, low-risk PTC globally. While active surveillance is deemed appropriate for patients with small, intrathyroidal PTC lacking aggressive cytopathology, local invasion, or clinically detectable metastases, and has shown favorable outcomes such as a low growth rate, rare regional or distal lymph node metastases, and low mortality (26, 27), Chinese patients often experience anxiety and nervousness due to the potential diagnosis of even a small PTC. As a result, immediate treatment is typically sought based on the psychological state of the patient, and preoperative fine needle biopsy is mandated before definitive therapy according to official guidelines in China (28, 29). On the other hand, long-term QoL considerations are paramount in the management of indolent, slow-growing PTC, particularly in the current era of conservative management. Options have expanded to include minimally invasive approaches; however, unlike active surveillance, any invasive therapy could potentially diminish QoL to varying degrees. Therefore, the burden of surveillance and the level of concern should be carefully weighed when determining the most suitable approach (30).

Acknowledgment of the limitations of the current study is crucial. Firstly, the relatively modest sample size may have reduced the statistical power of our findings, highlighting the need for a larger size trial. Secondly, our inclusion was limited to patients with PTC ≤ 5mm in size, necessitating future studies to incorporate a wider range of PTC sizes. Lastly, as this study was conducted at a single institution, external validation is essential before widespread clinical implementation.

In conclusion, for PTC ≤5mm, both RFA and LA exhibited similar cancer control outcomes and superior quality of life on par with surgery, while minimizing complications. These findings underscore the promise of RFA and LA as potential standard treatments for small PTCs, subject to further confirmation in future studies.

Data availability statement

The original contributions presented in the study are included in the article/supplementary material. Further inquiries can be directed to the corresponding author.

Ethics statement

The Henan Cancer Hospital Institutional Research Committee approved this study, and written informed consent agreements for medical research were obtained from all patients before undergoing initial treatment. The studies were conducted in accordance with the local legislation and institutional requirements. The participants provided their written informed consent to participate in this study.

Author contributions

WG: Writing – original draft, Writing – review & editing. RZ: Writing – original draft, Writing – review & editing. SZ: Writing – original draft, Writing – review & editing. YZ: Writing – original draft, Writing – review & editing. CZ: Writing – original draft, Writing – review & editing. DZ: Writing – original draft, Writing – review & editing.

Funding

The author(s) declare financial support was received for the research, authorship, and/or publication of this article. The manuscript was sponsored by Henan provincial Medical Science and Technology Research Project (No.LHGJ20200181).

Conflict of interest

The authors declare that the research was conducted in the absence of any commercial or financial relationships that could be construed as a potential conflict of interest.

Publisher's note

References

1. Li X, Yan L, Xiao J, Li Y, Yang Z, Zhang M, et al. Long-term outcomes and risk factors of radiofrequency ablation for T1N0M0 papillary thyroid carcinoma. *JAMA Surg*. (2024) 159:51–8. doi: 10.1001/jamasurg.2023.5202

2. Liu Q, Song M, Zhang H. Choice of management strategy for papillary thyroid microcarcinoma: active surveillance or immediate surgery? *J Cancer*. (2024) 15:1009–20. doi: 10.7150/jca.91612

3. Chung SR, Baek JH, Choi YJ, Lee JH. Thermal ablation for the management of papillary thyroid microcarcinoma in the era of active surveillance and hemithyroidectomy. *Curr Oncol Rep*. (2022) 24:1045–52. doi: 10.1007/s11912-022-01268-2

4. Cao XJ, Wang SR, Che Y, Liu J, Cong ZB, He JF, et al. Efficacy and safety of thermal ablation for treatment of solitary T1N0M0 papillary thyroid carcinoma: A multicenter retrospective study. *Radiology*. (2021) 300:209–16. doi: 10.1148/radiol.2021202735

5. Cao XJ, Liu J, Zhu YL, Qi L, Liu G, Wang HL, et al. Efficacy and safety of thermal ablation for solitary T1bN0M0 papillary thyroid carcinoma: A multicenter study. *J Clin Endocrinol Metab*. (2021) 106:e573–81. doi: 10.1210/clinem/dgaa776

6. Zhou W, Ni X, Xu S, Zhang L, Chen Y, Zhan W. Ultrasound-guided laser ablation versus microwave ablation for patients with unifocal papillary thyroid microcarcinoma: A retrospective study. *Lasers Surg Med*. (2020) 52:855–62. doi: 10.1002/lsm.23238

7. Kim HJ, Cho SJ, Baek JH. Comparison of thermal ablation and surgery for low-risk papillary thyroid microcarcinoma: A systematic review and meta-analysis. *Korean J Radiol*. (2021) 22:1730–41. doi: 10.3348/kjr.2020.1308

8. Chen S, Mao Y, Chen G. Economic effect between surgery and thermal ablation for patients with papillary thyroid microcarcinoma: a systemic review and meta-analysis. *Endocrine*. (2022) 76:9–17. doi: 10.1007/s12020-022-02991-3

9. Shen K, Xue S, Xie Y, Wang H, Li J, Sun Y, et al. Comparison of thermal ablation and routine surgery for the treatment of papillary thyroid microcarcinoma: a systematic review and Meta-analysis. *Int J Hyperthermia*. (2020) 37:913–24. doi: 10.1080/02656736.2020.1777331

10. Zheng L, Dou JP, Liu FY, Yu J, Cheng ZG, Yu XL, et al. Microwave ablation vs. surgery for papillary thyroid carcinoma with minimal sonographic extrathyroid extension: a multicenter prospective study. *Eur Radiol*. (2023) 33:233–43. doi: 10.1007/s00330-022-08962-6

11. Ledesma-Leon T, Solis-Pazmino P, Lincango EP, Figueroa LA, Ellenhorn J, Nasseri Y, et al. Ablation techniques or active surveillance compared to surgical resection in patients with low-risk papillary thyroid cancer: a systematic review and meta-analysis. *Endocrine*. (2024) 83:330–41. doi: 10.1007/s12020-023-03502-8

12. Tang L, Qu RW, Park J, Simental AA, Inman JC. Prevalence of occult central lymph node metastasis by tumor size in papillary thyroid carcinoma: A systematic review and meta-analysis. *Curr Oncol*. (2023) 30:7335–50. doi: 10.3390/curroncol30080532

13. Zhang X, Chen W, Fang Q, Fan J, Feng L, Guo L, et al. Lateral lymph node metastases in T1a papillary thyroid carcinoma: stratification by tumor location and size. *Front Endocrinol (Lausanne)*. (2021) 12:716082. doi: 10.3389/fendo.2021.716082

14. Cibas ES, Ali SZ. The 2017 bethesda system for reporting thyroid cytopathology. *Thyroid*. (2017) 27:1341–6. doi: 10.1089/thy.2017.0500

15. Choi Y, Jung SL. Efficacy and safety of thermal ablation techniques for the treatment of primary papillary thyroid microcarcinoma: A systematic review and meta-analysis. *Thyroid*. (2020) 30:720–31. doi: 10.1089/thy.2019.0707

16. Xu S, Huang H, Huang Y, Qian J, Wang X, Xu Z, et al. Comparison of lobectomy vs total thyroidectomy for intermediate-risk papillary thyroid carcinoma with lymph node metastasis. *JAMA Surg*. (2023) 158:73–9. doi: 10.1001/jamasurg.2022.5781

17. Wang Z, Qi P, Zhang L, Zhang B, Liu X, Shi Q, et al. Is routine drainage necessary after thyroid surgery? A randomized controlled trial study. *Front Endocrinol (Lausanne)*. (2023) 14:1148832. doi: 10.3389/fendo.2023.1148832

18. Min Y, Wang X, Chen H, Chen J, Xiang K, Yin G. Thermal ablation for papillary thyroid microcarcinoma: how far we have come? *Cancer Manag Res*. (2020) 12:13369–79. doi: 10.2147/CMAR.S287473

19. Tong M, Li S, Li Y, Li Y, Feng Y, Che Y. Efficacy and safety of radiofrequency, microwave and laser ablation for treating papillary thyroid microcarcinoma: a systematic review and meta-analysis. *Int J Hyperthermia*. (2019) 36:1278–86. doi: 10.1080/02656736.2019.1700559

20. Mauri G, Hegedüs L, Bandula S, Cazzato RL, Czarniecka A, Dudeck O, et al. European thyroid association and cardiovascular and interventional radiological society of europe 2021 clinical practice guideline for the use of minimally invasive treatments in Malignant thyroid lesions. *Eur Thyroid J*. (2021) 10:185–97. doi: 10.1159/000516469

21. Gao X, Yang Y, Wang Y, Huang Y. Efficacy and safety of ultrasound-guided radiofrequency, microwave and laser ablation for the treatment of T1N0M0 papillary thyroid carcinoma on a large scale: a systematic review and meta-analysis. *Int J Hyperthermia*. (2023) 40:2244713. doi: 10.1080/02656736.2023.2244713

22. Teng DK, Li WH, Du JR, Wang H, Yang DY, Wu XL. Effects of microwave ablation on papillary thyroid microcarcinoma: A five-year follow-up report. *Thyroid*. (2020) 30:1752–8. doi: 10.1089/thy.2020.0049

23. Li Y, Huo SN, Lu NC, Peng LL, Wei Y, Zhao ZL, et al. A comparative study of quality of life in patients with papillary thyroid carcinoma undergoing microwave ablation vs. *Total thyroidectomy. Int J Hyperthermia*. (2023) 40:2250935. doi: 10.1080/02656736.2023.2250935

24. Lan Y, Luo Y, Zhang M, Jin Z, Xiao J, Yan L, et al. Quality of life in papillary thyroid microcarcinoma patients undergoing radiofrequency ablation or surgery: A comparative study. *Front Endocrinol (Lausanne)*. (2020) 11:249. doi: 10.3389/fendo.2020.00249

25. Lan Y, Jin Z, Zhang Y, Song Q, Xiao J, Yan L, et al. Factors associated with health-related quality of life in papillary thyroid microcarcinoma patients undergoing radiofrequency ablation: a cross-sectional prevalence study. *Int J Hyperthermia*. (2020) 37:1174–81. doi: 10.1080/02656736.2020.1812738

26. Pace-Asciak P, Russell JO, Tufano RP. The treatment of thyroid cancer with radiofrequency ablation. *Tech Vasc Interv Radiol*. (2022) 25:100825. doi: 10.1016/j.tvir.2022.100825

27. Cho SJ, Suh CH, Baek JH, Chung SR, Choi YJ, Chung KW, et al. Active surveillance for small papillary thyroid cancer: A systematic review and meta-analysis. *Thyroid*. (2019) 29:1399–408. doi: 10.1089/thy.2019.0159

28. Chinese Society of Clinical Oncology (CSCO) diagnosis and treatment guidelines for persistent/recurrent and metastatic differentiated thyroid cancer 2018 (English version). *Chin J Cancer Res*. (2019) 31:99–116. doi: 10.21147/j.issn.1000-9604.2019.01.06

29. Society of Tumor Ablation Therapy of the Chinese Anti-Cancer Association, Ablation Expert Committee of the Chinese Society of Clinical Oncology (CSCO), Chinese Medical Doctor Association College of Interventionalists Tumor Ablation Committee and Chinese Bethune Spirit Research Association Endocrinology and Diabetes Branch Interventional Endocrine Committee. Expert consensus on thermal ablation of papillary thyroid cancer (2024 edition). *Zhonghua Nei Ke Za Zhi*. (2024) 63:355–64. doi: 10.3760/cma.j.cn112138-20231104-00296

30. Pace-Asciak P, Russell JO, Tufano RP. Review: Improving quality of life in patients with differentiated thyroid cancer. *Front Oncol*. (2023) 13:1032581. doi: 10.3389/fonc.2023.1032581

frontiers | Frontiers in Endocrinology

TYPE Original Research
PUBLISHED 22 August 2024
DOI 10.3389/fendo.2024.1364782

OPEN ACCESS

EDITED BY
Pia Pace-Asciak,
University of Toronto, Canada

REVIEWED BY
Subhash Kumar Tripathi,
Seattle Children's Research Institute, United States
Ricardo Pujol Borrell,
Autonomous University of Barcelona, Spain

*CORRESPONDENCE
Huibin Huang
huibinhuang@aliyun.com

†These authors have contributed equally to this work

RECEIVED 03 January 2024
ACCEPTED 25 July 2024
PUBLISHED 22 August 2024

CITATION
Jiang Z, Cai H, Lin Y, Lin R, Chen L and Huang H (2024) T-cell exhaustion-related genes in Graves' disease: a comprehensive genome mapping analysis.
Front. Endocrinol. 15:1364782.
doi: 10.3389/fendo.2024.1364782

T-cell exhaustion-related genes in Graves' disease: a comprehensive genome mapping analysis

Zhengrong Jiang[1†], Huiyao Cai[1†], Yizhao Lin[2], Ruhai Lin[1], Lijun Chen[1] and Huibin Huang[1*]

[1]Department of Endocrinology, Second Affiliated Hospital of Fujian Medical University, Quanzhou, Fujian, China, [2]Department of Internal Medicine, Gutian County Hospital of Ningde City, Ningde, Fujian, China

Background: T-cell exhaustion (Tex) can be beneficial in autoimmune diseases, but its role in Graves' disease (GD), an autoimmune disorder of the thyroid, remains unknown. This study investigated Tex-related gene expression in GD patients to discern the potential contributions of these genes to GD pathogenesis and immune regulation.

Methods: Through gene landscape analysis, a protein–protein interaction network of 40 Tex-related genes was constructed. mRNA expression levels were compared between GD patients and healthy control (HCs). Unsupervised clustering categorized GD cases into subtypes, revealing distinctions in gene expression, immune cell infiltration, and immune responses. Weighted gene co-expression network analysis and differential gene expression profiling identified potential therapeutic targets. RT-qPCR validation of candidate gene expression was performed using blood samples from 112 GD patients. Correlations between Tex-related gene expression and clinical indicators were analyzed.

Results: Extensive Tex-related gene interactions were observed, with six genes displaying aberrant expression in GD patients. This was associated with atypical immune cell infiltration and regulation. Cluster analysis delineated two GD subtypes, revealing notable variations in gene expression and immune responses. Screening efforts identified diverse drug candidates for GD treatment. The Tex-related gene *CBL* was identified for further validation and showed reduced mRNA expression in GD patients, especially in cases of relapse. *CBL* mRNA expression was significantly lower in patients with moderate-to-severe thyroid enlargement than in those without such enlargement. Additionally, *CBL* mRNA expression was negatively correlated with the disease-specific indicator thyrotropin receptor antibodies.

Conclusion: Tex-related genes modulate GD pathogenesis, and their grouping aids subtype differentiation and exploration of therapeutic targets. *CBL* represents a potential marker for GD recurrence.

KEYWORDS

Graves' disease, T-cell exhaustion, weighted gene co-expression network analysis, *CBL*, enlargement of thyroid gland

Introduction

Graves' disease (GD) is a prevalent autoimmune thyroid disorder that affects an estimated 0.5–2% of the global population (1). GD commonly manifests as symptomatic thyrotoxicosis, dysregulated hormone levels, and the presence of thyrotropin receptor antibodies (TRAb), conditions that can lead to life-threatening hyperthyroid crisis in some cases, leading to considerable morbidity and mortality (2). A thorough understanding of the etiology and pathogenesis of GD is necessary for the development of precise diagnostic methods and effective therapeutic interventions. Central to GD pathology is discernible derangement of T-cell functionality, which prompts a cascade of events that lead to the breakdown of immune tolerance, aberrant immunoregulation, heightened B-cell reactivity, and ultimately injury to the thyroid and associated tissues (3). However, the nuanced mechanisms responsible for the alterations in T-cell function observed in GD remain incompletely understood.

T lymphocytes, commonly referred to as T cells, assume a central role as effectors in the immune system and are mobilized in response to antigenic stimuli. This orchestrated response entails rapid T-cell proliferation and differentiation, culminating in the development of both effector T cells and memory T cells—a process indispensable for the preservation of immune homeostasis. Dysregulation of T-cell function is intricately associated with the onset of autoimmune pathologies (4). Specifically, T-cell exhaustion (Tex) represents a consequential deviation in T-cell differentiation, evoked by prolonged exposure to antigenic stimulation and/or inflammation (5). Hallmarks of Tex include progressive functional decline, sustained elevation of inhibitory receptors, alterations in transcription factor expression and utilization, and metabolic perturbations. Importantly, exhausted T cells lack the antigen-independent homeostatic proliferative capacity exhibited by memory T cells (6). The well-established connection of Tex with viral infections and compromised anti-tumor responses highlights its pivotal role. Within the tumor microenvironment, Tex may contribute to a waning anti-tumor immune response, fostering immune tolerance. Conversely, in autoimmune diseases, Tex may be beneficial, as depleted T cells modulate autoimmune responses through immunoregulatory mechanisms, thereby contributing to the restoration of immune homeostasis (7). Existing research underscores the correlation between the transcriptional profile of Tex and the therapeutic efficacy and prognosis across diverse autoimmune diseases, including systemic lupus erythematosus (SLE), type 1 diabetes mellitus, antineutrophil cytoplasmic antibody-associated vasculitis disease, rheumatoid arthritis (RA), and idiopathic pulmonary fibrosis (8). Although Tex has been studied in many autoimmune diseases, little evidence for its role in GD can be found in the current literature. An in-depth exploration of Tex within the context of GD would provide important insight into the precise mechanisms that underlie abnormal T-cell function in this specific autoimmune thyroid disorder.

In the present study, we first delineated molecular subtypes of GD by scrutinizing the expression profiles of Tex-related genes in the peripheral blood mononuclear cells (PBMCs) of GD patients. Through a meticulous analysis of Tex-related gene expression, we elucidated distinctive immune characteristics across these identified subtypes. For these subtypes, we performed co-expression analyses to identify key molecules that could serve as targets for potential molecularly-targeted drugs. This pioneering approach not only sheds light on the intricate immune landscape in GD but also introduces a novel research avenue for the prospective diagnosis and treatment of this autoimmune thyroid disorder.

Materials and methods

Data collection and pre-processing

For use in this study, the GSE71956 dataset was retrieved from the NCBI's GEO database (https://www.ncbi.nlm.nih.gov/geo/). This microarray dataset, focusing on *Homo sapiens*, includes gene expression data collected from the PBMCs of 31 GD patients and 18 healthy controls (HCs), for a total of 49 samples (9, 10).

Data processing involved translating probes into symbols based on platform-specific correspondences. Probes corresponding to multiple genes were carefully removed, and those converging on the same symbol were consolidated into a median value. Subsequently, 40 Tex-related genes were identified (11). Gene sets from the GOBP and KEGG pathways, obtained from the MSigDb database (https://www.gsea-msigdb.org/gsea/msigdb/, version msigdb_v2023.1.Hs_GMTs), were included in further analysis using the ssGSEA algorithm to quantify pathway activity scores. Concurrently, we retrieved a set of 17 immune response genes from the Immport database (https://www.immport.org/shared/genelists). Utilizing the ssGSEA algorithm, immune response scores were

computed for each sample in the GSE71956 dataset. The study also included 17 human leukocyte antigen (HLA) genes (12), and correlation analyses were conducted for 13 relevant genes. The four genes not included in the latter analyses were *HLA-J* and *HLA-DRB6*, which were absent from the GSE71956 dataset, and *HLA-A* and *HLA-B*, which were previously identified as key drivers in Tex.

Protein-protein interaction network construction

Interactions among Tex-related genes were systematically explored using the STRING protein interactions database (https://www.string-db.org/). These interactions formed the basis for constructing PPI networks.

Identification of differentially expressed Tex-related genes in GD patients

The Wilcoxon rank-sum test, with a stringent significance threshold set at $P<0.05$, was applied to identify differential expression of Tex-related genes between two delineated groups.

Classification of GD subtypes using expression profiles of Tex-related genes

Unsupervised cluster analysis, utilizing the ConsensusClusterPlus package, identified different disease subtypes based on the expression profiles of Tex-related genes. The clustering method employed Euclidean distance, with km clustering and 1000 replications to ensure stability. Differences in pathway activity, immune response score, HLA gene expression, immune cell infiltration score, and T-cell depletion-related gene expression were examined between subtypes.

Identification of key module genes in GD subtypes

To construct scale-free co-expression gene networks by weighted gene co-expression network analysis (WGCNA), stringent criteria included setting scale-free R^2 to 0.8 and a minimum threshold of 30 genes within a module. Subsequently, correlation analyses evaluated the relationship between modules and sample phenotypic features, using Pearson's correlation coefficients for Module Eigenvectors (MEs), signifying the most emblematic genes within each module. Core genes, integral to different subtypes, were identified through rigorous screening based on gene significance (GS) ≥0.6 and module membership (MM) ≥0.8.

Differential gene expression analysis across GD subtypes

The R-package limma identified differentially expressed genes (DEGs) within diverse subtype samples, employing stringent criteria of $|\log2FC| \geq 1$ and adj. $P<0.05$.

Functional enrichment analysis across GD subtypes

Functional annotation of DEGs between subtypes was completed using the R package clusterProfiler, with parameters including pvalueCutoff = 0.05 and pAdjustMethod = "BH." This facilitated the annotation of potential functions of genes that diverged between subtypes, predicting their molecular functions.

Identification of subtype hub genes and exploration of therapeutics via PPIs

WGCNA was performed to identify core genes for each subtype. Then PPI networks were constructed based on core DEGs. Subtype hub genes were selected based on those with the top 5 connectivity, and interactions between these genes and drugs were investigated using the DGIdb database (https://www.dgidb.org/, v4.2.0). Sankey diagrams were prepared to provide concise and informative visualization of the interactions between drugs and genes.

Participant inclusion and blood sample collection

Peripheral blood samples were systematically collected from 112 GD patients and 47 HCs at the Second Hospital of Fujian Medical University between June 2023 and November 2023. The diagnostic criteria for GD encompassed clinical manifestations of thyrotoxicity, elevated serum thyrotropin receptor antibodies (TRAb), reduced serum thyrotropin (TSH), and other pertinent indicators (13). Individuals in the HC group had normal thyroid function and thyroid autoantibody levels, and individuals were excluded if they had a chronic inflammatory or autoimmune disorder, a prior thyroid condition or surgery, an infectious disease, or a malignant tumor, or if they were pregnant or breastfeeding.

Within the GD patient cohort, 70 cases were primary, signifying the patients had not received previous treatment for thyroid or ocular conditions. Based on the degree of thyroid enlargement (confirmed by palpation and ultrasound), these 70 patients were categorized into two groups: those without thyroid enlargement or with Grade I enlargement were included in the non-severe thyroid enlargement GD group (NSTEGD), while those with Grade II-III enlargement were included in the severe thyroid enlargement GD group (STEGD). In contrast, 42 cases were recurrent, marked by the recurrence of symptoms and serological changes meeting the diagnostic criteria for GD within 2 years of discontinuing prescribed medication, as directed by the treating physician (14).

Ethical approval was obtained from the Ethics Committee of the Second Hospital of Fujian Medical University (Ethics No. 2023-488). The general information of the study participants is presented in Supplementary Table S1. PBMCs were isolated through concentration gradient centrifugation and cryopreserved in serum-free cryopreservative for backup.

RNA extraction and reverse transcription quantitative polymerase chain reaction

Total RNA was isolated from PBMCs using TRIzol (Thermo Fisher Scientific, Waltham, MA, USA) for reverse transcription. The resulting RNA was transcribed into cDNA using the PrimeScript RT Master Mix kit (Takara, Dalian, China), and then cDNA amplification was achieved using the TB Green Premix Ex Taq II kit (Takara). Primers targeting the CBL gene and *GAPDH* were synthesized by Shanghai Sangon (Shanghai, China). The experiment was repeated three times. The specific primer sequences were:

CBL-forward:5'-ACTGCTTCTAAGGCTGCTTCTGG-3',R:5'-GGCGGTGGTGGTGGAAGATC-3'.GAPDH-forward:5'-TGCCACTCCTCCACCTTTG-3',R:5'-CGAACCACCCTGTTGCTGT-3'.

Statistical analysis

Bioinformatics analyses were conducted using R version 4.1.2. Test for significance included the Wilcoxon rank-sum test for two-group comparisons and the Kruskal–Wallis tests for multiple-group comparisons. The chromosomal distribution of Tex-related genes across 23 chromosome pairs was visualized using the R package RCircos.

Target gene validation was performed using IBM SPSS Statistics 23.0 and GraphPad Prism 8.0, employing the $2^{-\Delta Ct}$ method for relative gene expression in clinical samples. Normal data distribution was confirmed with the Shapiro–Wilk test, and data variance was assessed with the F-test. Normally distributed data were expressed as mean ± standard deviation, with between-group comparisons performed using the Student's test or corrected t-test (Welch's method). Non-normally distributed data were presented as median and quartiles, and between-group comparisons were performed used the Mann–Whitney test.

Correlations between the candidate gene *CBL* and FT3, FT4, and TSH levels were examined by Pearson's correlation analysis, while the correlation between the candidate gene *CBL* and TRAb level was investigated by Spearman's rank correlation analysis.

Results

Tex-related gene landscape in GD patients

This study began with a comprehensive analysis of 40 Tex-related genes, and the results revealed an even distribution across chromosomes, indicating genome-wide dispersion (Figure 1A). Subsequent PPI network analysis highlighted extensive interactions, emphasizing notable connectivity among genes such as *IL7R*, *CCR7*, *JAK1*, and *CBL* (Figure 1B), suggesting their potential importance in Tex-related gene interactions. Spearman's correlation analysis demonstrated significant correlations in gene expression. The most pronounced was a positive correlation between *IL7R* and *B2M* expression, and a negative correlation between *IL7R* and *MET* exhibited the largest absolute value (Figure 1C), implying shared functional roles for these genes.

Comparison of the mRNA expression levels of Tex-related genes between healthy and GD samples revealed upregulation of two genes (*MET* and *SFMBT2*) and downregulation of four genes (*JAK1*, *CBL*, *B2M*, and *HLA-B*) in GD (Figures 1D-F).

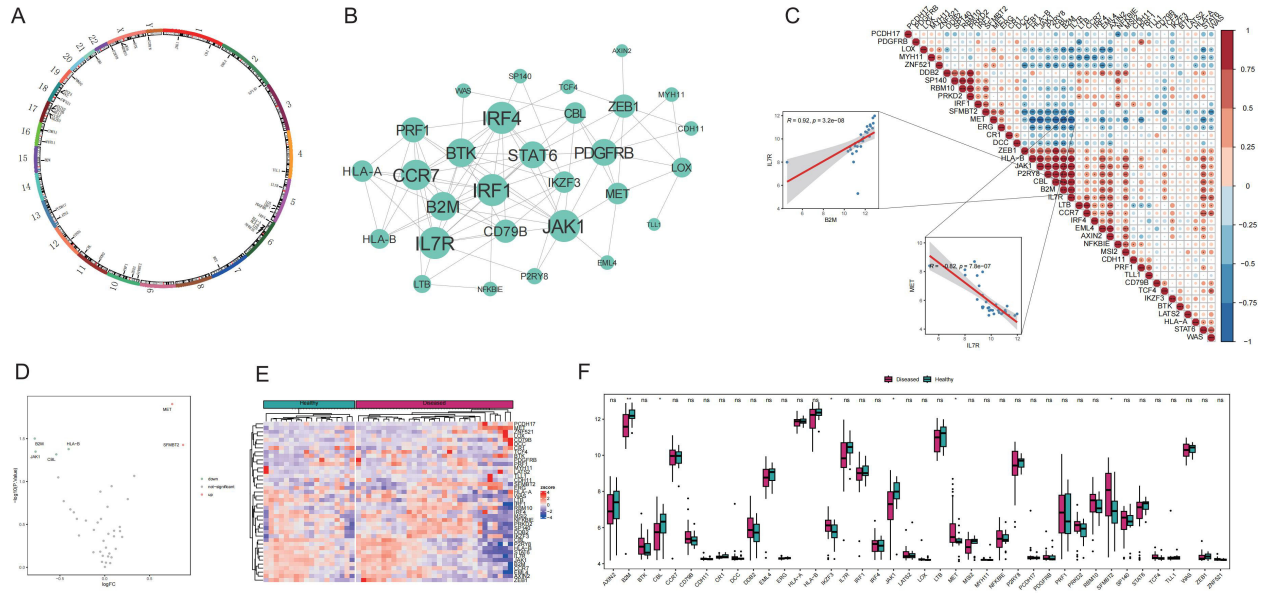

FIGURE 1
Expression of T-cell exhaustion (Tex)-related genes in the Graves' disease (GD) genetic landscape. A: Chromosomal distribution of Tex-related genes. B: Protein–protein interaction (PPI) network of Tex-related genes. C: Heat map depicting expression correlation of Tex-related genes in disease samples. D: Volcano map illustrating differences in Tex-related gene expression between the healthy control (HC) and GD groups. E: Heat map displaying the expression levels of Tex-related genes in the HC and GD groups. F: Expression distribution map of differentially expressed Tex-related genes. ns (p>0.05), *P<0.05, **P<0.01.

Involvement of Tex-related genes in immune regulation of GD

The potential roles of Tex-related genes in the pathogenesis of GD were investigated through a systematic analysis. Initial comparisons focused on HLA gene expression, immune cell infiltration scores, and immune response scores in different normal and GD patient samples. Spearman correlation analyses were performed to assess the relationships of HLA gene expression, immune cell infiltration scores, and immune response scores with Tex-related gene expression in GD patient samples. The results revealed down-regulation of three HLA genes (*HLA-C*, *HLA-E*, and *HLA-F*) in GD patient samples (Figure 2A). Further analyses demonstrated significant correlations between the expression of most aberrantly expressed HLA genes in GD and Tex-related genes (Figure 2B). Compared with HC samples, GD patient samples exhibited significantly higher infiltration scores for five immune cell types, specifically activated B cells, activated dendritic cells, central memory CD8 T cells, macrophages, and neutrophils (Figure 3A). Substantial correlations were observed between the immune cell infiltration scores in GD patient samples and the expression levels of Tex-associated genes. Notably, *CBL*, a Tex-related gene found to be differentially expressed in GD, showed a significant negative correlation with immune cell enrichment in GD (Figure 3B).

Six immune response scores, including those for Chemokine Receptors, Cytokine Receptors, Interleukin Receptors, TGFβ Family Members, and TNF Family Members Receptors, were significantly different between GD patient samples and HC samples (Figure 4A). Significant correlations were found between immune response scores and the expression of Tex-related genes. Of particular interest was a close correlation between *CBL* expression and the significantly enriched immune responses in samples from GD patients (Figure 4B). These results suggest that the expression of Tex-related genes may impact GD progression through immunomodulatory effects.

Classification of GD subtypes based on Tex-related gene expression

To elucidate the expression patterns of Tex-related genes associated with GD, we performed unsupervised cluster analysis, which classified 31 GD patient samples into two subtypes: Subtype1 (n=25) and Subtype2 (n=6), based on the expression profiles of 40 Tex-related genes (Figures 5A-C). The two disease subtypes were effectively determined by expression of T cell depletion-related genes (Figure 5D), with 21 Tex-related genes showing significantly differential expression, including notably *CBL*, which exhibited abnormally high expression in Subtype1 (Figure 5E).

Comparisons between subtypes revealed differences in pathway activity, HLA gene expression, immune cell infiltration score, and immune response score. Specifically, the results revealed significant distinctions in the pathway activities of the ECM RECEPTOR INTERACTION, ERBB SIGNALING PATHWAY, and MTOR SIGNALING PATHWAY between the subtypes (Figures 6A, B). Additionally, 17 immune cell infiltration scores, including those for activated B cells, activated dendritic cells, and activated CD8+ T cells, differed significantly between the subtypes (Figure 6C). The expression of 8 HLA genes and immune response scores related to cytokine receptors, natural killer cells, cytotoxicity, and the T-cell receptor (TCR) signaling pathway also showed significant differences between the two subtypes (Figures 6D, E). These findings suggest the presence of two distinct disease subtypes within GD that have divergent immunological characteristics based on the distinct expression patterns of Tex-related genes.

Identification of potential therapeutic drugs through WGCNA and subtype hub DEG analysis

To explore key molecules associated with the GD subtypes, WGCNA was performed on the top 50% of genes and identified 21 modules (Figures 7A, B). Based on the calculated correlation coefficient, the turquoise module was most positively correlated with Subtype1, and the magenta module was most positively correlated with Subtype2 (Figure 7C). These modules were considered key modules for Subtype1 and Subtype2, respectively, and 1441 and 59 module core genes were screened based on GS and MM, respectively (Figures 7D, E).

Upon application of the limma package, 3041 DEGs with upregulated expression in Subtype1 and 577 DEGs with upregulated expression in Subtype2 were identified (Figure 7F). Enrichment analysis was conducted on these DEGs (Figures 7G, H), and the intersection of core genes with upregulated genes in each subtype yielded 1235 core DEGs in Subtype1 (Figure 7I) and 44 core DEGs in Subtype2 (Figure 7J).

To identify potential therapeutic targets and drugs, subtype hub genes and drug molecules were screened using the PPI network and DGIdb database. From the constructed PPI networks for Subtype1 and Subtype2, the top 5 hub genes were selected based on node connectivity (Figures 8A, C). The hub genes for Subtype1 were *HSPA5*, *MYC*, *EEF2*, *EP300*, and *POLR2B*, while those for Subtype2 were *RAX2*, *P2R2B*, and *P2R2B*. Queries of interactions between hub genes and drugs in the DGIdb database revealed interactions of *MYC* and *EIF2AK4* with various drugs (Figures 8B, D). Examples include *novo*biocin, glutamine, and thioguanine for *MYC* and haloperidol, Hesperadin, and quetiapine for *EIF2AK4*.

CBL mRNA expression in PBMCs of GD patients

Based on the general association of Tex with a favorable prognosis in autoimmune diseases (7), we examined whether Tex-related driver genes are abnormally downregulated in GD patient samples. Considering the results of a literature review, the *CBL* gene was chosen for validation of its expression in GD patient-derived PBMCs. *CBL* mRNA demonstrated abnormally downregulated expression in GD patients (Figure 9A, P=0.043).

10.3389/fendo.2024.1364782

Furthermore, compared with that in samples from the primary group, *CBL* mRNA expression was lower in samples from the recurrent group (Figure 9B, *P*=0.020). *CBL* mRNA expression was significantly lower in GD patients with moderate-to-severe thyroid enlargement than in those without such enlargement (Figure 9C, *P*=0.002). Correlation analysis revealed a negative correlation between *CBL* mRNA expression and TRAb levels in GD patients. However, no significant associations were observed between *CBL* expression and the levels of FT3, FT4, and TSH (Table 1). These findings suggest that the Tex-related gene *CBL* may play a crucial immunoregulatory role in the pathogenesis of GD.

Discussion

GD is an autoimmune thyroid disorder characterized by elevated TRAb levels, lymphocytic infiltration, and tissue hyperactivation, with effects on multiple systems (2). T-cell

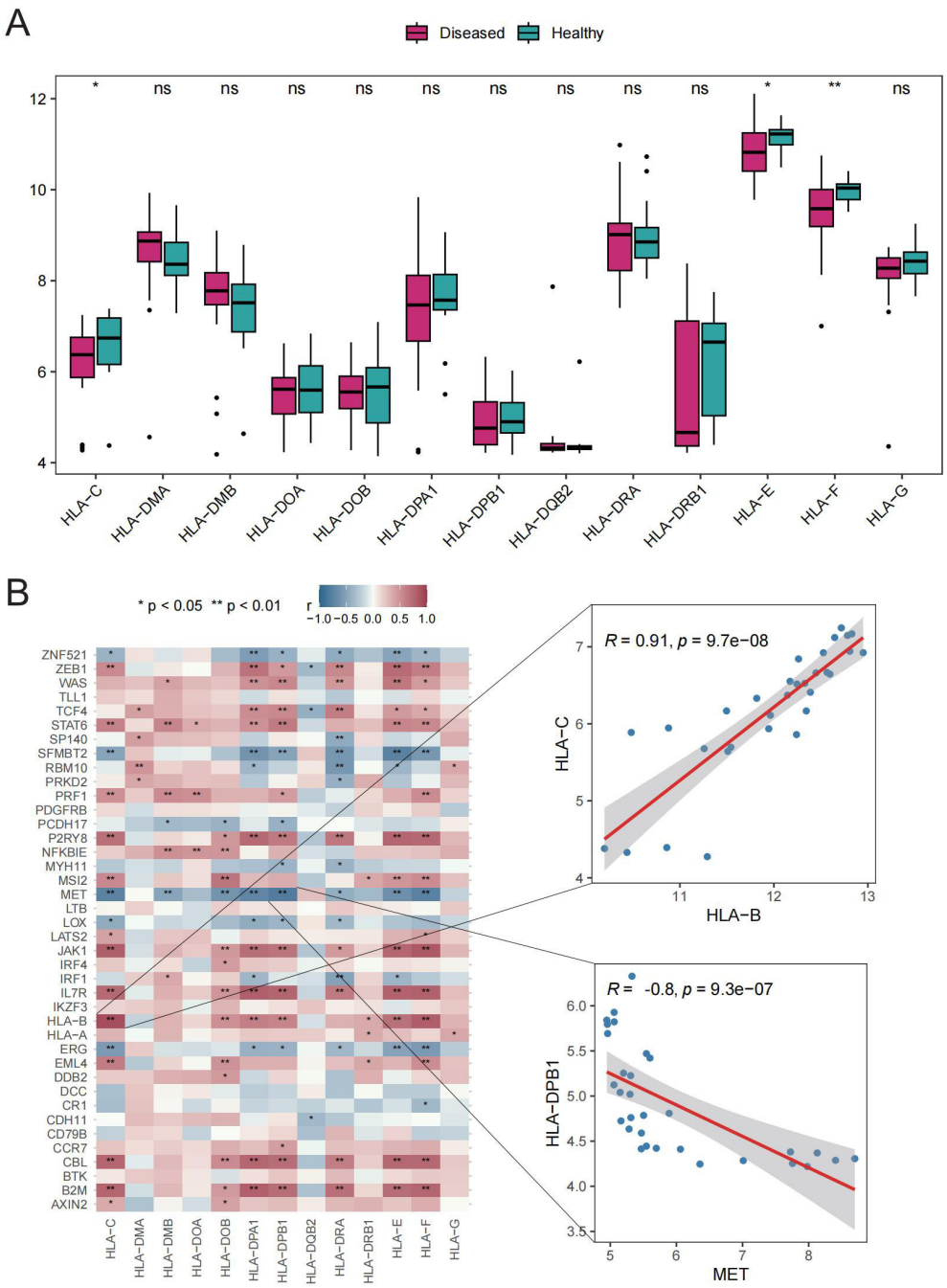

FIGURE 2
HLA gene analysis. A: Box plot showing gene expression differences between the HC and GD groups. B: Spearman correlation of Tex-related gene expression in GD samples. ns (p>0.05), *P<0.05, **P<0.01.

dysfunction is pivotal in GD pathogenesis and progression, and Tex, a distinct T-cell functional state, has been implicated in various autoimmune disorders (15). This study explored alterations of Tex-related gene expression in GD, and the results provide insight on the Tex phenotype and potential regulatory mechanisms. By identifying hub genes associated with different subtypes of GD, potential therapeutic avenues are revealed, offering theoretical support and guiding future investigations into the roles of Tex-related genes in GD pathogenesis.

In autoimmune diseases, a complex interplay of factors, including prolonged antigenic stimulation, restricted CD4+ T-cell responses, limited co-stimulation during initial T-cell activation, diminished gamma-chain cytokine signaling, and characteristics of the tissue microenvironment (e.g., hypoxia, nutrient deficiencies, pH abnormalities), contributes to T-cell differentiation along exhaustion pathways (16). Tex results in substantial alterations in effector function, cytokine responses, and metabolic profiles, accompanied by specific transcriptional changes (17). Recent investigations have identified Tex in several autoimmune diseases, which exhibit abnormal expression of inhibitory receptors and altered gene profiles. For instance, Tex phenotype manifestation has been observed in pancreatic islet-specific CD8 T cells in type 1 diabetes (18). Frenz et al. demonstrated increased expression of inhibitory receptors programmed cell death protein 1 (PD-1) and cytotoxic T-lymphocyte associated protein 4 (CTLA-4) in CD4+ T cells from RA patients (19), while another study in ANCA-associated vasculitis patients revealed dysregulated expression of Tex-related genes in CD8+ T cells (20). Additionally, A et al. reported a depleted T regulatory cell 2 (Treg2) cell phenotype and elevated expression of Tex-related genes in SLE patients (21). The present investigation aimed to elucidate the intricate interactions of Tex-related genes in GD, and the results reveal aberrant expression of Tex-related genes in PBMCs of GD patients, suggesting a potential role for Tex in GD pathogenesis.

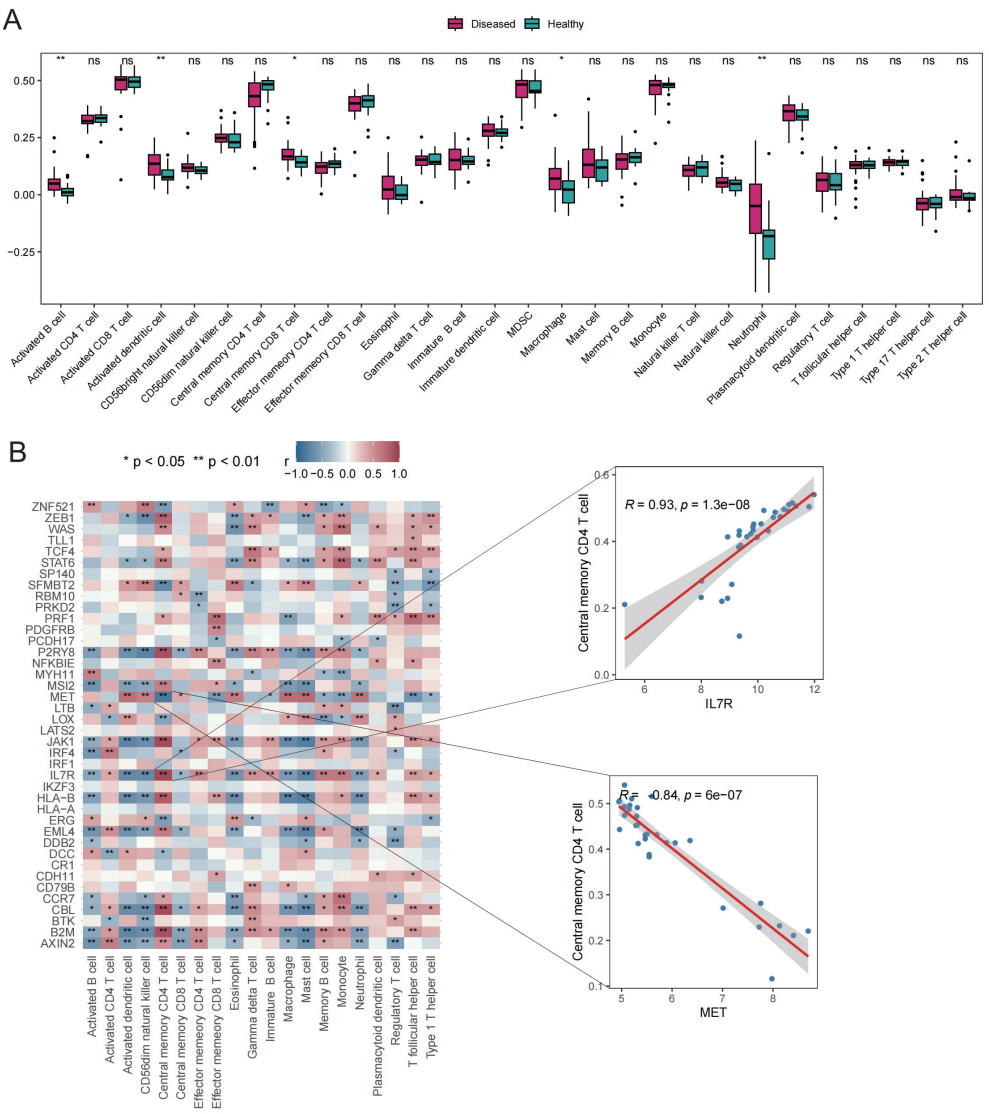

FIGURE 3
Immune cell infiltration scores. A: Box plot depicting expression of top 20 genes in the HC vs. GD groups. B: Spearman correlation of gene expression related to Tex in GD samples. ns (p>0.05), *P<0.05, **P<0.01.

Marked by the expression of inhibitory receptors like programmed death ligand 1 (PD-L1), lymphocyte activation gene 3 (LAG-3), T-cell immunoglobulin and mucin domain 3 (TIM-3), cluster of differentiation 244 (CD244), CD160, and T cell immunoglobulin and ITIM domain (TIGIT), crucially modulate autoimmune responses, negatively regulating immunopathological pathways through adjustments in their transcriptional expression profiles (8). Tex is integral to maintaining immune homeostasis, although it does not alter the initial disease progression direction. For example, the elevated PD-L1 expression in synovial tissue and fluid of RA patients suggests the key role of the PD-1/PD-L1 co-inhibitory pathway in immune homeostasis regulation in RA (22). In Crohn's disease, functional enrichment of Tex-related genes indicates their significance in various lymphocyte and immune activation pathways. Conversely, in SLE patients, aberrant expression of Tex-related genes in Tregs is associated with the nuclear factor kappa B (NF-κB) signaling pathway (21). These insights underscore the pivotal regulatory role of Tex in diverse autoimmune diseases. Previous studies implicated activated dendritic cells, macrophages, and neutrophils in the autoimmune and inflammatory responses of GD. These cells contribute through antigen presentation, cytokine secretion, and inflammatory mediator release. Furthermore, B cells

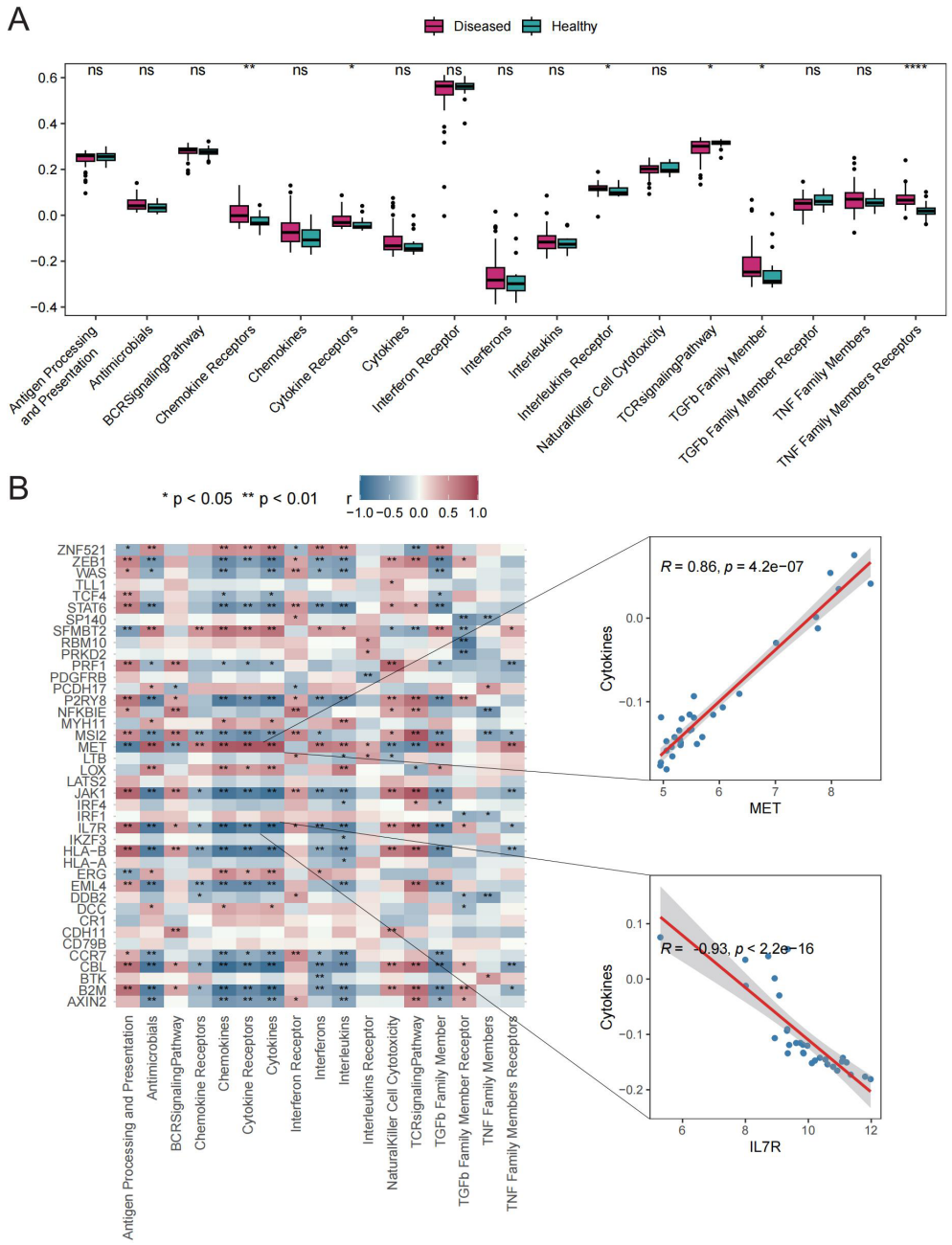

FIGURE 4
Immune response scores. A: Box plot showing differences in immune response scores between the HC and GD groups. B: Spearman correlation analysis for Tex-related gene expression in GD samples. ns (p>0.05), *P<0.05, **P<0.01, ****P<0.0001.

10.3389/fendo.2024.1364782

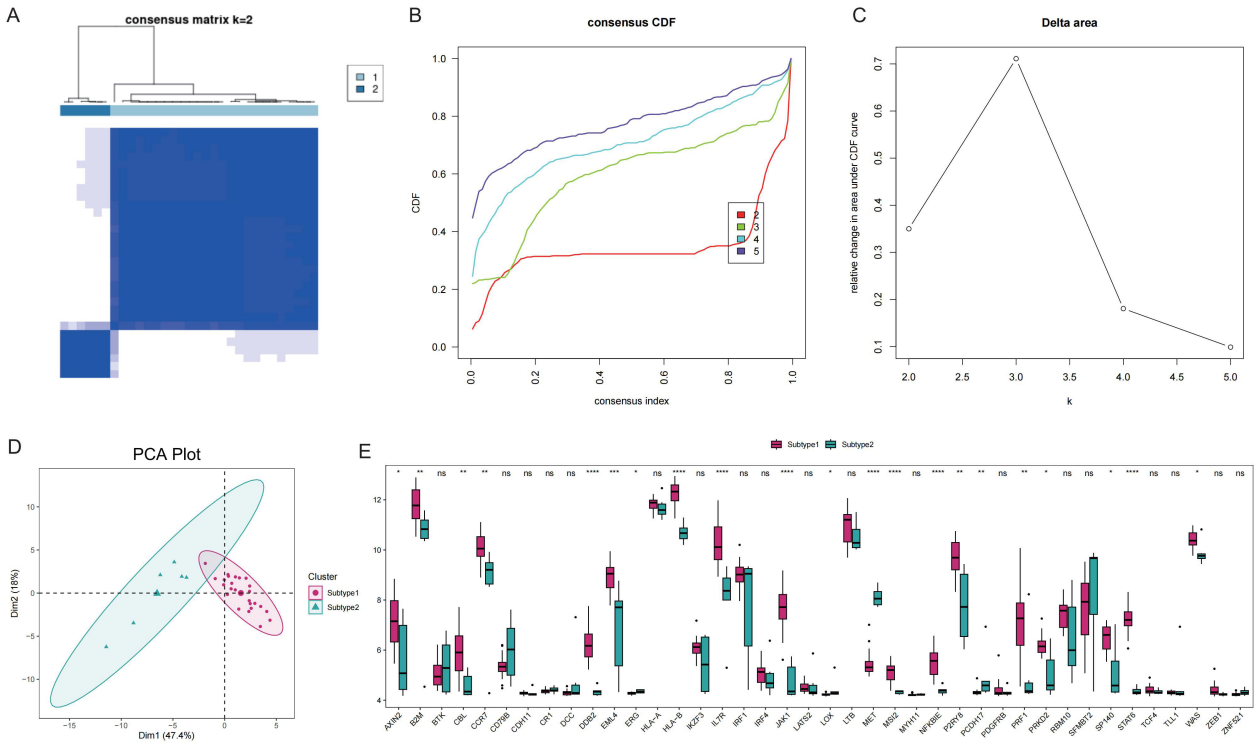

FIGURE 5
Disease subtype analysis. A: Consistent clustering of Tex-related genes; Subtype1 and Subtype2 represent two subgroups. B: Cumulative distribution function (CDF) plot; C: Delta Area Plot; D: Principal component analysis of T cell exhaustion-related genes; E: Box plots of Tex-related gene expression in the two subtypes. ns (p>0.05), *P<0.05, **P<0.01, ***P<0.001, and ****P<0.0001.

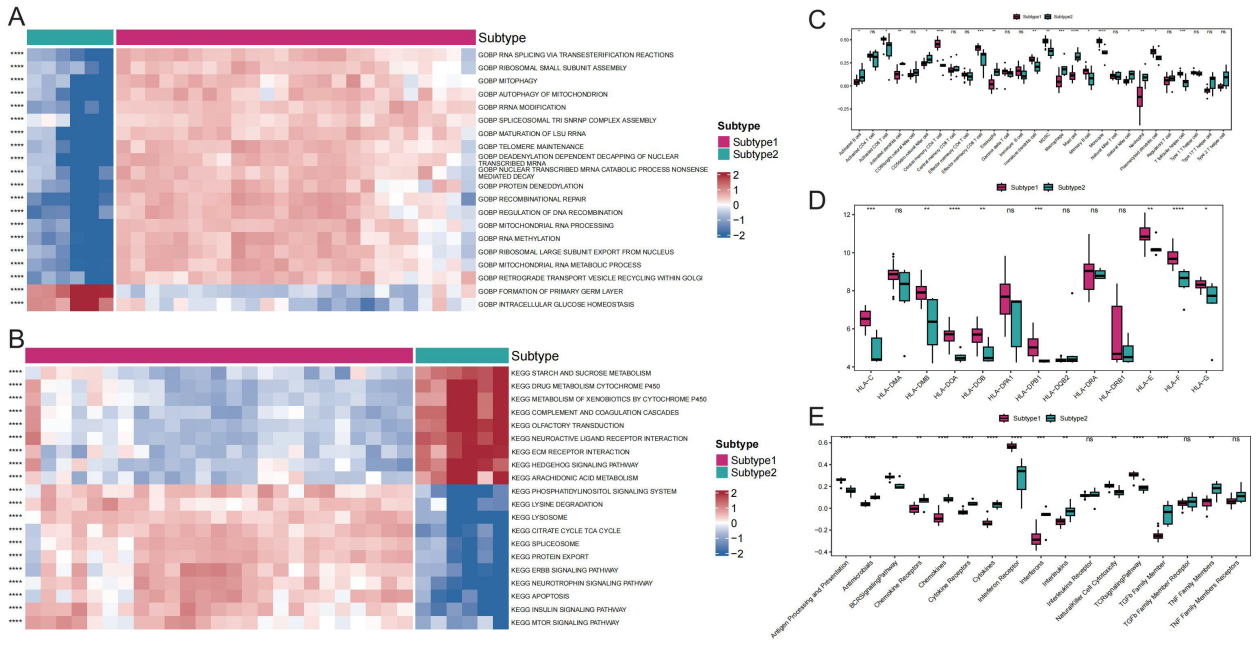

FIGURE 6
Comparison of immune responses between subtypes of GD. A: Heat map of differential gene ontology biological process (GOBP) pathway activity between GD subtypes. B: Heat map of differential Kyoto Encyclopedia of Genes and Genomes (KEGG) pathway activity between GD subtypes. C: Differential immune cell infiltration scores between GD subtypes. D: Comparison of HLA gene expression between GD subtypes. E: Differential immunoreactivity scores between GD subtypes. ns (p>0.05), *P<0.05, **P<0.01, ***P<0.001, and ****P<0.0001.

10.3389/fendo.2024.1364782

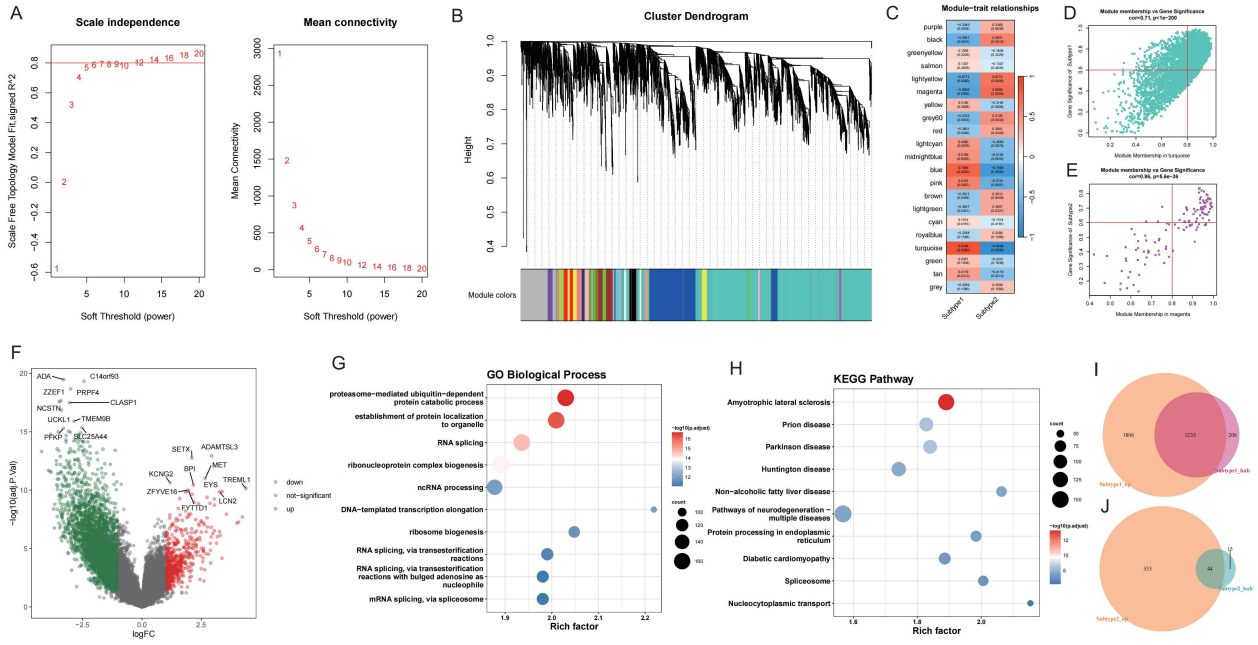

FIGURE 7
WGCNA screening of core genes for key modules of each GD subtype. A: Analysis of network topology for various soft-thresholding powers. B: Gene dendrogram and module colors. C: Module-feature correlation. D-E: Turquoise and magenta module screening for core genes. F: Volcano map of differentially expressed genes between GD subtypes; Subtype1 is control. G-H: Enrichment analysis of differentially expressed genes between GD subtypes. I-J: Wayne's diagram of core genes and upregulated genes in each subtype.

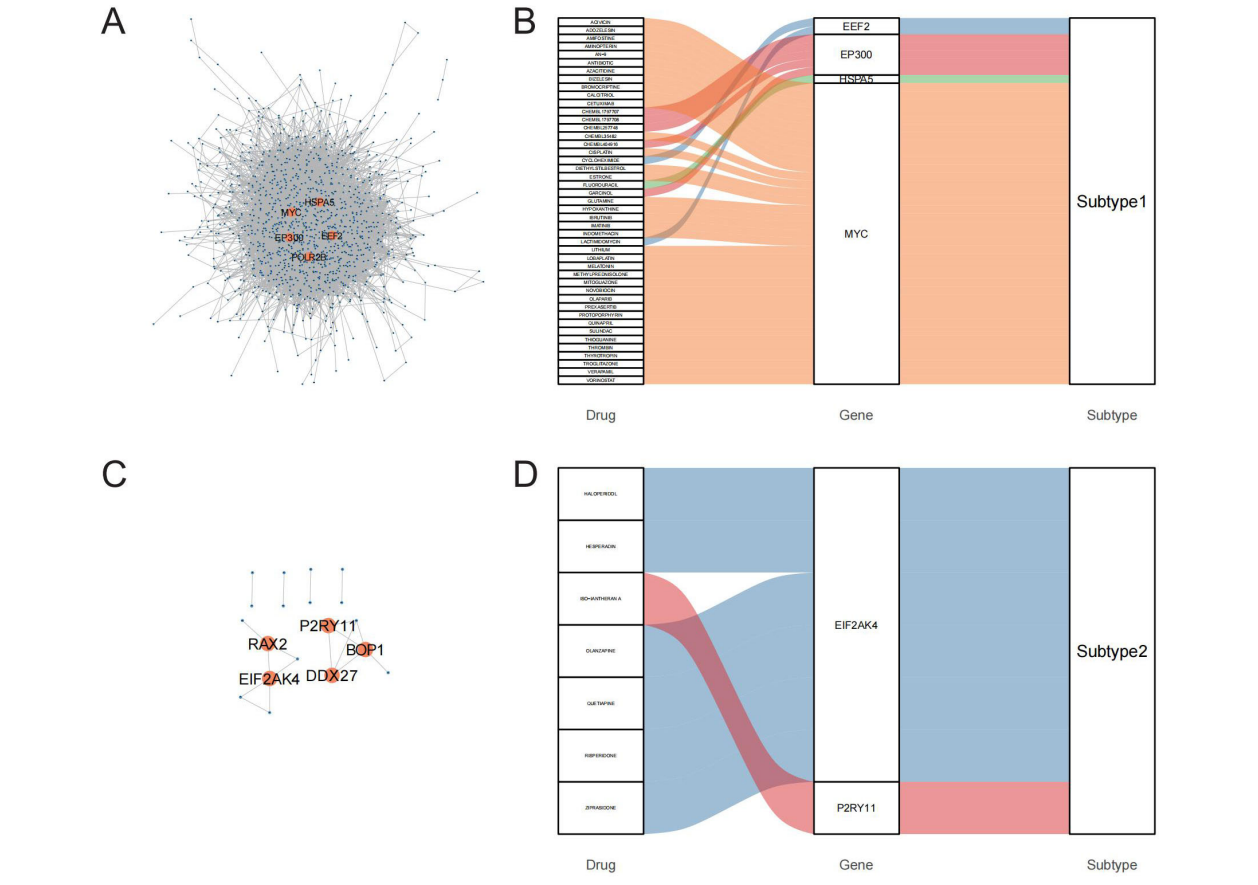

FIGURE 8
PPI networks identify hub genes for mining of potential drugs. A-C: PPI networks of core differentially expressed genes (DEGs) between the GD subtypes; A is Subtype1, C is Subtype2. B-D: Interactions of hub genes of GD subtypes with drugs.

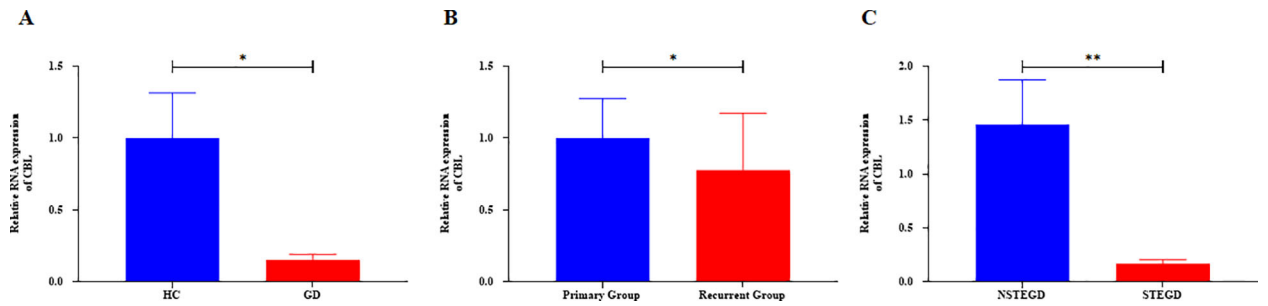

FIGURE 9
Expression of Tex-related gene *CBL* in PBMCs of GD patients. A: Abnormal downregulation of *CBL* mRNA expression in GD patients. B: Lower *CBL* mRNA expression in the recurrent group compared with the primary group. C: Lower *CBL* mRNA expression in GD patients with moderate-to-severe thyroid enlargement compared to those without such enlargement. The error bars presented on multiple panels represent the Standard Error of the Mean (SEM), **P*<0.05, ***P*<0.01. GD: Graves' disease patient group, HC: healthy control group, NSTEGD: those without thyroid enlargement or with Grade I enlargement GD, STEGD: those with Grade II-III enlargement GD.

activated by helper CD4+ T cells produce autoantibodies, intensifying the autoimmune response (23). Our study reveals that Tex-related gene expression in GD patients may regulate the recruitment of immune cells, such as activated dendritic cells, macrophages, neutrophils, and activated B cells, thereby participating in chemokine and cytokine receptor-mediated immune responses. Accordingly, we hypothesize that aberrantly expressed Tex-related genes in GD may influence disease development and progression by modulating the GD immune response. However, further functional experimental studies are required to confirm this hypothesis.

In our comprehensive exploration of the relationship between clinical phenotypes and Tex-related genes in GD patients, unsupervised cluster analysis revealed 40 Tex-related genes capable of classifying sequenced GD cases into two subtypes. These subtypes exhibited significant disparities in gene expression, immune cell infiltration, and immune response enrichment, consistent with previous findings (21). These findings suggest the involvement of Tex-related genes in the phenotypic variation of GD patients through immunomodulatory functions. Furthermore, through the identification of core genes expressed in different GD subtypes, we pinpointed potential therapeutic agents such as novobiocin, glutamine, thioguanine, haloperidol, Hesperadin, and quetiapine. Specifically, glutamine, which is known for its immune-modulating properties, has demonstrated modulatory effects in RA (24). Thioguanin, a nucleoside analog widely used in immunomodulatory therapies, has applications in treating Crohn's disease, autoimmune hepatitis, lupus nephritis, and transplant rejection prevention (25). Haloperidol, an antipsychotic, exhibits a potential modulating effect on pro-inflammatory T-cell function and has shown therapeutic efficacy in a rat model of RA, despite being primarily indicated for psychiatric disorders (26). Hesperadin, an antioxidant, has demonstrated efficacy in treating RA and experimental allergic encephalomyelitis (27). Quetiapine has been reported to reduce autoimmune-mediated demyelination by inhibiting T-cell responses (28). While the use of these drugs in GD remains unreported, drawing from previous studies, we posit that these drugs targeting Tex-associated genes may present novel avenues for GD treatment.

TABLE 1 Correlation analysis between CBL expression and laboratory indicators.

Variable	r	*P*
FT3 (pmol/L)	-0.05	0.563
FT4 (pmol/L)	0.01	0.924
TSH (mIU/L)	0.02	0.833
TRAb (IU/ml)	-0.29	0.002**

**P <0.01.

For further analysis in GD patients, *CBL* was selected as a candidate gene due to its abnormally low expression in GD samples and its role in negatively regulating the immune infiltration of various cell types and immune responses. RT-qPCR analysis confirmed the abnormally low expression of *CBL* in PBMCs of GD patients, consistent with microarray sequencing results, and revealed a negative correlation with the level of TRAb—a crucial diagnostic indicator for GD involving the aberrant activation of pro-inflammatory lymphocytes, including T cells. These findings support the results of our comprehensive bioinformatics analysis, suggesting a potential role for the Tex-related gene *CBL* in the abnormal immune regulation of GD. When GD cases were categorized into primary and relapse groups, significantly lower *CBL* mRNA expression was observed in the relapse group. In patients with newly diagnosed GD, clinical phenotypes can be separated according to the presence of moderate-to-severe thyroid enlargement and the absence of such enlargement. We found that *CBL* mRNA expression was significantly downregulated in the former group. *CBL* encodes an E3 ubiquitin-protein ligase, acting as a negative regulator in various signaling pathways (29). Previous studies have reported a pro-Tex role for *CBL* in diseases such as esophageal cancer, in which *CBL* interacts with SPRY1 to promote Tex, contributing a pro-cancer effect. Additionally, studies on *CBLB*, a closely related homolog of *CBL*, have demonstrated its promotion of Tex (30). Therefore, we hypothesize that the low expression of *CBL* in GD patients may promote GD relapse and thyroid enlargement by inhibiting Tex. However, mechanistic studies are required to further validate this hypothesis.

Our study has some limitations. Our findings were primarily derived from comprehensive bioinformatics analyses, and initial validation through RT-qPCR was conducted for only one Tex-related gene. Additionally, the small sample size necessitates

additional functional experimental validation and expansion of the clinical sample size. These steps are crucial for a comprehensive assessment of the exact role of Tex-related genes in the pathogenesis and prognosis of GD. Recent advancements in technologies such as single-cell sequencing, multiparameter flow cytometry, and high-dimensional mass cytometry offer opportunities to explore T-cell heterogeneity, various phenotypes, functions, and transcriptional programs. Our group plans to conduct in-depth studies in these areas for a more nuanced understanding of the role of Tex in GD.

Conclusions

In summary, Tex may be integral to the pathogenesis and prognostic mechanisms of GD. Our study provides initial insights, indicating that the Tex-related gene *CBL* is associated with immunomodulatory functions and holds promise as a prognostic biomarker for disease relapse. However, this finding requires further validation in more comprehensive studies.

Data availability statement

The original contributions presented in the study are included in the article/Supplementary Materials. Further inquiries can be directed to the corresponding author.

Ethics statement

The studies involving humans were approved by the Medical Ethics Committee of the Second Affiliated Hospital of Fujian Medical University (Ethics No. 2023-488). The studies were conducted in accordance with the local legislation and institutional requirements. The participants provided their written informed consent to participate in this study.

Author contributions

ZJ: Writing – original draft, Writing – review & editing. HH: Writing – original draft, Writing – review & editing. HC: Writing – review & editing. YL: Data curation, Formal analysis, Writing – review & editing. RL: Validation, Writing – review & editing. LC: Validation, Writing – review & editing.

Funding

The author(s) declare financial support was received for the research, authorship, and/or publication of this article. This study was supported by the Startup Fund for scientific research, Fujian Medical University (Grant number: 2021QH1117), the Quanzhou Guiding Science and Technology Programme projects in the field of medical and health care (Grant number: 2021N019S) and the Fujian Natural Science Foundation Project (Grant number: 2021J01252).

Acknowledgments

We also thank all of the participants.

Conflict of interest

The authors declare that the research was conducted in the absence of any commercial or financial relationships that could be construed as a potential conflict of interest.

Publisher's note

Supplementary material

The Supplementary Material for this article can be found online at: https://www.frontiersin.org/articles/10.3389/fendo.2024.1364782/full#supplementary-material

References

1. Smith TJ, Hegedüs L. Graves' Disease. *N Engl J Med*. (2016) 375:1552–65. doi: 10.1056/NEJMra1510030

2. Antonelli A, Fallahi P, Elia G, Ragusa F, Paparo SR, Ruffilli I, et al. Graves' disease: Clinical manifestations, immune pathogenesis (cytokines and chemokines) and therapy. *Best Pract Res Clin Endocrinol Metab*. (2020) 34:101388. doi: 10.1016/j.beem.2020.101388

3. Hansen M, Cheever A, Weber KS, O'Neill KL. Characterizing the interplay of lymphocytes in graves' Disease. *Int J Mol Sci*. (2023) 24. doi: 10.3390/ijms24076835

4. Chopp L, Redmond C, O'Shea JJ, Schwartz DM. From thymus to tissues and tumors: A review of T-cell biology. *J Allergy Clin Immunol*. (2023) 151:81–97. doi: 10.1016/j.jaci.2022.10.011

5. Álvarez-Sierra D, Marín-Sánchez A, Gómez-Brey A, Bello I, Caubet E, Moreno-Llorente P, et al. Lymphocytic thyroiditis transcriptomic profiles support the role of checkpoint pathways and B cells in pathogenesis. *Thyroid*. (2022) 32:682–93. doi: 10.1089/thy.2021.0694

6. Wherry EJ, Kurachi M. Molecular and cellular insights into T cell exhaustion. *Nat Rev Immunol*. (2015) 15:486–99. doi: 10.1038/nri3862

7. Osum KC, Burrack AL, Martinov T, Sahli NL, Mitchell JS, Tucker CG, et al. Interferon-gamma drives programmed death-ligand 1 expression on islet β cells to limit T cell function during autoimmune diabetes. *Sci Rep*. (2018) 8:8295. doi: 10.1038/s41598-018-26471-9

8. Collier JL, Weiss SA, Pauken KE, Sen DR, Sharpe AH. Not-so-opposite ends of the spectrum: CD8(+) T cell dysfunction across chronic infection, cancer and autoimmunity. *Nat Immunol*. (2021) 22:809–19. doi: 10.1038/s41590-021-00949-7

9. Limbach M, Saare M, Tserel L, Kisand K, Eglit T, Sauer S, et al. Epigenetic profiling in CD4+ and CD8+ T cells from Graves' disease patients reveals changes in genes associated with T cell receptor signaling. *J Autoimmun*. (2016) 67:46–56. doi: 10.1016/j.jaut.2015.09.006

10. Zhang Y, Wei J, Zhou H, Li B, Chen Y, Qian F, et al. Identification of two potential immune-related biomarkers of Graves' disease based on integrated bioinformatics analyses. *Endocrine*. (2022) 78:306–14. doi: 10.1007/s12020-022-03156-y

11. Zhang Z, Chen L, Chen H, Zhao J, Li K, Sun J, et al. Pan-cancer landscape of T-cell exhaustion heterogeneity within the tumor microenvironment revealed a progressive roadmap of hierarchical dysfunction associated with prognosis and therapeutic efficacy. *EBioMedicine*. (2022) 83:104207. doi: 10.1016/j.ebiom.2022.104207

12. Zhang X, Zhang S, Yan X, Shan Y, Liu L, Zhou J, et al. m6A regulator-mediated RNA methylation modification patterns are involved in immune microenvironment regulation of periodontitis. *J Cell Mol Med*. (2021) 25:3634–45. doi: 10.1111/jcmm.16469

13. Ross DS, Burch HB, Cooper DS, Greenlee MC, Laurberg P, Maia AL, et al. 2016 american thyroid association guidelines for diagnosis and management of hyperthyroidism and other causes of thyrotoxicosis. *Thyroid*. (2016) 26:1343–421. doi: 10.1089/thy.2016.0229

14. Cho YY, Chung YJ. Vitamin D supplementation does not prevent the recurrence of Graves' disease. *Sci Rep*. (2020) 10:16. doi: 10.1038/s41598-019-55107-9

15. Belk JA, Daniel B, Satpathy AT. Epigenetic regulation of T cell exhaustion. *Nat Immunol*. (2022) 23:848–60. doi: 10.1038/s41590-022-01224-z

16. Ogura H, Preston-Hurlburt P, Perdigoto AL, Amodio M, Krishnaswamy S, Clark P, et al. Identification and analysis of islet antigen-specific CD8(+) T cells with T cell libraries. *J Immunol*. (2018) 201:1662–70. doi: 10.4049/jimmunol.1800267

17. Laban S, Suwandi JS, Unen van V, Pool J, Wesselius J, Höllt T, et al. Heterogeneity of circulating CD8 T-cells specific to islet, neo-antigen and virus in patients with type 1 diabetes mellitus. *PloS One*. (2018) 13:e0200818. doi: 10.1371/journal.pone.0200818

18. Linsley PS, Long SA. Enforcing the checkpoints: harnessing T-cell exhaustion for therapy of T1D. *Curr Opin Endocrinol Diabetes Obes*. (2019) 26:213–8. doi: 10.1097/MED.0000000000000488

19. Frenz T, Grabski E, Buschjäger D, Vaas LA, Burgdorf N, Schmidt RE, et al. CD4(+) T cells in patients with chronic inflammatory rheumatic disorders show distinct levels of exhaustion. *J Allergy Clin Immunol*. (2016) 138:586–589.e10. doi: 10.1016/j.jaci.2016.04.013

20. McKinney EF, Lee JC, Jayne DR, Lyons PA, Smith KG. T-cell exhaustion, co-stimulation and clinical outcome in autoimmunity and infection. *Nature*. (2015) 523:612–6. doi: 10.1038/nature14468

21. Guo C, Liu Q, Zong D, Zhang W, Zuo Z, Yu Q, et al. Single-cell transcriptome profiling and chromatin accessibility reveal an exhausted regulatory CD4+ T cell subset in systemic lupus erythematosus. *Cell Rep*. (2022) 41:111606. doi: 10.1016/j.celrep.2022.111606

22. Globig AM, Mayer LS, Heeg M, Andrieux G, Ku M, Otto-Mora P, et al. Exhaustion of CD39-expressing CD8(+) T cells in crohn's disease is linked to clinical outcome. *Gastroenterology*. (2022) 163:965–981.e31. doi: 10.1053/j.gastro.2022.06.045

23. Purnamasari D, Soewondo P, Djauzi S. Dendritic cells in Graves' disease. *Acta Med Indones*. (2015) 47:61–9.

24. Nakaya M, Xiao Y, Zhou X, Chang JH, Chang M, Cheng X, et al. Inflammatory T cell responses rely on amino acid transporter ASCT2 facilitation of glutamine uptake and mTORC1 kinase activation. *Immunity*. (2014) 40:692–705. doi: 10.1016/j.immuni.2014.04.007

25. Legué C, Legros L, Kammerer-Jacquet S, Jézequel C, Houssel-Debry P, Uguen T , et al. Safety and efficacy of 6-thioguanine as a second-line treatment for autoimmune hepatitis. *Clin Gastroenterol Hepatol*. (2018) 16:290–1. doi: 10.1016/j.cgh.2017.07.032

26. Fahmy Wahba MG, Shehata Messiha BA, Abo-Saif AA. Ramipril and haloperidol as promising approaches in managing rheumatoid arthritis in rats. *Eur J Pharmacol*. (2015) 765:307–15. doi: 10.1016/j.ejphar.2015.08.026

27. Qi W, Lin C, Fan K, Chen Z, Liu L, Feng X, et al. Hesperidin inhibits synovial cell inflammation and macrophage polarization through suppression of the PI3K/AKT pathway in complete Freund's adjuvant-induced arthritis in mice. *Chem Biol Interact*. (2019) 306:19–28. doi: 10.1016/j.cbi.2019.04.002

28. Mei F, Guo S, He Y, Wang L, Wang H, Niu J, et al. Quetiapine, an atypical antipsychotic, is protective against autoimmune-mediated demyelination by inhibiting effector T cell proliferation. *PloS One*. (2012) 7:e42746. doi: 10.1371/journal.pone.0042746

29. Lock P, S.T. I, Straffon AF, Schieb H, Hovens CM, Stylli SS. Spred-2 steady-state levels are regulated by phosphorylation and Cbl-mediated ubiquitination. *Biochem Biophys Res Commun*. (2006) 351:1018–23. doi: 10.1016/j.bbrc.2006.10.150

30. Kumar J, Kumar R, Singh Kumar A, Tsakem EL, Kathania M, Riese MJ, et al. Deletion of Cbl-b inhibits CD8(+) T-cell exhaustion and promotes CAR T-cell function. *J Immunother Cancer*. (2021) 9. doi: 10.1136/jitc-2020-001688

frontiers | Frontiers in Endocrinology

TYPE Methods
PUBLISHED 16 September 2024
DOI 10.3389/fendo.2024.1403087

OPEN ACCESS

EDITED BY
Pia Pace-Asciak,
University of Toronto, Canada

REVIEWED BY
Leonardo Rossi,
University of Pisa, Italy
Jared Shenson,
Orlando Health Cancer Institute, United States

*CORRESPONDENCE
Mario Rotondi
mario.rotondi@icsmaugeri.it

RECEIVED 18 March 2024
ACCEPTED 28 August 2024
PUBLISHED 16 September 2024

CITATION
Teliti M, Occhini A, Fonte R, Croce L, Calì B, Ripepi FA, Carbone A, Rotondi M and Chytiris S (2024) Recurrent laryngeal nerve monitoring by flexible laryngoscopy during thyroid radiofrequency ablation in the awake patient. *Front. Endocrinol.* 15:1403087. doi: 10.3389/fendo.2024.1403087

Recurrent laryngeal nerve monitoring by flexible laryngoscopy during thyroid radiofrequency ablation in the awake patient

Marsida Teliti[1,2], Antonio Occhini[3], Rodolfo Fonte[2], Laura Croce[1,2], Benedetto Calì[3], Federica Antonella Ripepi[1], Andrea Carbone[4], Mario Rotondi[1,2]* and Spyridon Chytiris[2]

[1]Department of Internal Medicine and Therapeutics, University of Pavia, Pavia, Italy, [2]Unit of Endocrinology and Metabolism, Laboratory for Endocrine Disruptors, Istituti Clinici Scientifici Maugeri IRCCS, Pavia, Italy, [3]Department of General and Minimally Invasive Surgery, Istituti Clinici Scientifici Maugeri IRCCS, Pavia, Italy, [4]Unit of Diabetology and Endocrinology, Medical-Oncologic Department, ASST Lodi, Lodi, Italy

Objective: Although radiofrequency ablation (RFA) is a safe and effective non-surgical treatment for benign thyroid nodules, injury to the recurrent laryngeal nerve (RLN), is a potential and feared complication. Intermittent voice checks have been proposed to monitor vocal cord (VC) function during RFA, but such assessment is highly subjective and effort-dependent.

Methods: We are here reporting the methodological use of flexible laryngoscopy (FL) for VC monitoring during bilateral thyroid RFA treatment. The patient, a 35-year-old woman, was referred to the Endocrinology Unit for subclinical hyperthyroidism due to bilateral autonomously functioning thyroid nodules.

Results: At the end of the treatment of the first nodule, the FL performed by an otorhinolaryngologist specialist allowed evaluating VC function and ruling out possible paralysis before proceeding with the contralateral RFA treatment. The patient was awake during the entire procedure and well tolerated the laryngoscopic examination. The TSH serum evaluations performed one month and 9 months after the procedure assessed an euthyroid state (TSH 3.2 mIU/L and 2.8 mIU/L, respectively).

Conclusion: During bilateral thyroid RFA the use of FL for VC monitoring treatment resulted in a safe, easy-to-perform, and effective strategy to minimize and anticipate RLN injury risk in the awake patient. The prevention of RLN damage is advisable in the case of single RFA treatment, while it should be strongly recommended when RFA is performed on bilateral nodules.

KEYWORDS

flexible laryngoscope, radiofrequency ablation, recurrent laryngeal nerve, bilateral, thyroid nodule

10.3389/fendo.2024.1403087

Introduction

Radiofrequency ablation (RFA) is an attractive and safe non-surgical approach for the treatment of benign non-functioning nodules as well as autonomously functioning thyroid nodules (AFTN) (1, 2). In experienced hands, the procedure has a low rate of complications. Indeed, according to the most recent and comprehensive meta-analysis, in patients undergoing RFA for benign thyroid nodules the incidence of overall complications has been reported to be ~ 2.0%, being the rate of major complications ~1.3% (3, 4). Advertent injury of the recurrent laryngeal nerve (RLN), during the RFA procedure is one of the feared complications (5). However, the overall rate of transient or permanent voice change following RFA has been reported to be ~ 1.40% based on subjective voice examination (2). To minimize RLNs damage, it has been proposed to leave a cuff of unablated posterior thyroid tissue immediately adjacent to the tracheoesophageal groove, or so-called "danger triangle," where the RLN is not visible but is expected to be present (1, 6). In addition, the slow injection of cold dextrose 5% for hydrodissection has proven to be an effective method for separating the target lesion from surrounding critical structures (4, 7). Lastly, the use of the 'moving shot technique' with a trans-isthmic approach further reduces the risk of this feared complication (1). However, despite these precautions, injury to the laryngeal nerves by their anatomical site remains a potential risk. Typically, patients present with hoarseness of voice during or immediately following the procedure. Indeed, intermittent voice checks have been proposed to monitor vocal cord (VC) function during RFA, but such assessment is highly subjective and effort-dependent (1). The observation of passive or active symmetrical VC movements during breathing or phonation by laryngeal ultrasonography is a further noninvasive and convenient method for assessing VC function (8). However, at present flexible laryngoscopy (FL) remains the gold standard exam for evaluating VC mobility and to anticipate potential RLN damage. At least theoretically, the prevention of RLN damage is advisable in the case of single RFA treatment, while it should be strongly recommended when RFA is to be performed on bilateral nodules. In this view, we here describe the methodological procedures of performing FL for vocal cord monitoring during RFA treatment of bilateral thyroid nodules.

Case discussion

We report the case of a 35-year-old woman who was referred to the Endocrinology Unit for subclinical hyperthyroidism diagnosed by a thyroid work-up performed for an assisted reproduction program. Throughout the last years, the patients experienced a progressive decrease in serum TSH (from 0.74 mIU/ml to 0.19 mIU/ml at the last evaluation performed on March 2023). The thyroid ultrasound, performed by the same endocrinologist (S.C) who performed the RFA procedures, showed a normal sized gland in the presence of two nodules. The first nodule was located in the basal area of the right thyroid lobe, being hypoechoic, partially cystic, and internally vascularized, with diameters of 14.2x16.9x27.3 mm and an estimated volume of 3.44 ml (Figure 1); the second one, with the same ultrasound features, was located in the middle third of the left thyroid lobe, with diameters of 12.6x12.8x18.9 mm and an estimated volume of 1.59 ml (Figure 2). Both nodules corresponded to areas of increased radioisotope uptakes at thyroid scintiscan (without inhibition of the surrounding parenchyma). The patient was offered the following therapeutic options: 1) thyroid surgery (i.e. total thyroidectomy); 2) radioiodine ablation therapy; 3) ablation of the thyroid nodules by radiofrequency. The advantages and disadvantages of each therapeutic option were discussed with the patient. Owing to the fact that the patient was planning pregnancy and was starting a medically assisted reproduction program, radiofrequency ablation of both nodules appeared as the most suitable option.

Methods

RFA procedure was carried out on April 2023 in a sterile setting. Local anesthesia with Lidocaine 2% was administered at the skin

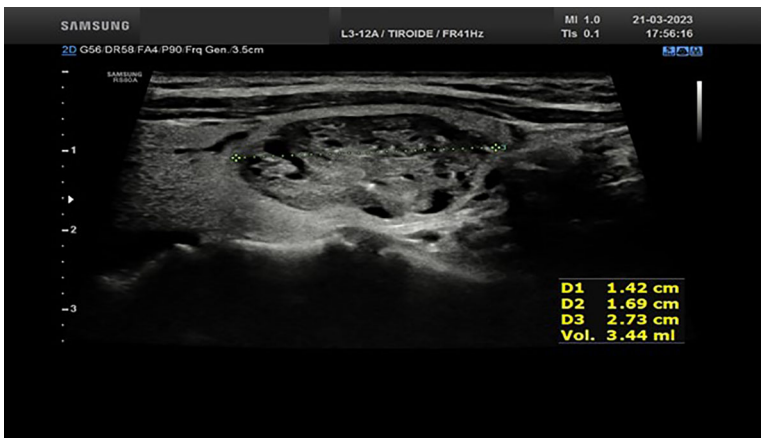

FIGURE 1
Ultrasound appearance of the thyroid right lobe nodule before RFA procedure.

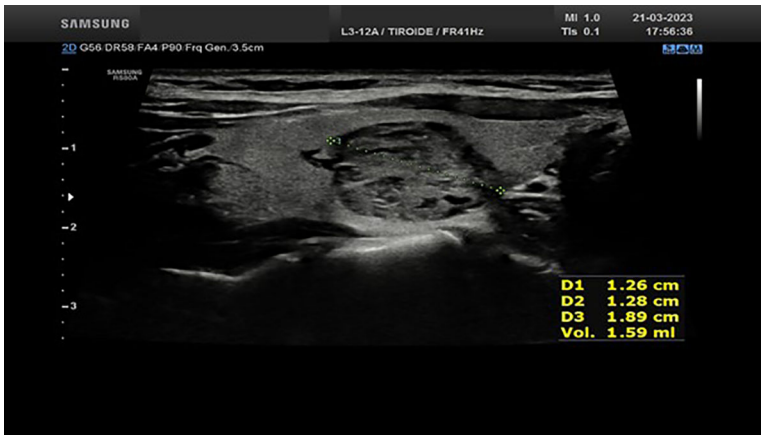

FIGURE 2
Ultrasound appearance of the thyroid left lobe nodule before RFA procedure.

puncture site and the perithyroidal space. No hydrodissection or anesthetic infusion was made in the peri- or under-capsular layer. The operator (S.C) was an endocrinologist with over 20 years of experience in thyroid imaging, fine-needle aspirations, core-needle biopsies, and percutaneous ethanol therapy who performs RFA treatment since 2018. During the procedure, the patient remained in a supine position with mild neck extension. The procedure was performed using an 18-gauge internally cooled electrode, 7 cm length with a 10 mm active tip. The US-guided moving-shot technique with a trans-isthmic approach was applied. At first, the right lobe nodule was treated (8.4 kJ were delivered in 9 min and 56 sec for a total of 8 ablations). The patient was advised to report pain, and voice testing was performed at regular intervals. When complete right nodule ablation was achieved, FL was performed by an otorhinolaryngologist. Briefly, FL was performed using a 30 cm long flexible Rhino-Laryngo-Fiberscope with a diameter of 3.5 mm. The patient was seated during the procedure. Before beginning, the patient was instructed to close her mouth and breathe gently through her nose. The tip of the endoscope was then advanced along the floor of the nose. The fiberscope was then maneuvered over the soft palate, allowing visualization of the vocal cords. This enabled the assessment of vocal cord mobility, to assess the normal motility of the VC. VC function was evaluated between the two procedures. Afterwards, treatment of the nodule at the left lobe proceeded (9.3 kJ were delivered in 10 min and 50 sec for a total of 5 ablations). A few hours after an US of the neck was performed: the right lobe nodule measures were 16.3x20x25.7 mm vs 14.2x16.9x27.3 mm (estimated volume 4.39 ml vs 3.44 ml); the left lobe nodule measures were 15.6x14.9x16.4 mm vs 12.6x12.8x18.9 mm (estimated volume 1.99 ml vs 1.59 ml). Minimal perithyroid inflammatory tissue was present with no visible hematomas. The absence of dysphonia after the end of the RFA procedure did not prompt us to repeat FL.

Results

FL performed at the end of the right thyroid nodule's RFA treatment recorded normal right VC function. The patient was awake in the surgery room. Symmetric spontaneous and volitional VC movements, including swallowing, were documented before proceeding with the treatment of the contralateral nodule. The patient well tolerated the procedure.

Ultrasound and biochemical follow-up

Approximately one month after the procedure, the right basal nodule measures 14.1x16.7x19.3 mm (estimated vol 2.39 ml vs 3.44 ml, Figure 3); the medium left nodule measures 13.2x11.4x14.3 mm (estimated vol 1.12 ml vs 1.59 ml, Figure 4). Both nodules appear completely treated, occupied by a hypoechoic area, a result of the treatment. One month after the procedure, the thyroid function was restored (TSH 3.2 mIU/L). At the last serum TSH assessment on January 2024, euthyroidism was confirmed (TSH 2.8 mIU/L).

Conclusion

We report the use of FL for VC monitoring during RFA treatment of bilateral functioning thyroid nodules in the awake patient. At the end of the treatment of the first nodule, the laryngoscopic examination allowed evaluating VC function and ruling out possible paralysis before proceeding with the contralateral procedure.

Recently, the use of FL for VC monitoring during RFA has been documented by Valcavi et al. for a patient under general sedation with a large thyroid nodule (9). FL was performed throughout the thyroid RFA to support the operator during the procedure. In the absence of documented thermal injury, the operator was comfortable in proceeding with extensive ablation of the nodule. The Authors propose that this approach should be recommended for large thyroid nodules to reduce the risk of undetected injury during the procedure. Of note, Fung et al. (8), first reported the use of intra-operative laryngeal ultrasonography (iLUSG) during thyroid RFA. Compared to FL, transcutaneous laryngeal ultrasound can offer some advantages including the fact that it is

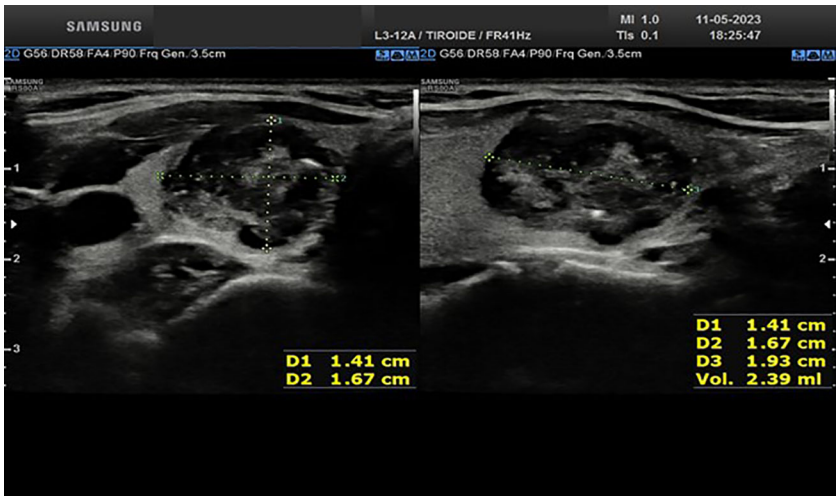

FIGURE 3
Ultrasound appearance of the thyroid right lobe nodule one month after RFA procedure.

a non-invasive and easy-to-learn method. More importantly, iLUSG would not require the involvement of an otolaryngologist, being easily performed by physicians skilled in neck ultrasound. However, some limitations to the use of iLUSG should be acknowledged. Indeed, previous evidence showed that the presence of calcified laryngeal cartilage, which is mostly found in older male patients, could prevent accurate VC function assessment (10, 11). Nevertheless, the role of ultrasound in this context is highly promising and certainly warrants further investigation (12). The issue of potential VC damage following RFA is particularly relevant when bilateral nodules are treated, as VC function can be normal during treatment, but it may occur post treatment due to the procedure-induced edema.

Some peculiarities of the here reported case deserve to be highlighted: i) the patient was awake; ii) early detection of RFA-induced VC paralysis would have prevented potential bilateral injury, as undetected injury during RFA may result in unilateral or, even worse, bilateral RLN damage. Taken together it could be suggested that independently of nodule size, FL should be performed when treating bilateral nodules. Indeed, the use of a trans-isthmic approach even by an experienced operator may not be sufficient to prevent RLN injury. Thus, an additional measure of safety could be represented by a direct evaluation of VC functional integrity before proceeding with the treatment of the contralateral nodule. If RLN injury is detected, the procedure can be stopped immediately to limit further neural damage, and timely remedies such as intra-operative injection of cold 5% dextrose can be performed (13).

In conclusion, we are reporting the first case of the use of FL for VC monitoring during bilateral thyroid RFA treatment as a safe, easy to perform, and effective strategy to minimize RLN injury risk in the awake patient.

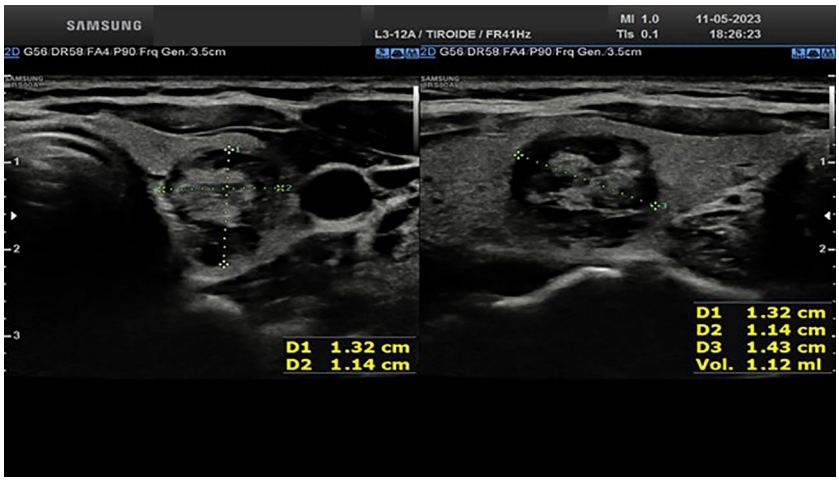

FIGURE 4
Ultrasound appearance of the thyroid left lobe nodule one month after RFA procedure.

Data availability statement

The original contributions presented in the study are included in the article/supplementary material, further inquiries can be directed to the corresponding author.

Ethics statement

Ethical approval was not required for the studies involving humans because ethical review and approval were not required for this study in accordance with the local legislation and institutional requirements. The studies were conducted in accordance with the local legislation and institutional requirements. The participants provided their written informed consent to participate in this study. Written informed consent was obtained from the individual(s) for the publication of any potentially identifiable images or data included in this article.

Author contributions

MT: Writing – review & editing, Data curation, Writing – original draft. AO: Writing – review & editing, Methodology. RF: Writing – review & editing. LC: Writing – review & editing. BC: Methodology, Writing – review & editing. FR: Writing – review & editing, Data curation. AC: Data curation, Writing – review & editing. MR: Writing – review & editing, Conceptualization. SC: Conceptualization, Writing – original draft, Writing – review & editing.

Funding

The author(s) declare financial support was received for the research, authorship, and/or publication of this article. This research was partially funded under the National Recovery and Resilience Plan (NRRP), Mission 4 Component 2 Investment 1.4 - Call for tender No. 3138 of 16 December 2021, rectified by Decree n.3175 of 18 December 2021 of Italian Ministry of University and Research funded by the European Union – NextGenerationEU. This research was partially supported through the Ricerca Corrente funding of the Italian Ministry of Health.

Conflict of interest

The authors declare that the research was conducted in the absence of any commercial or financial relationships that could be construed as a potential conflict of interest.

Publisher's note

All claims expressed in this article are solely those of the authors and do not necessarily represent those of their affiliated organizations, or those of the publisher, the editors and the reviewers. Any product that may be evaluated in this article, or claim that may be made by its manufacturer, is not guaranteed or endorsed by the publisher.

References

1. Sinclair CF, Baek JH, Hands KE, Hodak SP, Huber TC, Hussain I, et al. General principles for the safe performance, training, and adoption of ablation techniques for benign thyroid nodules: an American thyroid association statement. *Thyroid*. (2023) 33 (10):1150–70. doi: 10.1089/thy.2023.0281

2. Chung SR, Suh CH, Baek JH, Park HS, Choi YJ, Lee JH. Safety of radiofrequency ablation of benign thyroid nodules and recurrent thyroid cancers: a systematic review and meta-analysis. *Int J Hyperthermia*. (2017) 33(8):920–30. doi: 10.1080/02656736.2017.1337936

3. Issa PP, Cironi K, Rezvani L, Kandil E. Radiofrequency ablation of thyroid nodules: a clinical review of treatment complications. *Gland Surg*. (2024) 13(1):77–86. doi: 10.21037/gs-22-539

4. Baek JH, Lee JH, Sung JY, Bae JI, Kim KT, Sim J, et al. Complications encountered in the treatment of benign thyroid nodules with us-guided radiofrequency ablation: A multicenter study. *Radiology*. (2012) 262(1):335–42. doi: 10.1148/radiol.11110416

5. Zhao ZL, Wei Y, Peng LL, Li Y, Lu NC, Yu MA. Recurrent laryngeal nerve injury in thermal ablation of thyroid nodules - risk factors and cause analysis. *J Clin Endocrinol Metab*. (2022) 107:E2930–7. doi: 10.1210/clinem/dgac177

6. Kim J, Baek JH, Lim HK, Ahn HS, Baek SM, Choi YJ, et al. 2017 Thyroid radiofrequency ablation guideline: Korean society of thyroid radiology. *Korean J Radiol*. (2018) 19(4):632–55. doi: 10.3348/kjr.2018.19.4.632

7. Chan WK, Sun JH, Liou MJ, Hsu CJ, Lu YL, Chou WY, et al. Novel and advanced ultrasound techniques for thyroid thermal ablation. *Endocrinol Metab*. (2024) 39 (1):40–6. doi: 10.3803/enm.2024.1917

8. Fung MMH, Lang BHH. Using intra-operative laryngeal ultrasonography as a real-time tool in assessing vocal cord function during radiofrequency ablation of the thyroid gland. *World J Surg*. (2022) 46:2206–11. doi: 10.1007/s00268-022-06596-9

9. Valcavi R, Gaino F, Novizio R, Mercante G. Vocal cord monitoring by flexible fiberoptic laryngoscopy during thyroid radiofrequency ablation. *VideoEndocrinology*. (2023) 10:41–3. doi: 10.1089/ve.2023.0012

10. Wong KP, Lang BHH, Chang YK, Wong KC, Chow FCL. Assessing the validity of transcutaneous laryngeal ultrasonography (TLUSG) after thyroidectomy: what factors matter? *Ann Surg Oncol*. (2015) 22:1774–80. doi: 10.1245/s10434-014-4162-z

11. Kandil E, Deniwar A, Noureldine SI, Hammad AY, Mohamed H, Al-Qurayshi Z, et al. Assessment of vocal fold function using transcutaneous laryngeal ultrasonography and flexible laryngoscopy. *JAMA Otolaryngol - Head Neck Surg*. (2016) 142(1):74–8. doi: 10.1001/jamaoto.2015.2795

12. Pace-Asciak P, Russell JO, Dhillon VK. Intraoperative neuromonitoring: evaluating the role of continuous IONM and IONM techniques for emerging surgical and percutaneous procedures. *Front Endocrinol (Lausanne)*. (2022) 13:823117. doi: 10.3389/fendo.2022.823117

13. Lee MK, Baek JH, Chung SR, Choi YJ, Lee YM, Kim TY, et al. Effectiveness of injecting cold 5% dextrose into patients with nerve damage symptoms during thyroid radiofrequency ablation. *Endocrinol Metab*. (2020) 35(2):407–15. doi: 10.3803/EnM.2020.35.2.407

frontiers | Frontiers in Endocrinology

TYPE Original Research
PUBLISHED 09 October 2024
DOI 10.3389/fendo.2024.1402522

OPEN ACCESS

EDITED BY
Pia Pace-Asciak,
University of Toronto, Canada

REVIEWED BY
Erivelto Martinho Volpi,
Hospital Alemão Oswaldo Cruz, Brazil
Iram Hussain,
University of Texas Southwestern Medical Center, United States

*CORRESPONDENCE
Iftikhar Malik
iftikhar.malik@fvsawi.com
Johnson Thomas
Johnson.Thomas@Mercy.net

RECEIVED 17 March 2024
ACCEPTED 23 September 2024
PUBLISHED 09 October 2024

CITATION
Malik I, Mitchell J and Thomas J (2024) Efficacy of echolaser smart interface-guided laser ablation in volume reduction of symptomatic benign thyroid nodules. *Front. Endocrinol.* 15:1402522. doi: 10.3389/fendo.2024.1402522

Efficacy of echolaser smart interface-guided laser ablation in volume reduction of symptomatic benign thyroid nodules

Iftikhar Malik[1]*, Janeil Mitchell[2] and Johnson Thomas[3]*

[1]Department of Endocrinology, Fox Valley Surgical Specialists, Appleton, WI, United States, [2]Division of Endocrine Surgery, Department of General Surgery, Fox Valley Surgical Specialists, Appleton, WI, United States, [3]Department of Endocrinology, Mercy Hospital, Springfield, MO, United States

Background: The management of benign symptomatic thyroid nodules until recent years has been limited to surgery, radioactive iodine treatment, or surveillance which is associated with the burden of morbidity of complications or symptom non-relief as well as cost. Laser ablation has emerged as a minimally invasive alternative, this uses laser energy to thermally ablate nodule tissue, leading to volume reduction and symptom relief. Long-term treatment response data is growing but remains limited in the United States. Our study aims to quantify the effectiveness of laser ablation in reducing the volume of thyroid nodules over a 12 to 18-month period.

Materials and methods: Retrospective review of data was conducted for 63 adults with cytologically benign, solid symptomatic thyroid nodules ranging from 1.333 cm^3 to 103.794 cm^3 in volume. Ultrasound-guided laser thermal ablation was performed on all nodules using EchoLaser X4 Smart Interface device with 1064 nm diode laser to deliver total ablation energy (joules), calculated per device guidelines. Serial sonographic volume measurements were conducted 1 month, 3 -6 months, 6 - 12 months, and 12 to 18 months post-ablation intervals.

Results: Study cohort was comprised of 63 thyroid nodules. reduction in nodule volume increased progressively over time, with median reductions of 46.05% [STD 21.8] at 1 month, 60.33% [STD 20.1] at 3-6 months, 68.69% [STD 18.8] at 6-12 months, and 64.04% [STD 19.27] at 12-18 months. A total of 62, 56, 42, and 17 nodules had available data for analysis at these respective intervals.

Conclusion: This study demonstrated a marked progressive reduction of thyroid nodule volume following ablation. The treatment appears to be consistently effective in reducing symptoms across a wide range of nodule sizes, although the

degree of volume reduction varies. The results of our study underscore the potential of laser ablation as a viable treatment option for thyroid nodules, with a sustained reduction in nodule volume observed over an extended post-procedure period.

KEYWORDS

laser ablation, thyroid nodule, echolaser, benign nodule, ablation

Introduction

Laser thyroid nodule ablation is a minimally invasive percutaneous technique utilized in the treatment of symptomatic, functional, and non-functional benign thyroid nodules (1). The incidence of thyroid nodules among the general population is on the rise, with up to 1 in 10 benign nodules observed to be symptomatic over an individual's lifetime, the number of patients potentially needing therapeutic intervention is also rising (2, 3). Historically, surgery has been the sole treatment option for solid nodules causing local discomfort or aerodigestive compression, but over the past two decades, percutaneous image-guided thermal ablation modalities including radiofrequency ablation, cryoablation, and microwave ablation, high-intensity focused ultrasound have emerged in as a potential treatment alternatives.

Laser thyroid ablation involves the application of thermal energy via a thin optical fiber inserted percutaneously into a target thyroid nodule creating a predictable zone of coagulative necrosis. Laser ablation has been shown to significantly reduce the volume of thyroid nodules leading to reduction of compressive symptoms and improved cosmetic outcomes for patients (4–7).

Clinical data continues to grow, illuminating procedural challenges and areas of research. One limitation to treatment efficacy in thermal ablation is possible regrowth of nodule tissue at ablated margins and need for retreatment for insufficient volume reduction and symptom control (8–10). Contributing factors are unclear, however commercial laser devices have developed image guidance packages to aid in volumetric ablation planning.

The primary objective of this study was to assess the effectiveness of percutaneous laser ablation under an ultrasound guidance platform with spatial overlay for treatment planning, [Echolaser Smart Interface] in volume reduction of symptomatic, benign thyroid nodules.

Materials and methods

Study design and data collection

This is a single center retrospective study. A retrospective electronic medical chart review was conducted at an outpatient endocrinology clinic, Fox Valley Surgical Specialists (FVSS) to identify all patients who were treated with laser ablation for thyroid nodules from January 2020 to December 2022.

Inclusion criteria included all adult patients undergoing laser ablation at FVSS. Patients lost to follow up after laser ablation without at least one follow up were excluded from the study.

Data collected from the charts included patient demographics (age and sex), results of fine needle aspiration biopsies, laboratory values including TSH, Free T4, and Free T3, and measurements from thyroid and neck ultrasound images. Baseline assessments, as documented in the chart were also collected and entered into a spreadsheet. This included patient history, physical exam, and thyroid nodule symptom assessment. Measurements of the nodule from the same day pre-ablation and post-ablation using ultrasound, TSH, Free T4, Free T3 values, as well as clinical notes on pre- and post-ablation symptoms and procedural complications were also collected. Thyroid nodule symptoms were assessed using questions with binary answers.

The study was approved by the Pearl IRB (2023-0298-DFT).

Changes in thyroid nodule volume in cm3 were measured using ultrasound at 1 month, 3 to 6 months, 6 to 12 months and 12 to 18 months after laser ablation. All descriptive and discrete data points were collected and entered into a password-projected computerized spreadsheet.

Laser ablation

Laser ablation procedures were completed in an outpatient endocrinology clinic under sterile conditions. The ablation site was thoroughly cleansed with antiseptic solution and sterile drapes were applied to create a barrier around the surgical field. Ultrasound probes were covered with sterile probe covers. The healthcare providers donned sterile gowns and gloves before entering the sterile field. Only sterile instruments and materials, including needles, were introduced into the field. Standard laser precautions were followed.

The Elesta ECHOLASER X4 laser system, developed by ElestaSpA based in Calenzano, Italy, was employed, augmented by its accompanying guidance software[Echolaser Smart Interface] (1). This system was approved for clinical use from the United

States Food and Drug Administration (FDA) under the 510(k) Premarket Notification pathway on September 4, 2018.The ECHOLASER X4 was utilized with a single diode laser source operating at a wavelength of 1064 nm and can deliver a maximum power output of 7 watts.

Total Laser energy for the nodule was calculated using device guidelines. Average energy delivered per nodule was 3461 Joules.

During thyroid nodule ablation, ultrasound guidance was utilized continuously during the ablation planning phase, needle insertion, and continuous monitoring of the ablation process. The introduction of the fiber into the thyroid nodule was facilitated using a 21-gauge needle introducer. The Echolaser Smart Interface (ESI) was employed to aid in the accurate placement and positioning of the needles into the target lesion. Laser energy transmission to the target site was achieved through the use of bare flat-tipped quartz optical fibers with a diameter of 300 µm, sourced from Oberon GmbH, Wildau, Germany

In all patients, local anesthesia using 1% Lidocaine without epinephrine was used. Hydrodissection technique was used not only for anesthesia but also to establish a protective buffer zone between the thyroid and vital structures, including the carotid arteries, jugular veins, and trachea. Our ablation approach primarily involved a trans-isthmic technique. As the targeted area underwent ablation, the fibers were repositioned to a fresh area. Nodule ablation was initiated from the inferior aspect and systematically progressed in an upward direction by the pullback technique (1).

Upon the conclusion of laser ablation, the removal of the fibers was carried out, accompanied by the extraction of the needle(s), and hemostasis was accomplished through the application of pressure at the respective site. Subsequent to the needle extraction, an evaluation of external bleeding was conducted through visual inspection. Furthermore, an assessment of internal bleeding and the potential for nodule rupture was performed by the investigator using neck ultrasound with Doppler flow.

Pain and complication evaluations were conducted immediately following Laser ablation and documented in the medical record. Subsequent follow-up assessments were scheduled at 1, 3, 6, and 12-month intervals following the conclusion of the study procedure. These follow-up visits encompassed comprehensive evaluations, including medical history reviews, physical examinations, and complete ultrasound of the neck with Doppler assessment. The continuous monitoring of adverse events was an integral part of the study protocol. Two investigators (IM or JM) conducted all physical examinations, data collection, ultrasound examinations with Doppler imaging, and administered the laser ablation procedure for all enrolled subjects.

Data collection and analysis

Neck ultrasound examinations, incorporating Doppler imaging, were conducted utilizing the GE Logiq P9 ultrasound system and ML6-16 probe. The volume of thyroid nodules, measured in milliliters, was determined using the formula: Nodule Volume = Length (cm) × Width (cm) × Depth (cm) × 0.525 (11). To assess the change in nodule size, the percentage reduction in nodule volume was calculated via the equation: (1 - Final Volume/Initial Volume) x100 (12). Additionally, thyroid function tests and symptomatology, both pre- and post-procedure were recorded and analyzed.

Data analysis and generation of descriptive statistics was completed using Python statistical libraries (13). Mean, median volume changes during each interval, standard deviation, interquartile range, change in volume for each interquartile range over each time interval specified in the study were calculated. Efficacy of laser ablation was assessed by the change in volume over time after laser ablation.

Results

In this study, we evaluated the efficacy of laser ablation in reducing the volume of cytologically-benign solid thyroid nodules. The analysis encompassed data from various time intervals post-procedure: 1 month, 3-6 months, 6-12 months, and 12-18 months. A total of 62, 56, 42, and 17 nodules had available data for analysis of these respective intervals. Sixty-three patients were included in the study, consisting of 58 women and 5 men. Benign functioning and non functioning nodules were included in the study. One patient was lost to follow-up.

There were 58 females and 5 males in the study cohort with ages ranging from 26 to 85 years. Median age was 61. Pre-procedure nodule volume ranged from 1.333 cm^3 to 103.794 cm^3. Median volume was 9.595 cm^3.

The median reduction in thyroid nodule volume was 46% [STD 21.8] at 1 month and observed to increase progressively over time. Figure 1 illustrates the mean percentage reduction in thyroid nodule volume over sequential post-ablation intervals following laser therapy.

Four distinct time frames are reported in Figure 1: 1 month (blue box), 3-6 months (orange box), 6-12 months (green box), and 12-18 months (red box) post-treatment. The bar corresponding to the 1-month interval exhibits a 45.5.% reduction in nodule volume, indicating initial response to the ablation procedure. Subsequent time intervals show progressive volume reduction, with the 3-6 months interval displaying a 60.1% decrease, the 6-12 months interval a 68.1% decrease, and the 12-18 months interval demonstrating a 68.1% decrease.

The distribution of percentage reduction in thyroid nodule volume across the four post-ablation time intervals: 1 month, 3-6 months, 6-12 months, and 12-18 months is presented as a violin plot in Figure 2. Each 'violin' encompasses a kernel density estimation illustrating the spread and probability density of the data at different percentage reductions. The central boxplot within each violin indicates the interquartile range (IQR) with a line marking the median percentage reduction.

The first violin(blue violin) for the 1-month interval shows a median reduction close to the 50% mark, with the majority of the data points spread around the median, indicating a consistent response among patients. The second violin (orange violin) for the 3-6 months interval displays a slightly higher median reduction, suggesting a variation in the response among patients as time

10.3389/fendo.2024.1402522

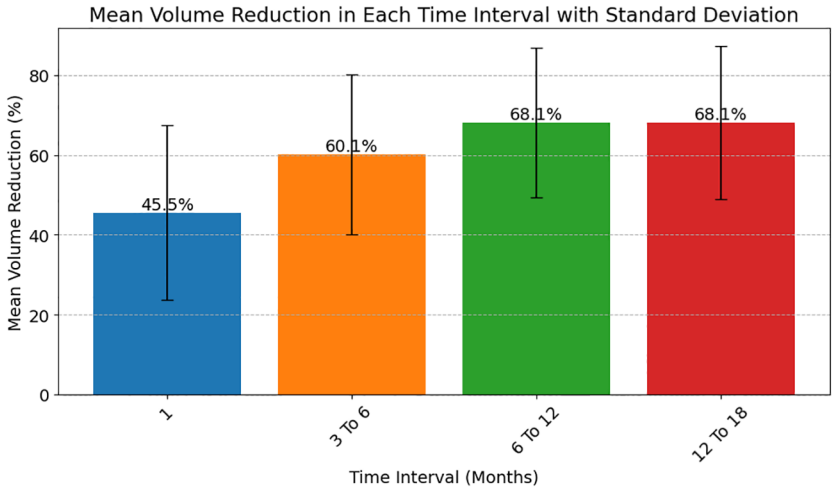

FIGURE 1
Post-ablation mean volume reduction in thyroid nodule volume at different time intervals.

progresses. The third violin (green violin) for the 6-12 months interval demonstrates a median that is higher still, with a broader distribution. The fourth violin (red violin) for the 12-18 months interval shows similar median reduction as the 6-12 month plot.

Volume reduction: subgroup analysis based on initial nodule volume

Figure 3, bar clusters revealed a few notable trends. At the 1-month interval, all quartiles demonstrate significant volume reduction. There was progressive volume reduction with increasing quartile at this stage. The 3-6 and 6-12 months interval shows a continued increase in volume reduction. But there was no statistically significant difference between the quartiles.

No immediate post procedure complications bleeding, difficulty swallowing were noted. No hospitalization after LA was reported. There was no clinically relevant change in thyroid function after laser ablation in patients with normal thyroid function. No patient had recurrent laryngeal, tracheal or esophageal damage. No subcutaneous burns or vascular damage occurred during or after the procedure. For patients not lost to follow-up (62 patients) and who had final symptom assessment, the majority of patients reported symptoms either resolved (n = 46, 85%) or improved (n=9, 16.6%) after LA. Of the 63 patients, 5 patients (7.9%) underwent second LA due to inadequate resolution of

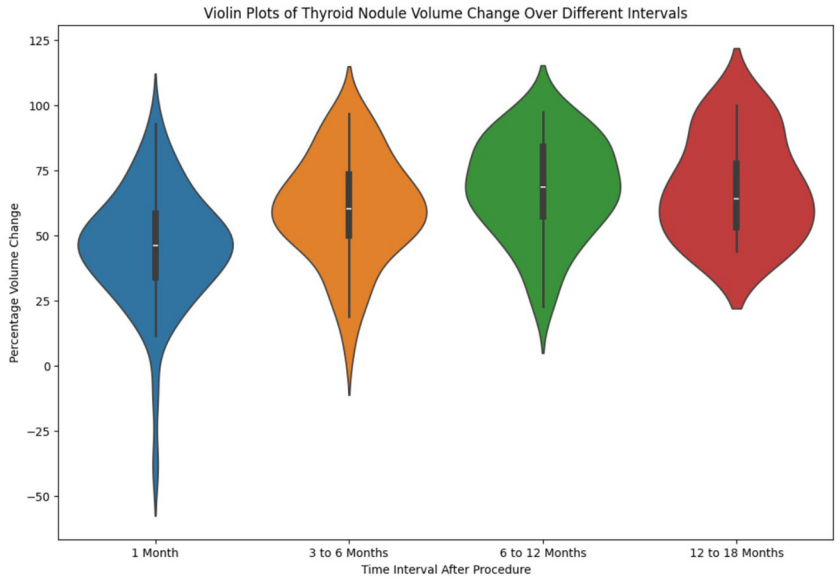

FIGURE 2
Distribution of thyroid volume reduction over different time intervals.

10.3389/fendo.2024.1402522

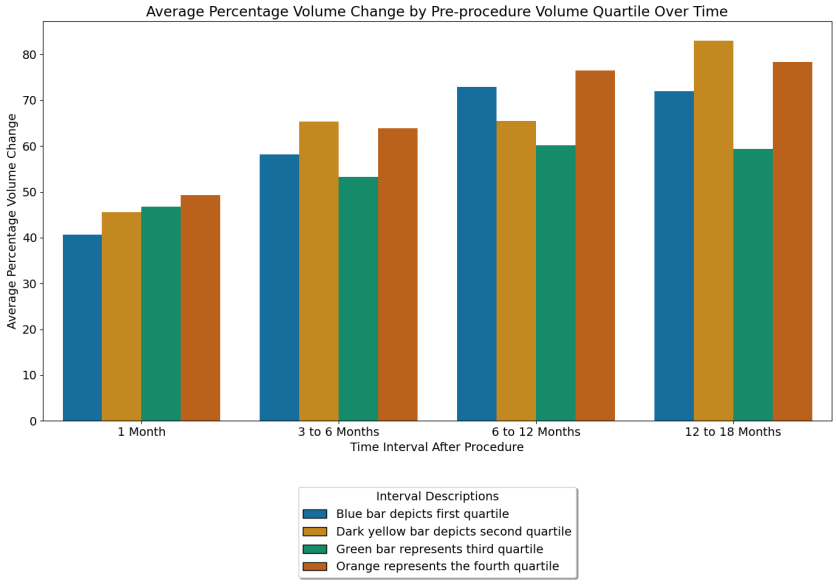

FIGURE 3
Mean percent volume change by pre-procedure volume quartile over time.

compressive symptoms. Of these 5 patients, the average volume reduction was 67.56% at 12 months.

Discussion

In this study, the Elesta Echolaser was employed to ablate benign symptomatic nodules, producing progressive reduction of nodule volume from initial ablation up to 12 months, and sustained mean reduction at 18 months. Initial volume reduction, within the first month, was most pronounced for the largest nodule. We observed an average volume reduction of approximately 12 cubic centimeters at 12 months following laser ablation of thyroid nodules. This aligns with findings from Rahal Júnior et al., where a reduction of about 60% in thyroid nodule volume was noted after a year (14). Average pre-procedure volume was 1.67cm3. Our subgroup analysis, which categorized nodules based on their initial volume, revealed differential responses to treatment. In the first month after treatment, volume reduction was proportional to the preprocedural volume. But later on in the study this trend disappeared. It is important to note that the correlation between pre-procedure nodule volume and percent reduction was generally weak, indicating that while size may influence the response initially, it is not the sole determinant of treatment success. Other potential factors that could affect the volume reduction includes, amount of energy applied and composition of the nodule (15).

Not all thyroid nodules are amenable to currently available minimally invasive procedures. Cystic or predominantly cystic nodules are best treated with aspiration or ethanol ablation (16). Nodules extending into the mediastinum may not be fully accessible percutaneously, and risks pneumothorax. Some researchers have reported regression of volume reduction long-term, thought to possibly represent inadequate margin ablation, leading to the possibility of recurrence. Since laser ablation relies on heat to destroy tissue, it can be difficult to definitively assess the success of the procedure during the treatment itself. Some centers in Europe and Asia use contrast enhanced ultrasound after ablation to identify the area of ablation (17). But this is not approved for use in the United States. We employed echolaser smart interface to aid in uniform spatial ablation using pullback technique along paths within a grid overlaying the thyroid nodule. The average percent reductions observed at 1 month (45.54%), 3-6 months (60.1%), 6-12 months (68%), and 12-18 months (68.1%) in our study are comparable to those reported in previous research (9, 18–21). Our study had only 63 participants and not all patients had 18 month follow up. It is unknown if the treatment effect will continue long-term, but results underscore the potential of laser ablation as an effective treatment for reducing the size of thyroid nodules. In recent years, a growing body of literature has supported LAs efficacy and safety. Studies have consistently reported significant reductions in nodule volume, improvement in local symptoms, and a low rate of complications (22). Our findings align with this emerging consensus, demonstrating a progressive decrease in nodule volume over 18 month period following laser ablation without significant complications (23).

In 2020 European Thyroid Association reviewed available data on thyroid thermal ablation techniques and published clinical guidelines (24). According to this guideline, image guided thermal ablation can be offered to adult patients who have pressure or cosmetic symptoms. This guideline also recommended dedicated training for the operator and discussion of potential side effects with the patients. A recent American Thyroid Association multidisciplinary consensus statement acknowledges the increasing adoption of thermal ablation techniques and calls for safe adoption and implementation in the United States (25). A pilot study in the United States demonstrated safe and effective Laser ablation in an outpatient setting (26).

As the prevalence of thyroid nodules increases, particularly in aging populations, treatments that offer reduced recovery times, lower complication rates, and preservation of thyroid function become increasingly valuable. Laser ablation fulfills these criteria, providing a viable option for patients who may not be ideal candidates for surgery or who prefer a less invasive approach to avoid surgical risks including laryngeal nerve injury (27). Minimally invasive procedures also have the potential to reduce healthcare spending. Studies comparing cost effectiveness of minimally invasive procedures to open thyroidectomy has shown potential significant cost savings (28, 29).

Our study contributes to the growing body of evidence supporting the use of laser ablation for the treatment of thyroid nodules. The observed reductions in nodule volume over time, coupled with the treatment's minimal invasiveness, position laser ablation as a promising alternative to surgery for suitable candidates. Future research should focus on multi-year long-term outcomes, the identification of factors predicting treatment response, and the refinement of patient selection criteria to further enhance the therapeutic potential of this technique.

Conclusion

The study conclusively demonstrates that laser ablation is a highly effective treatment for reducing the volume of thyroid nodules. With significant volume reductions observed at various post-procedure intervals, this minimally invasive technique shows promise for patients seeking alternatives to surgical intervention. The varying degrees of effectiveness based on initial nodule size, highlight the potential for tailored treatment approaches. Laser ablation thus offers a valuable addition to the therapeutic arsenal for thyroid nodules, combining efficacy with a favorable safety profile. This technique stands as a transformative approach in the management of thyroid nodules, aligning with the evolving landscape of patient-centered, minimally invasive medical care.

Data availability statement

The raw data supporting the conclusions of this article will be made available by the authors, without undue reservation.

Ethics statement

The studies involving humans were approved by Pearl Institutional Review Board. The studies were conducted in accordance with the local legislation and institutional requirements. Written informed consent for participation was not required from the participants or the participants' legal guardians/next of kin in accordance with the national legislation and institutional requirements.

Author contributions

IM: Conceptualization, Data curation, Investigation, Methodology, Project administration, Resources, Supervision, Validation, Writing – original draft, Writing – review & editing. JM: Investigation, Methodology, Project administration, Writing – original draft, Writing – review & editing. JT: Conceptualization, Formal analysis, Visualization, Writing – original draft, Writing – review & editing.

Funding

The author(s) declare that no financial support was received for the research, authorship, and/or publication of this article.

Acknowledgments

We would like to thank the Endocrine team at FVSS (Fox Valley Surgical Specialist), special thanks to Kayla Keefe RN, Katie Cantie MA and the administration at FVSS for supporting the study.

Conflict of interest

The authors declare that the research was conducted in the absence of any commercial or financial relationships that could be construed as a potential conflict of interest.

Publisher's note

Supplementary material

The Supplementary Material for this article can be found online at: https://www.frontiersin.org/articles/10.3389/fendo.2024.1402522/full#supplementary-material

References

1. Gambelunghe G, Stefanetti E, Avenia N, De Feo P. Percutaneous ultrasound-guided laser ablation of benign thyroid nodules: results of 10-year follow-up in 171 patients. *J Endocr Soc*. (2021) 5:bvab081. doi: 10.1210/jendso/bvab081

2. Mu C, Ming X, Tian Y, Liu Y, Yao M, Ni Y, et al. Mapping global epidemiology of thyroid nodules among general population: A systematic review and meta-analysis. *Front Oncol*. (2022) 12:1029926. doi: 10.3389/fonc.2022.1029926

3. Durante C, Costante G, Lucisano G, Bruno R, Meringolo D, Paciaroni A, et al. The natural history of benign thyroid nodules. *JAMA*. (2015) 313:926–35. doi: 10.1001/jama.2015.0956

4. Oddo S, Balestra M, Vera L, Giusti M. Benign thyroid nodule unresponsive to radiofrequency ablation treated with laser ablation: a case report. *J Med Case Rep*. (2018) 12:127. doi: 10.1186/s13256-018-1628-9

5. Papini E, Bizzarri G, Pacella CM. Percutaneous laser ablation of benign and Malignant thyroid nodules. *Curr Opin Endocrinol Diabetes Obes*. (2008) 15:434. doi: 10.1097/MED.0b013e32830eb89a

6. Papini E, Bizzarri G, Novizio R, Guglielmi R. Laser ablation for thyroid nodules has come to age—a review. *Ann Thyroid*. (2023) 8:4–4. doi: 10.21037/aot-22-26

7. Gambelunghe G, Fatone C, Ranchelli A, Fanelli C, Lucidi P, Cavaliere A, et al. A randomized controlled trial to evaluate the efficacy of ultrasound-guided laser photocoagulation for treatment of benign thyroid nodules. *J Endocrinol Invest*. (2006) 29:RC23–26. doi: 10.1007/BF03347368

8. Sim JS, Baek JH. Long-term outcomes following thermal ablation of benign thyroid nodules as an alternative to surgery: the importance of controlling regrowth. *Endocrinol Metab Seoul Korea*. (2019) 34:117–23. doi: 10.3803/EnM.2019.34.2.117

9. Pacella CM, Mauri G, Achille G, Barbaro D, Bizzarri G, Feo P, et al. Outcomes and risk factors for complications of laser ablation for thyroid nodules: A multicenter study on 1531 patients. *J Clin Endocrinol Metab*. (2015) 100:3903–10. doi: 10.1210/jc.2015-1964

10. Mauri G, Pacella CM, Papini E, Solbiati L, Goldberg SN, Ahmed M, et al. Image-guided thyroid ablation: proposal for standardization of terminology and reporting criteria. *Thyroid Off J Am Thyroid Assoc*. (2019) 29:611–8. doi: 10.1089/thy.2018.0604

11. Seo SH, Kim TH, Kim SH, Lee SH, Kim JT, Park DW, et al. Predicting the size of benign thyroid nodules and analysis of associated factors that affect nodule size. *Chonnam Med J*. (2015) 51:97–101. doi: 10.4068/cmj.2015.51.2.97

12. American Thyroid Association Change in Thyroid Nodule Volume Calculator. Available online at: https://www.thyroid.org/professionals/calculators/thyroid-with-nodules/ (Accessed June 21, 2023).

13. van Rossum G. Python reference manual (1995). Available online at: https://ir.cwi.nl/pub/5008 (Accessed January 22, 2024).

14. Junior AR, Falsarella PM, Mendes GF, Hidal JT, Andreoni DM, Lúcio J, et al. Ablação percutânea com laser de nódulos benignos de tireoide: um estudo de acompanhamento de um ano. *Einstein São Paulo*. (2018) 16. doi: 10.31744/einstein_journal/2018AO4279

15. Negro R, Salem TM, Greco G. Laser ablation is more effective for spongiform than solid thyroid nodules. A 4-year retrospective follow-up study. *Int J Hyperth Off J Eur Soc Hyperthermic Oncol North Am Hyperth Group*. (2016) 32:822–8. doi: 10.1080/02656736.2016.1212279

16. Park HS, Yim Y, Baek JH, Choi YJ, Shong YK, Lee JH. Ethanol ablation as a treatment strategy for benign cystic thyroid nodules: a comparison of the ethanol retention and aspiration techniques. *Ultrasonography*. (2019) 38:166–71. doi: 10.14366/usg.18033

17. Ma S, Zhou P, Wu X, Tian S, Zhao Y. Detection of the single-session complete ablation rate by contrast-enhanced ultrasound during ultrasound-guided laser ablation for benign thyroid nodules: A prospective study. *BioMed Res Int*. (2016) 2016:9565364. doi: 10.1155/2016/9565364

18. Døssing H, Bennedbaek FN, Hegedüs L. Effect of ultrasound-guided interstitial laser photocoagulation on benign solitary solid cold thyroid nodules - a randomised study. *Eur J Endocrinol*. (2005) 152:341–5. doi: 10.1530/eje.1.01865

19. Papini E, Guglielmi R, Bizzarri G, Graziano F, Bianchini A, Brufani C, et al. Treatment of benign cold thyroid nodules: a randomized clinical trial of percutaneous laser ablation versus levothyroxine therapy or follow-up. *Thyroid Off J Am Thyroid Assoc*. (2007) 17:229–35. doi: 10.1089/thy.2006.0204

20. Papini E, Rago T, Gambelunghe G, Valcavi R, Bizzarri G, Vitti P, et al. Long-term efficacy of ultrasound-guided laser ablation for benign solid thyroid nodules. Results of a three-year multicenter prospective randomized trial. *J Clin Endocrinol Metab*. (2014) 99:3653–9. doi: 10.1210/jc.2014-1826

21. Achille G, Zizzi S, Di Stasio E, Grammatica A, Grammatica L. Ultrasound-guided percutaneous laser ablation in treating symptomatic solid benign thyroid nodules: Our experience in 45 patients. *Head Neck*. (2016) 38:677–82. doi: 10.1002/hed.23957

22. Trimboli P, Castellana M, Sconfienza LM, Virili C, Pescatori LC, Cesareo R, et al. Efficacy of thermal ablation in benign non-functioning solid thyroid nodule: A systematic review and meta-analysis. *Endocrine*. (2020) 67:35–43. doi: 10.1007/s12020-019-02019-3

23. Jasim S, Patel KN, Randolph G, Adams S, Cesareo R, Condon E, et al. American association of clinical endocrinology disease state clinical review: the clinical utility of minimally invasive interventional procedures in the management of benign and Malignant thyroid lesions. *Endocr Pract*. (2022) 28:433–48. doi: 10.1016/j.eprac.2022.02.011

24. Papini E, Monpeyssen H, Frasoldati A, Hegedüs L. 2020 European thyroid association clinical practice guideline for the use of image-Guided ablation in benign thyroid nodules. *Eur Thyroid J*. (2020) 9:172–85. doi: 10.1159/000508484

25. Sinclair CF, Baek JH, Hands KE, Hodak SP, Huber TC, Hussain I, et al. General principles for the safe performance, training, and adoption of ablation techniques for benign thyroid nodules: an American thyroid association statement. *Thyroid Off J Am Thyroid Assoc*. (2023) 33:1150–70. doi: 10.1089/thy.2023.0281

26. Thomas J, Ledger GA, Haertling T. Effects of ultrasound-guided laser ablation therapy on symptomatic benign thyroid nodules, using echoLaser – results of a pilot study in the United States. *Endocr Pract*. (2023) 29:942–7. doi: 10.1016/j.eprac.2023.08.015

27. Culp JM, Patel G. Recurrent Laryngeal Nerve Injury (2024). StatPearls Publishing. Available online at: http://www.ncbi.nlm.nih.gov/books/NBK560832/ (Accessed March 12, 2024). StatPearls.

28. Miller JR, Tanavde V, Razavi C, Saraswathula A, Russell JO, Tufano RP. Cost comparison between open thyroid lobectomy and radiofrequency ablation for management of thyroid nodules. *Head Neck*. (2023) 45:59–63. doi: 10.1002/hed.27213

29. Schalch MS, Costa ACN, de Souza RP, Guerra FLB, Guerreiro R, De Cicco R. Radiofrequency ablation of thyroid nodules: prospective cost-effectiveness analysis in comparison to conventional thyroidectomy. *Arch Endocrinol Metab*. (2021) 65:752–7. doi: 10.20945/2359-3997000000411

Frontiers in Endocrinology

Explores the endocrine system to find new therapies for key health issues

The second most-cited endocrinology and metabolism journal, which advances our understanding of the endocrine system. It uncovers new therapies for prevalent health issues such as obesity, diabetes, reproduction, and aging.

Discover the latest Research Topics

See more →

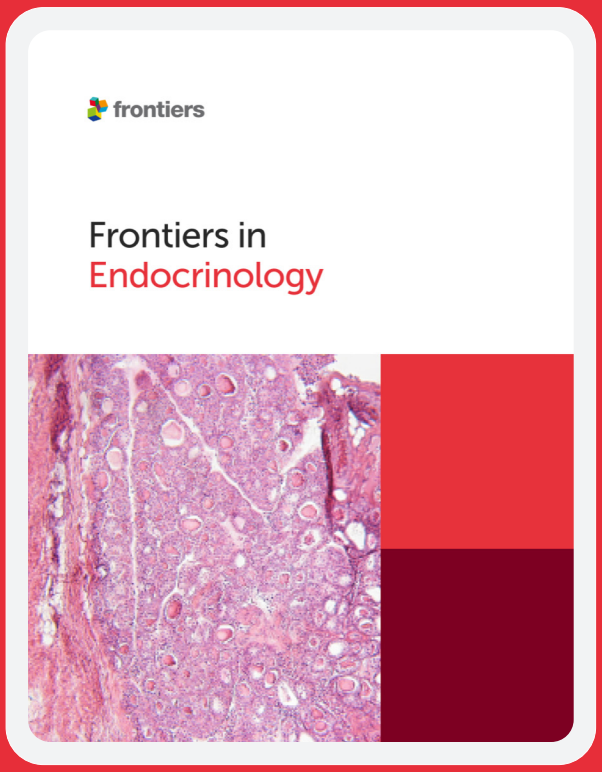

Frontiers

Avenue du Tribunal-Fédéral 34
1005 Lausanne, Switzerland
frontiersin.org

Contact us

+41 (0)21 510 17 00
frontiersin.org/about/contact